UNIVERSITY OF SOUTHAMPTON

Faculty of Engineering and Physical Sciences
School of Electronics and Computer Science

Impact of Moisture and Thermal Ageing on Space Charge Characteristics in Natural Ester Liquid-Impregnated Paper Insulation System

by

Hyungjin Yoon

ORCiD: 0000-0002-6097-8487

A thesis for the degree of
Doctor of Philosophy

January 2024

University of Southampton

Abstract

Faculty of Engineering and Physical Sciences
School of Electronics and Computer Science

Doctor of Philosophy

Impact of Moisture and Thermal Ageing on Space Charge Characteristics in Natural Ester Liquid-Impregnated Paper Insulation System

by Hyungjin Yoon

The HVDC technology has facilitated the long-distance transmission of large amounts of power. This benefit of HVDC technology allows for the decentralisation of energy resources, enabling the utilisation of remote renewable resources such as offshore wind farms. To keep the HVDC power transformer operating reliably, it is crucial to design the insulation system effectively. In HVDC power transformers, the predominant dielectric materials are cellulose and mineral oil. Mineral oil is still utilised in HVDC power transformers due to its strong dielectric strength and cooling function. However, the limitations of mineral oil, such as poor biodegradability, high fire risk, and scarcity, have motivated the development of an alternative. As a consequence of its high biodegradability, low fire risk, and renewability, natural ester liquid has been seen as a promising dielectric liquid to replace mineral oil. Despite this, more research is being conducted to determine the viability of using natural ester liquid in the HVDC power transformer. Therefore, a comparative study between natural ester liquid and mineral oil is critical.

The HVDC power transformer, unlike the AC system, is subjected to AC, DC, and AC-DC combined stresses. Under DC conditions, space charge accumulation is a common occurrence in dielectric materials. Space charge accumulation is undesired in the oil-paper insulation system because it enhances the electric field in certain areas, which accelerates the insulation's degradation and may even cause it to fail prematurely. To study the space charge characteristics, the pulsed electroacoustic (PEA) technique was applied.

One of the most unwelcome by-products of oil-paper insulation systems is moisture, which aids the penetration of space charges deeper into the oil-impregnated paper. Natural ester liquid is hydrophilic and may absorb water actively from cellulose. As a result, investigating space charge characteristics in natural ester liquid-impregnated paper and mineral oil-impregnated paper under moisture impact circumstances is critical.

During the HVDC power transformer operation, hot spots might form close to the windings. Therefore, the long-term operation of the HVDC power transformer results in the thermal ageing of oil-paper insulating systems. The space charge characteristics of oil-impregnated papers can be influenced by a number of variables, including physical and chemical impacts under thermal ageing conditions. Comparing natural ester liquid with mineral oil under thermal ageing circumstances can provide additional data for determining if natural ester liquid can be employed as the dielectric liquid for HVDC power transformers.

This thesis investigated the effect of moisture and thermal ageing on natural ester liquid-impregnated papers by comparing it with mineral oil-impregnated paper. Moisture and thermal ageing are considered major factors in deteriorating insulating materials. Natural ester liquid and mineral oil have different chemical structures, which react differently with moisture and thermal ageing. Especially under different moisture conditions, natural ester liquid delayed the accumulation of heterocharges compared to mineral oil. This indicates that natural ester liquid can behave as an inhibitor of heterocharge accumulation in the oil-paper system. Natural ester liquid has ester linkages in its chemical structure, making it more polar than mineral oil. Hence, natural ester liquids can dissolve more by-products like water and acids because of their greater polarity, contributing to improved cellulose conditions during thermal ageing.

Regarding the space charge decay, natural ester liquid showed a faster charge dissipation rate than mineral oil. When the polarity is reversed, faster charge dissipation of natural ester oil can help mitigate the negative effect of polarity reversal. From a dielectric point of view, natural ester liquid can provide advantages such as faster charge dissipation, an inhibitor for heterocharge accumulation, and higher breakdown strength. However, additional research is still required to accept natural ester liquid for HVDC converter transformers fully.

Contents

List of Figures

List of Tables

Declaration of Authorship

I declare that this thesis and the work presented in it is my own and has been generated by me as the result of my own original research.

I confirm that:

1. This work was done wholly or mainly while in candidature for a research degree at this University;
2. Where any part of this thesis has previously been submitted for a degree or any other qualification at this University or any other institution, this has been clearly stated;
3. Where I have consulted the published work of others, this is always clearly attributed;
4. Where I have quoted from the work of others, the source is always given. With the exception of such quotations, this thesis is entirely my own work;
5. I have acknowledged all main sources of help;
6. Where the thesis is based on work done by myself jointly with others, I have made clear exactly what was done by others and what I have contributed myself;
7. Parts of this work have been published as:

   Conferences:

   H. Yoon and G. Chen, "Impact of Moisture on Space Charge Characteristics in Natural Ester Oil-Impregnated Paper," in 2020 IEEE 3rd International Conference on Dielectrics (ICD), 2020.

   H. Yoon and G. Chen, "Impact of Thermal Ageing on Space Charge Characteristics in Natural Ester Oil-impregnated Paper," in 2021 IEEE Conference on Electrical Insulation and Dielectric Phenomena (CEIDP), 2021.

   Journals:

   H. Yoon and G. Chen, "Space Charge Characteristics of Natural Ester Oil-Impregnated Paper With Different Moisture Contents," in IEEE Transactions on Dielectrics and Electrical Insulation, vol. 29, no. 6, pp. 2139-2146, Dec. 2022.

   H. Yoon, G. Chen and I. L. Hosier, "Influence of Thermal Aging on Dielectric Properties of Natural Ester Oil-Impregnated Paper," in IEEE Transactions on Dielectrics and Electrical Insulation, vol. 30, no. 3, pp. 1337-1344, June 2023

   H. Yoon, I. L. Hosier, and G. Chen, "Impact of Moisture on Space Charge Characteristics of Multilayer of Natural Ester Oil-impregnated Paper," in IEEE Transactions on Dielectrics and Electrical Insulation, 2023 **(Under Review)**

Signed:.. Date:..................

Acknowledgements

My research is about space charge dynamics related to natural ester oil and has been completed with a lot of help.

First of all, I would like to express my sincere gratitude to my supervisor, Professor George Chen. He provided a lot of motivation and insightful guides for my research.

Also, I would like to thank Alan Welford and Charlie Reed for providing a lot of help in the Tony Davies High Voltage Laboratory.

Many thanks to Phicket Ketsamee, Dr. Ian L Hoiser, Dr. Orestis Vryonis, and Dr. Suuny Chaudhary that they shared various viewpoints.

Finally, I would like to thank my family for providing support and deep understanding during my PhD programme.

To my brother . . .

Definitions and Abbreviations

HVDC	High Voltage Direct-Current
HVAC	High Voltage Alternating-Current
DC	Direct-Current
AC	Alternating-Current
LCC	Line Communicated Converter
VSC	Voltage Source Converter
CSC	Current Source Converter
IGBT	Insulated-Gate Bipolar Transistor
PWM	Pulse Width Modulation
PB	Pressboard
PR	Polarity Reversal
DP	Degree of Polymerisation
BCT	Bipolar Charge Transport
PEA	Pulsed Electroacoustic
PVDF	Polyvinylidene Fluoride
ε	Permittivity
$tan\delta$	Loss Tangent
σ, σ_{dc}	Conductivity, DC conductivity
$E, E_{applied}, E_{max}$	Electric Field, Applied Electric Field, Maximum Electric Field
ΔE	Electric Field Distortion Rate
Q_{total}	Total Amount of Charges

ppm	Part Per Million
ρ	Charge Density
S	Electrode Area
Hz	Hertz

Chapter 1

Introduction

1.1 Background

Efficient bulk power transport necessitates a high level of technology due to the exponentially rising energy demand. As a result, High Voltage Direct-Current (HVDC) technology is gaining popularity because, in contrast to High Voltage Alternating-Current (HVAC) technology, it can transmit large amounts of energy over long distances with high-efficiency [1].

The HVDC technology is more advantageous than HVAC economically. If AC and DC systems require similar insulating technologies for peak voltage, the DC system, which uses only two conductors, can transmit more power than the AC system, which requires three conductors [2]. Moreover, as illustrated in Figure 1.1, the DC system utilises more inexpensive transmission towers in terms of space and cost. Although

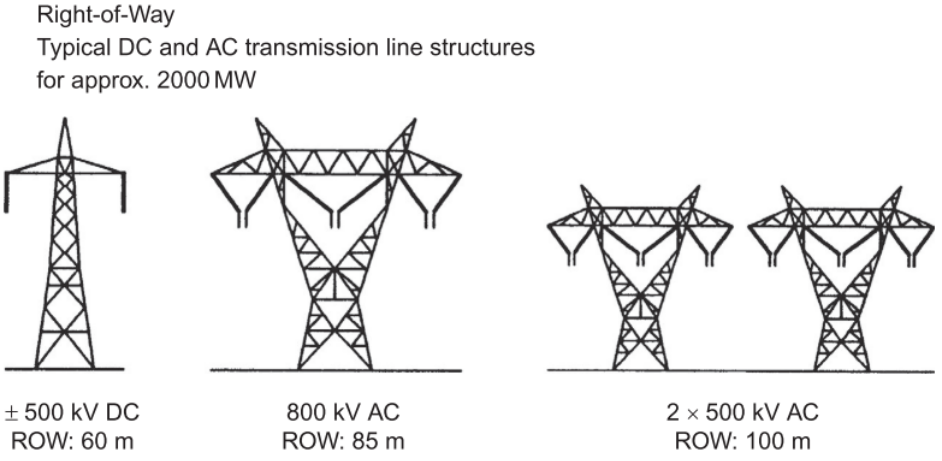

FIGURE 1.1: Tower Structures for DC and AC Transmission System [2]

HVAC technology is considered economically advantageous for short-distance bulk

power transmissions due to relatively lower initial installation costs. However, long-distance bulk power transmissions, which exceed the break-even distance, are better suited for HVDC transmission systems than HVAC transmission systems, as depicted in Figure 1.2 [2]. The break-even distance is where the overall investment cost for HVAC exceeds the overall investment for HVDC. Therefore, after reaching this point, HVDC shows better economic viability over HVAC for longer transmission, making itself the preferred option. According to [3], for overhead lines, the break-even distance is between 800 km and 1000 Km, whilst for submarine cable, the break-even distance is approximately 50 Km.

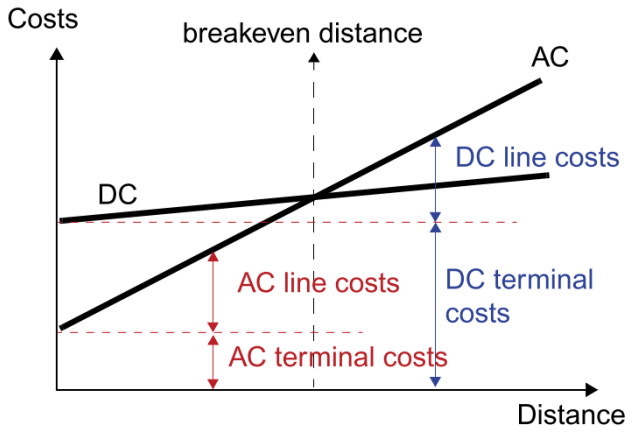

FIGURE 1.2: Cost Comparison of AC and DC Systems [2]

HVDC transmission systems have technological advantages over HVAC. Due to the absence of frequency, the HVDC transmission system can fully utilise the conductor's cross-section without skin effect, thereby increasing the transmission efficiency [1]. Furthermore, the absence of these frequencies allows asynchronous interconnection between two different frequency AC systems [2].

The HVDC converter transformer plays a critical role in ensuring the sustainability of the power supply in the HVDC transmission system. HVDC power transformers are equipped with converter stations that enable the conversion of AC to DC or DC to AC in the transmission process [4]. In contrast to traditional HVAC transmission systems, the HVDC power transformer is subjected to multiple stresses, including AC, DC, and DC polarity reversal [5]. Regarding HVDC technology, a line-commutated converter (LCC) and a voltage-sourced converter (VSC) are two primary devices in order to convert electric power from AC to DC or vice versa [6]. LCC can manage higher voltage and current levels than VSC [6]. On the other hand, VSC can provide greater operational flexibility than LCC [6]. Thus, the polarity reversal is only valid for LCC due to its limited flexibility. The behaviour of the electric field in the HVDC transformer insulation system is determined by the type of stress. These stresses produce various electric field distributions that affect the performance of the HVDC transformer [5]. The AC field is impacted by the dielectric permittivity, while the DC field is mainly affected

by electrical conductivity [7]. Therefore, different electric stresses produce different electric field distributions, so designing the HVDC transformer insulation system requires careful attention [7].

The electrical insulation technology has a significant effect on the performance and service life of HVDC power transformers [8]. As the main insulation system of an HVDC power transformer, oil-papers typically suffer from space charge accumulation. Significantly, the DC electric field can lead it the formation of space charges in oil-papers [9]. Space charges in dielectrics locally intensify the electric field, which accelerates the ageing of the oil-paper and sometimes causes a premature breakdown in the HVDC power transformer [9]. Therefore, studying the space charge dynamics contributes to a greater understanding of the insulation system for HVDC power transformers.

In HVDC power transformers, the most common insulating materials are mineral oil and cellulose paper. Although paper is an efficient and economical solid insulating material, it is often combined with mineral oil [10]. Mineral oil has been used to enhance both the electrical insulation and cooling functions of HVDC power transformers. Due to its outstanding dielectric properties, mineral oil is the most frequently used dielectric liquid in HVDC power equipment [11]. However, despite its desirable properties, mineral oil also has some significant drawbacks. First, its relatively low flash point of about 160°C causes a significant fire hazard [11]. Furthermore, the extremely poor biodegradability of mineral oil poses a serious hazard to the environment when leakage occurs.

The shortcomings of mineral oil have increased attention to natural ester liquid as a viable substitute for transformer applications. Because natural ester liquid has a high flash point (above 300°C), it provides a significantly lower fire risk than mineral oil. Furthermore, natural ester liquid can achieve high biodegradability because it is produced from a plant-based resource [11]. While natural ester liquid is already used as the dielectric liquid in low- and medium-voltage transformers, further investigation is required before it can be fully utilised in HVDC power transformers [12].

Moisture, caused by ageing or water ingress, is one of the most hazardous byproducts because it can accelerate the ageing process and result in a substantial decrease in breakdown voltage [13]. Moreover, the operation of the HVDC power transformer generates a hot spot inside, leading to thermal ageing of the oil-paper [14]. These deteriorating factors can have a significant influence on the dielectric properties of the oil-paper insulation system.

Therefore, it is vital to investigate the space charge characteristics of the natural ester liquid-paper insulation system compared to that of the mineral oil-paper insulation system under the influence of moisture and thermal ageing. The objective of this study is to assess the suitability of natural ester liquid as the dielectric liquid in HVDC power transformers by comparing it to mineral oil.

1.2 Research Questions

Since the PEA method came out in the 1980s, many researchers have done space charge measurements on dielectrics [15]. Research on natural ester liquid under DC conditions is relatively insufficient because mineral oil has been predominantly used in HVDC power transformers. Moisture and thermal ageing are the main factors that reduce the performance of oil-paper insulation. They have a substantial impact on the space charge characteristics of oil-paper, which may accelerate the degradation process. Therefore, the purpose of this study is to investigate the applicability of natural ester liquid as the dielectric liquid for HVDC power transformers. The investigation was done by comparing the space charge characteristics of natural ester liquid-paper and mineral oil-paper.

Four research questions are set for this thesis:

- How does moisture affect the space charge dynamics of single-layer natural ester liquid-impregnated paper?
- How does thermal ageing affect the space charge dynamics and physicochemical properties of single-layer natural ester liquid-impregnated paper?
- How does moisture affect the space charge dynamics in a double layer made of natural ester liquid and natural ester liquid-impregnated paper?
- How does polarity reversal under different moisture conditions affect the space charge dynamics in double layers composed of natural ester liquid and natural ester liquid-impregnated paper?

1.3 Objectives of This Research

The main insulating materials for HVDC power transformers are transformer oil and paper. This study focuses on investigating the electrical properties of natural ester liquid. As natural ester liquid is derived from plants, it is renewable, making it an environmentally friendly option with high biodegradability. Despite its current use in low and medium-voltage power transformers, further research is needed before applying natural ester liquid to HVDC power transformers.

This research makes a contribution to the field by space charge characteristics of natural ester liquid-impregnated paper under the influence of moisture and thermal ageing.

The existing studies mainly focus on a single layer of natural ester liquid-impregnated paper, while this study explored the multilayer of oil gap and natural ester liquid-impregnated paper by comparing it with mineral oil. Therefore, this research aims to contribute by providing data on the applicability of natural ester liquid as HVDC power transformer oil, achieved through a comparison of its electrical properties with mineral oil.

1.4 Structure of This Report

This report investigated the space charge characteristics of natural ester liquid-impregnated paper and mineral oil-impregnated paper. This report consists of 8 chapters.

Chapter 1 introduces this report's background, research questions, and structure.

Chapter 2 provides a comprehensive literature review, facilitating a deeper understanding of the research materials and methodology.

Chapter 3 introduces the methodology for experiments and provides the background of each experimental measurement.

Chapter 4 explored how moisture affects the space charge dynamics of single-layer natural ester liquid-impregnated paper by comparing it with mineral oil-impregnated paper.

Chapter 5 explored how thermal ageing influenced the space charge dynamics of single-layer natural ester liquid-impregnated paper by comparing it with mineral oil-impregnated paper.

Chapter 6 studied the impact of moisture on space charge characteristics of multilayer of natural ester liquid-impregnated paper.

Chapter 7 investigated the polarity reversal effect on space charge characteristics of multilayer of natural ester liquid-impregnated paper with different moisture contents.

Chapter 8 discussed the conclusion.

Chapter 9 discussed the potential future research.

Chapter 2

Literature Review

2.1 High Voltage Direct-Current(HVDC) Technology

As the conventional power system, HVAC transmission systems dominate most power grids, and they are economic systems due to their relatively inexpensive equipment. The HVAC transmission system has the advantage of relatively easy voltage change and an electric field rotation [16]. Besides, the HVAC transmission system is more convenient for interrupting AC current in comparison with HVDC transmission systems [16].

Nevertheless, the rapid increase in energy demand has emphasised the necessity for more power generation and long-distance power transmission. Unfortunately, HVAC transmission systems show a number of shortcomings for long-distance bulk power transfer in terms of efficiency, stability, and interconnection between two asynchronous AC systems [2]. Therefore, the HVDC transmission system is being increasingly considered an alternative to overcome the drawbacks of HVAC technology.

Early DC transmission systems have confronted various problems such as high installation costs, changing voltage levels, harmony generations, and difficulty in controlling [2]. However, most shortcomings of DC transmission systems have been resolved thanks to the development of semiconductor and insulation technology, enabling the transmission of bulk power over long-distance efficiently [2]. Furthermore, the effective bulk power transmission over long-distance facilitates the utilisation of remote renewable energy such as offshore wind farms [16].

Due to the numerous advantages of HVDC technology, the HVDC transmission system is currently regarded as the future main power system. Therefore, a thorough understanding of HVDC technology is necessary for the efficient transfer of large amounts of power.

2.1.1 Overview of HVDC Transmission System

Initial power transmission systems implemented direct current (DC) technology, but electrical energy was produced adjacent to consumers to prevent significant energy losses caused by excessively low voltage levels [17]. On the other hand, the early ac system could efficiently transform from low- and high-voltage levels, which was adequate to transmit power over long-distance compared to the DC system, and this led the AC system to become the dominant technology [17]. Nevertheless, technological advances in semiconductors and power electronics have enabled to overcome the drawbacks of DC systems [17]. Moreover, this showed that the DC system has considerable potential as a next-generation power transmission system.

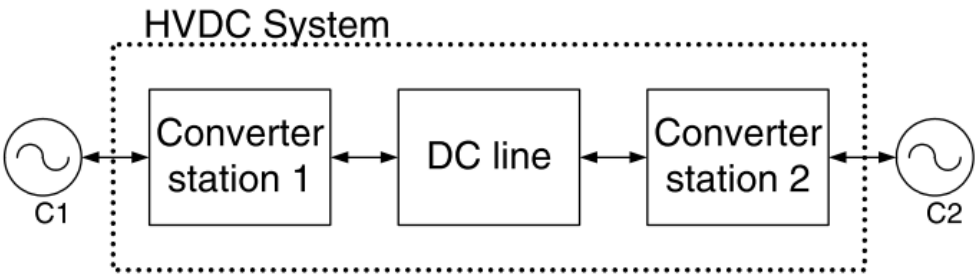

FIGURE 2.1: Simplified Schematic of Overall HVDC Transmission System [2]

Figure 2.1 represents the simplified schematic of the overall HVDC transmission system. The basic concept behind the HVDC transmission system is to transfer electrical energy from one AC system to another through interconnected HVDC links, comprising two converter stations and DC lines [2]. As shown in Figure 1.2, HVDC technology offers greater economic advantages than HVAC technology, especially for long-distance power transmission. HVAC transmission system imposes a significant inductance on the power transmission line for long-distance bulk power transfer [2]. As the length of the AC cable increases, the charging current also increases accordingly. Consequently, the cable can be significantly influenced by reactive current, primarily due to capacitance, which disturbs the flow of additional useful power [16]. This imposed inductance must be compensated to achieve reliable and sustainable operations. Consequently, the HVAC transmission system regarding long-distance inevitably requires reactive compensation for long cables, which causes extra cost [2], [16].

In addition, as depicted in Figure 2.2 (a), the conductor is subject to the skin effect due to the presence of frequency in HVAC technology. As the frequency rises, the current is pushed to the surface of the conductor, making it challenging to use the conductor's cross-section entirety [2]. In contrast, HVDC technology is unaffected by frequency, so it is free from skin effects. Thus, the entire cross-section of the conductor can be

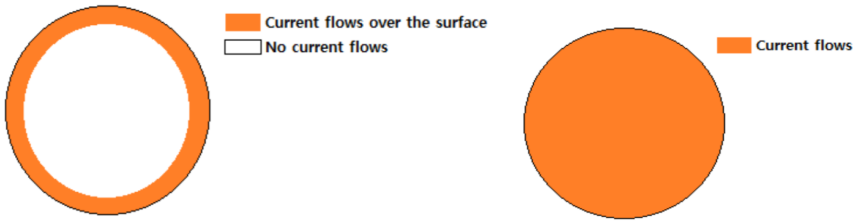

(A) HVAC(Skin Effect) (B) HVDC(No Skin Effect)

FIGURE 2.2: Skin Effect on Conductor between HVAC and HVDC Systems

fully utilised, as shown in Figure 2.2 (b), which achieves higher efficiency than HVAC technology [2], [4].

It is not possible to connect two systems using different frequencies with an AC connection [16]. Furthermore, it is difficult to establish an AC connection unless both systems operate simultaneously, even if they use the same frequency [16]. However, asynchronous interconnection can be achieved through HVDC technology between two AC systems at different rated frequencies (e.g. 50 and 60 Hz) or the same frequencies with asynchronous systems [18]. HVDC technology enables interconnected systems to maintain their original power quality, including frequency and voltage levels, independently [18]. Also, replacing circuit breakers and limiting current is unnecessary since HVDC technology does not require a large increase in the short circuit capacity of two interconnected AC systems [18]. Since the advanced control capability of HVDC systems also functions as a firewall between interconnected systems, catastrophic cascading failures, and power outages in the power grid can be prevented efficiently [17].

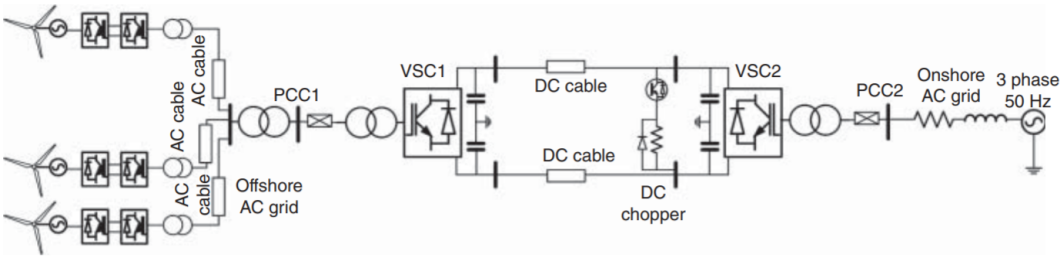

FIGURE 2.3: Offshore Wind Farm with HVDC Interconnection [19]

Due to the efficiency of HVDC systems in long-distance transmission, remote renewable energy sources, such as offshore wind farms, can be effectively utilised, as illustrated in the Figure 2.3 [19], [20]. Since there are no length restrictions on the HVDC transmission system, the availability of decentralised energy resources with HVDC technology has the potential to provide numerous economic and environmental benefits [17].

2.1.2 Line Communicated Converter(LCC)-HVDC Technology

HVDC transmission systems typically utilise either Line Commutated Converter (LCC) or Voltage Source Converter (VSC) technologies [6]. The commercialisation of the mercury-arc valve in the 1950s enabled the utilisation of HVDC transmission systems. Afterwards, the development of thyristors in the 1970s improved HVDC technology, enabling the design of more simplified and compact converter stations [6]. Therefore, this section focuses mainly on thyristor-based LCC-HVDC technology.

The line commutated converter (LCC)-HVDC system is depicted in Figure 2.4. LCC is also called a current source converter (CSC), and it utilises thyristors in converter stations [21]. The prominent role of the thyristor is to function as a bi-stable switch that is triggered by a gate pulse. This state is maintained unless the current becomes zero, at which point it can be switched off. Therefore, it requires the current to pass through zero in order to be reset [21].

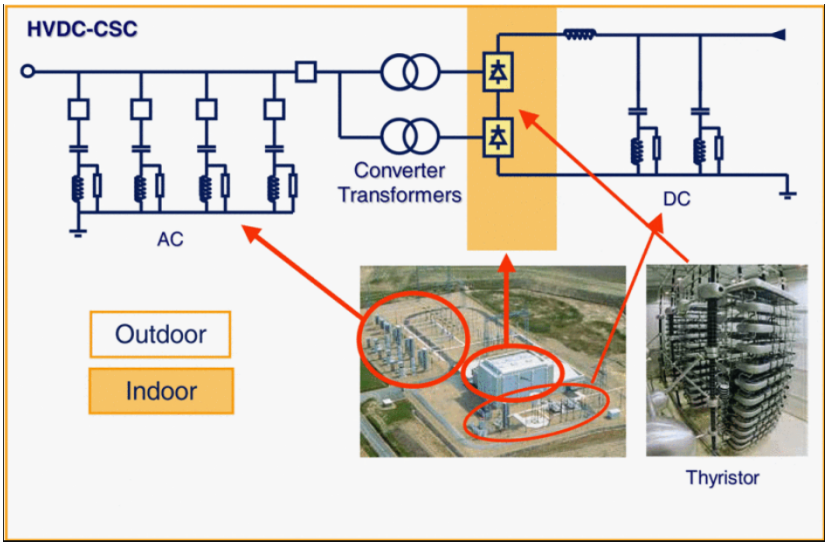

FIGURE 2.4: LCC(CSC)-HVDC System [22]

Figure 2.5 indicates the different types of LCC-HVDC connection and the converter transformer is mainly connected to the 6-pulse thyristor bridge or 12-pulse thyristor bridge [23]. In LCC-HVDC technology, a synchronised voltage source is necessary to operate converters and basic components with three-phase, the full-wave bridge called the 6-pulse bridge, are leveraged for HVDC conversion [22]. In a 6-pulse bridge, six switching processes produce a six times larger harmonic ripple than the fundamental frequency with respect to the DC output voltage [22]. Each 6-pulse bridge is integrated with six controlled switching elements or thyristor valves, containing series-connected thyristors to obtain the desired dc voltage rating [22]. Regarding the 12-pulse bridge, the two 6-pulse bridges in the DC terminal are integrated with the AC voltage source phase shifted by 30 degrees [22]. Then, two 6-pulse bridges can be connected in series,

increasing the DC voltage and reducing some AC current and DC voltage harmonics, but 12-pulse bridges still face some harmonics [22]. The feature of AC current harmonic is 12n±1, and the feature of DC voltage harmonic is 12n in the 12-pulse bridge [22].

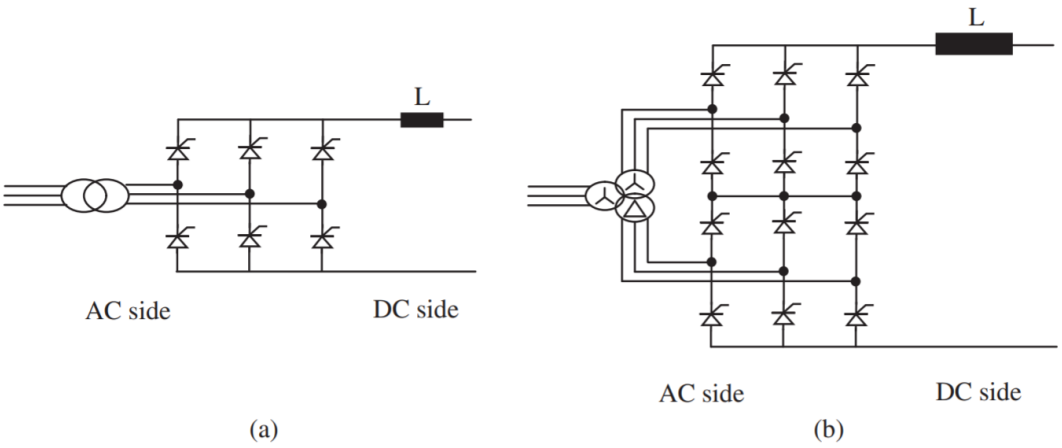

FIGURE 2.5: Basic Circuit of HVDC Connection. (a) 6-pulse LCC (b) 12-pulse LCC [23]

Firing angle α represents the angle that the thyristor switches on and off and μ represents the commutation angle [23]. Figure 2.6 (a) shows the waveform without commutation overlap (μ=0°) in the 6-pulse thyristor converter, while Figure 2.6 (b) depicts the waveform in the 6-pulse thyristor converter, which is affected by the commutation overlap (μ=9°) [23].

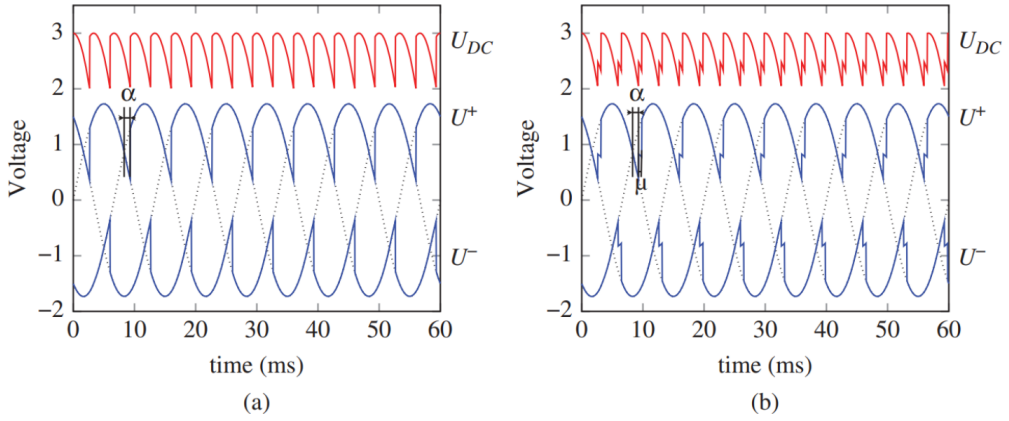

FIGURE 2.6: Typical Waveforms of the 6-pulse Thyristor Converter. (a) 6-pulse converter waveform without commutation angle (α=27°and μ=0°) (b) 6-pulse converter waveform with commutation angle (α=27°and μ=9°) [23]

LCC-HVDC technology is controlled by regulating the firing angle α on the converting and inverting sides [21]. Controlling the firing angle α enables the unidirectional line commutated DC flow, injected into a receiving AC system [21]. The output current then remains constant, which is why LCC technology is also known as CSC [21]. In a classic HVDC system, the current always flows in one direction, so the polarity of the voltage must be changed for the reverse power flow [23]. The commutation angle μ in the thyristor converter is generated by the inductance, which results in a short overlap

period while transferring the current between two conducted branches of the converter [23]. Reducing harmonics in AC systems requires additional filters and converters with a higher level of pulses, such as 12, 18, or 24-pulse [23]. Most classic HVDC systems have the 12-pulse thyristor converter that can cancel out harmonics $(6 \pm 1 + k \times 12)$ such as 5th, 7th, and 17th [23]. Therefore, 12-pulse converters as basic devices can enhance harmonic performance on both the AC and DC sides. Also, they can simplify filtering devices and save space and construction costs [24].

Achieving the high voltage must require connecting several thyristors in series [23]. A single thyristor can withstand up to 8.5kV, and it allows the current up to 5kA [23]. Typically, redundancy is required to prevent a single thyristor failure, which may lead to the malfunction of the overall HVDC link [23].

2.1.3 Voltage Source Converter(VSC)-HVDC Technology

The core component used in the voltage source converter (VSC) technology is the transistor such as the Insulated Gate Bipolar Transistor (IGBT) [25]. Figure 2.7 depicts the equivalent circuit of the VSC-HVDC system. LCC-HVDC technology has dominated the HVDC transmission system due to its high voltage rating, efficiency, and low cost. However, LCC-HVDC technology utilising thyristors at line frequency is at risk for commutation failures caused by AC-side converter faults. [26]. In particular, these failures can cause a substantial reduction in voltage on the AC system, which is linked to the LCC-HVDC transmission system [26]. Therefore, the AC system linked to the LCC-HVDC transmission system must be stable in order to prevent AC system failures, which can cause a substantial interruption to the voltage waveform [26].

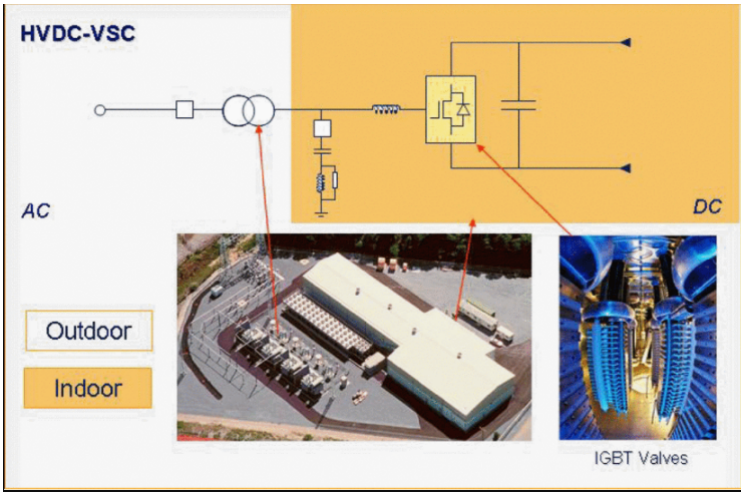

FIGURE 2.7: VSC-HVDC System [22]

Thus, the VSC-HVDC technology has been developed to compensate for the shortcomings of LCC-HVDC technology. Even though VSC-HVDC technology still shows

lower performance for efficiency and power capacity than LCC-HVDC technology, the improved controllability of VSC-HVDC technology is suitable for weak AC systems and offshore networks [26]. In LCC-HVDC technology, the switch can only be turned on, and the next current must go through zero for the switch to reset to the off state. VSC-HVDC technology, in contrast, utilises electrical switches with both "on" and "off" functions [25]. The voltage source converter utilises the pulse width modulation (PWM), which can control both the phase and amplitude [27]. Consequently, controlling the phase and amplitude enables independent regulation of active and reactive power and enhances controllability of voltage and frequency [27].

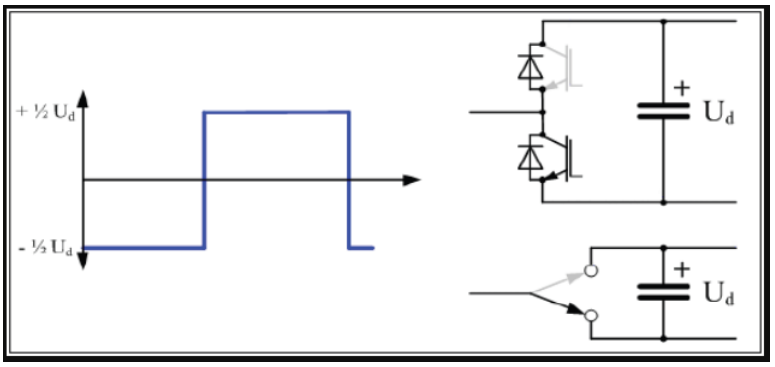

FIGURE 2.8: Two-level VSC-HVDC System [21]

VSC-HVDC technology starts with a two-level converter, and it has switching equipment to produce two levels of voltage($+\frac{1}{2}\ U_{dc}$ and $-\frac{1}{2}\ U_{dc}$) complementarily on the AC output of the converter as shown in Figure 2.8 [21]. This complementary function allows only one switch to be turned on at a time, while the other remains in an off-state because turning both switches on simultaneously would result in a capacitor short circuit across the DC link. Then, this may harm the switching device in the converter due to the over-current [21].

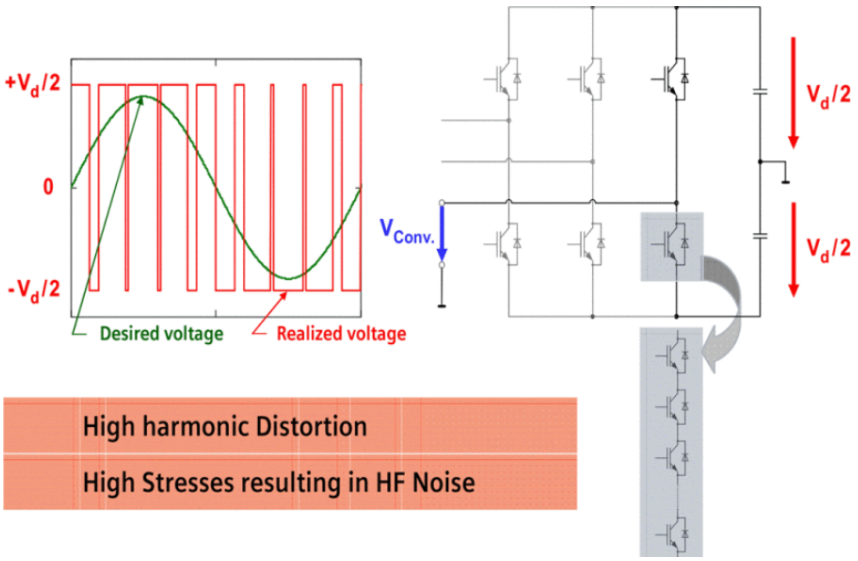

FIGURE 2.9: The Principle of Two-Level Converter [28]

Figure 2.9 shows that the PWM pulse package generates the converter voltage, but it is somewhat different from the desired voltage (green line), so more filters are required to obtain a clean sinusoidal wave [28]. The initial VSC-HVDC technology has been developed based on two or three levels of voltage source converters via high frequency (1-2 kHz) PWM, but this causes a high rate of converter losses, which is up to 2-3% [27]. The PWM mechanism demands the switch be operated "on and off" numerous times per cycle. Therefore, this high switching frequency leads to the low efficiency of the overall transmission of the two-level converter in comparison with LCC-HVDC technology [21]. Consequently, this high switching frequency reduces the overall transmission efficiency of the two-level converter in comparison to LCC-HVDC technology [21]. The conventional two-level or three-level converter with PWM switches the full DC voltage in large steps, leading to high harmonic distortion and increased transient stress [27]. Notably, high transient stress can result in high-frequency noise [27]. Therefore, in VSC-HVDC technology, reducing harmonic distortion and improving the efficiency of voltage source converters is achieved through the use of multi-level converters, starting with the three-level converter [21].

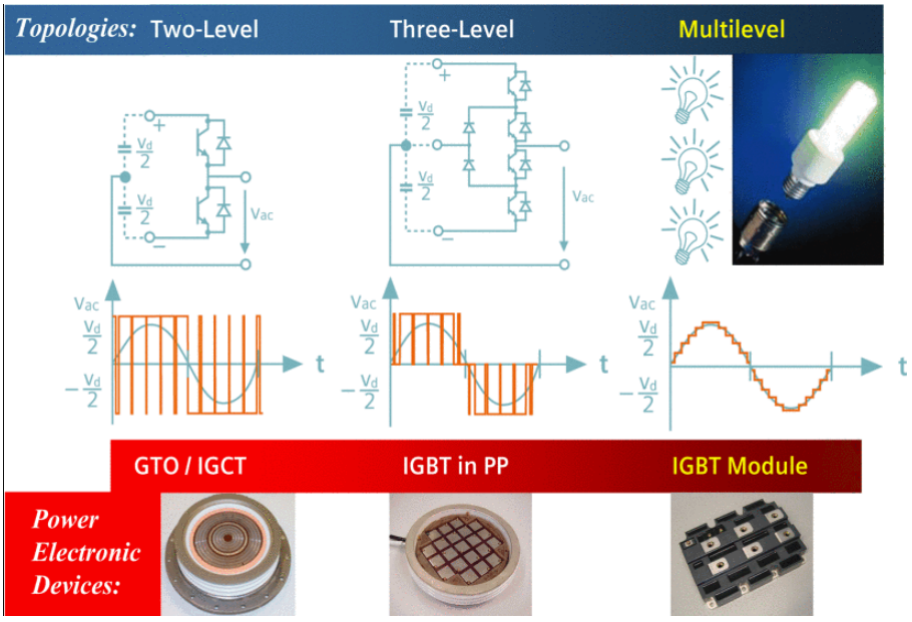

FIGURE 2.10: VSC with Different Levels [28]

Figure 2.10 represents the different levels of the VSC-HVDC system. Producing ac voltage from a large number of smaller voltage steps can reduce the large voltage steps with respect to PWM operation and this finer gradation can lower harmonic proportions [6], [28]. Then, this technique can be used in multi-level converters. Figure 2.11 shows that the ratio of converter modules regulates the ac bus voltage. Regulating only two voltage levels enables it to obtain the desired ac bus voltage without operating all semiconductors simultaneously [6]. This method can achieve a relatively lower switching frequency, resulting in lower losses in comparison with two-level or three-level converters [6], [28]. Thus, multi-level converters function as the controllable voltage source

via many discrete voltage steps, which generate the desired ac voltage with adjustable magnitude and phase angle at the ac terminal [6]. LCC-HVDC technology inevitably requires many reactive compensators and ac filters, but a relatively lower number of devices are necessary for VSC-HVDC technology. Thus, it can accomplish low footprints [6].

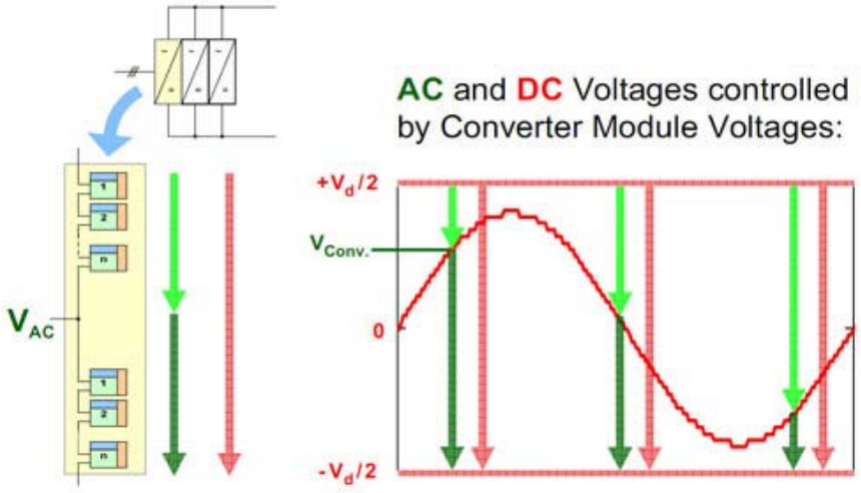

FIGURE 2.11: Voltage Control for VSC-HVDC Multi-Level [6]

Despite the advantages of VSC-HVDC technology, there are still disadvantages to overcome. Typically, VSC-HVDC technology, particularly multi-level, needs a larger number of semiconductors compared to LCC-HVDC technology [19]. VSC-HVDC technology typically requires higher costs because the unit cost of an IGBT in VSC-HVDC technology is higher than that of a comparable thyristor in LCC-HVDC technology [19]. IGBT switches and modules have a lower power capacity than thyristors, which demand more power for electronic devices [19].

2.1.4 LCC-HVDC vs VSC-HVDC

HVDC power transmission systems are recognised as the technology of the next generation due to their unique advantages over HVAC. Submarine power transmission is made possible by HVDC technology, which is more cost-effective and technically superior to HVAC technology over distances greater than $600-800$km [19]. As mentioned previously, HVDC technology is mainly classified into two techniques: LCC-HVDC and VSC-HVDC. LCC and VSC technologies each have benefits and drawbacks, so the application of HVDC technology requires careful investigation. The following information, Table 2.1, is a comparison between LCC-HVDC and VSC-HVDC.

TABLE 2.1: LCC-HVDC vs VSC-HVDC [21]

LCC-HVDC	VSC-HVDC
Based on the thyristor	Based on IGBT
The semiconductor can accept voltages of either polarity	Current in either direction can be accepted
High overload ability	Low overload ability
AC and DC harmonic filters are required to eliminate distortion and harmonics	It does not require a filter because it creates harmonics at an insignificant level
Reactive power control efficiency is low	Reactive power control efficiency is high
It requires a large space, which dominated by harmonic filters	It requires much less space compared to LCC technology
Reversing power direction can be achieved by changing the polarity of the voltage	Reversing power direction can be achieved by changing current direction
It is capable of accepting high voltages up to $\pm$1100kV	It is capable of accepting high voltages up to $\pm$500kV
Most LCC technology is used for a long-distance bulk power transmission	VSC technology is frequently used for power transmission from remote areas where renewable energy exists such as offshore wind farm

2.2 HVDC Converter Transformer

The demand for electric energy is soaring dramatically worldwide. Since power sources located near the consumption centre are primarily being utilised, research is underway to efficiently transmit electricity from remote renewable energy sources [29]. The high efficiency of HVDC technology facilitates to transfer of a large amount of power over long-distance. The HVDC converter transformer is a critical electric appliance that enables effective and reliable power transmission and distribution [29].

As depicted in Figure 2.12, HVDC converter transformers are heavy and complicatedly designed because they must withstand AC and DC electric fields simultaneously [2]. Furthermore, the effectiveness of the HVDC transmission system is heavily reliant on HVDC converter transformers. The most crucial role of the HVDC converter transformer is involved in the voltage transformation between AC supply and the HVDC transmission system and large tap ranges, which contain small steps, can provide essential adjustments in the voltage supply [30]. To further improve HVDC technology,

the next generation power grid, it is vital to understand the HVDC converter transformer thoroughly.

FIGURE 2.12: HVDC Converter Transformer (ABB) [29]

2.2.1 Electric Field Characteristics in HVDC Converter Transformer

In contrast to conventional HVAC transformers, HVDC converter transformers operate under significantly complex conditions with AC, DC, and AC-DC combined stresses affecting the valve windings [31]. Therefore, the appropriate insulation technique is necessary to maintain the high efficiency and reliability of the HVDC converter transformer [32]. Figure 2.13 illustrates the basic insulation structure of the HVDC converter transformer.

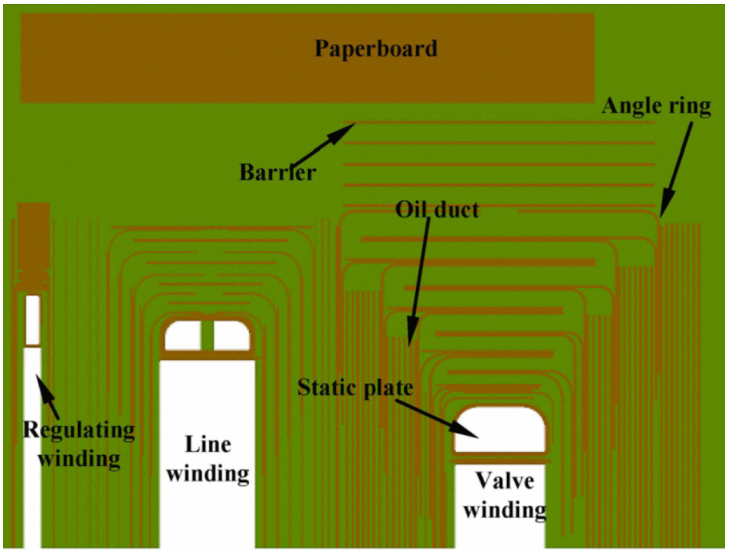

FIGURE 2.13: Basic Insulation Structure of HVDC Converter Transformer [8]

The primary insulating materials of the HVDC converter transformer are mineral oil and paper. Particularly, under DC stress, the electric field in insulating materials can be enhanced in a specific region due to space charge accumulation [31]. This enhanced electric field may accelerate the degradation of insulation materials, which can lead to a premature breakdown [31]. Insulating materials, such as transformer oil and cellulose paper, are used in both HVDC converter transformers and conventional transformers. However, the distribution of DC field characteristics significantly differs from AC conditions [33]. Figure 2.14 depicts the typical voltage application in HVDC systems, and Figure 2.15 represents electric field distribution under different voltage conditions.

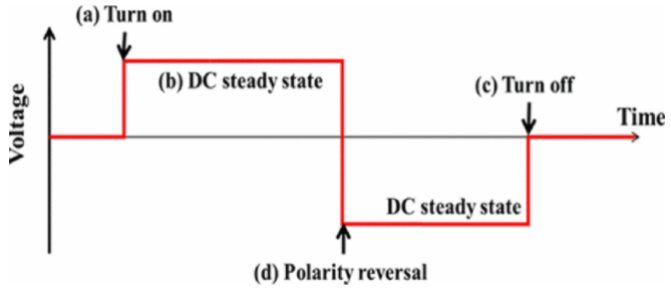

FIGURE 2.14: Voltage Applications in HVDC System [34]

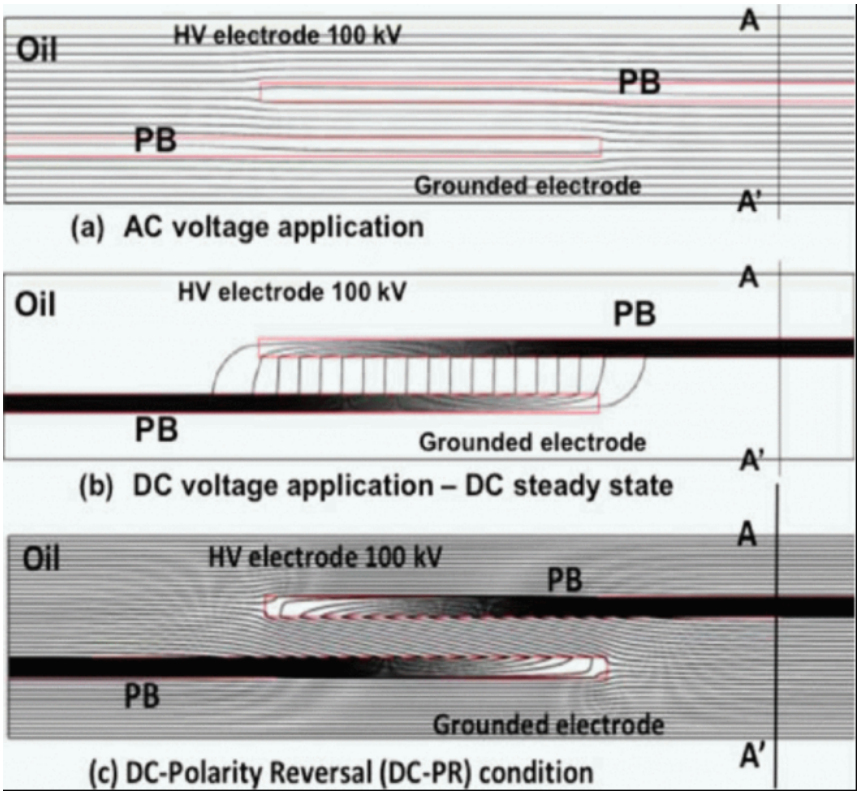

FIGURE 2.15: Electric Field Distributions with Different Voltage Condition: (a) AC Voltage Application, (b) DC-SS (steady state), (c) DC-PR (polarity reversal) [34]

As shown in Figure 2.15, electric fields tend to be uniformly distributed under the AC condition, while electric fields tend to be concentrated in a specific region under the DC-SS (steady state) condition [34]. The accumulated charges at DC-SS prior to the

DC-PR (polarity reversal) operation can cause a high electric field under DC-PR [34]. Polarity reversal remains restricted to LCC-HVDC due to its controllability constraints. Consequently, the electric field distribution at DC-SS before DC-PR operation may be essential to understanding the electrical insulation performance of oil and paper insulation systems [34].

2.3 Insulation System of HVDC Converter Transformer

The HVDC converter transformer plays a critical role in the power transmission system, and its efficiency has a significant impact on the overall performance of the system. The large transformer, like the HVDC converter transformer, is costly and complicatedly designed [35]. Therefore, the transformer condition should be carefully monitored to ensure high efficiency and longer service life [35]. Although there are many different factors involved in monitoring the condition of a transformer, special care needs to be given to the insulation system [35]. Also, appropriate insulation technology for active parts of the transformer is indispensable for safe and reliable operations [35].

During transformer operation, the insulation system inside the tank inevitably undergoes a degradation process such as thermal ageing, oxidation, and hydrolytic impact [35]. Paper and transformer oil are the critical materials that comprise the insulation system in the transformer. Degradation factors affect the electrical, chemical, and mechanical properties of papers and transformer oils. Thus, this section discusses the main insulating materials used in power transformers.

2.3.1 Cellulose

Cellulose is one of the primary insulating materials in the power transformer. Paper and pressboard are manufactured from cellulose for the insulation system, and cellulose has been widely accepted for power transformers due to its renewability and economic reasons [36].

The moisture adsorption curves in Figure 2.16 show how cellulose has a considerable hygroscopic characteristic. Despite having a decent dielectric strength and low dielectric loss, hygroscopic characteristic causes issues because moisture can negatively affect the insulation's capabilities. Typically, cellulose may retain between 4 and 8% moisture in the relative humidity range of 30 to 70% at room temperature (20 to 25°C) [37]. However, a freshly built transformer's insulation moisture content should be less than 0.5% to prevent the loss of dielectric strength and slow down the paper degradation and ageing [37]. Hence, the cellulose must be kept in a dry condition and impregnated with transformer oil to fill the voids, preventing partial discharge [36], [38]. The paper

functions as an electrical insulator, whereas the pressboard possesses both good electrical insulating properties and excellent mechanical strength. Due to this combination, power transformers with greater rated voltages can be manufactured [39].

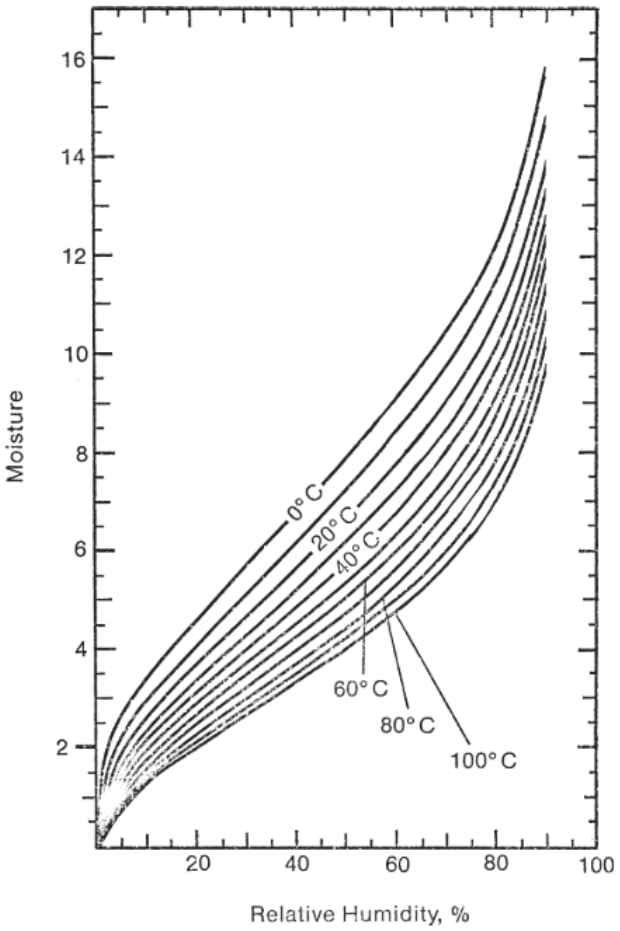

FIGURE 2.16: Moisture Absorption in Paper [36]

Figure 2.17 represents the paper and pressboard for the power transformer. Paper and pressboard are manufactured from wood through the Kraft chemical process, and this is why the paper is also called Kraft paper [36]. Wood for paper and pressboard can be either softwood or hardwood [36]. Wood is a natural resource, which includes a flexible tube of cellulose combined with lignin [36]. Lignin is a brownish aromatic polymer, but most lignin is eliminated from the wood through the pulping process [36]. Removing lignin provides high flexibility for papers and reduces impurities that can lead to discolouration and degradation of the paper [40].

Figure 2.18 depicts the chemical structure of glucose. Through glycosidic bonds, anhydroglucose forms a linear polymer that is called cellulose as described in Figure 2.19. The degree of polymerisation (DP) is the terminology to indicate the number of monomer units in the polymer structure, so the DP of cellulose can be defined as the average number of connected glucose rings [35]. This can be simply described as $[C_5H_{10}O_5]_n$, where n represents the degree of polymerisation [36].

FIGURE 2.17: Paper and Pressboard for the Power Transformer [36]

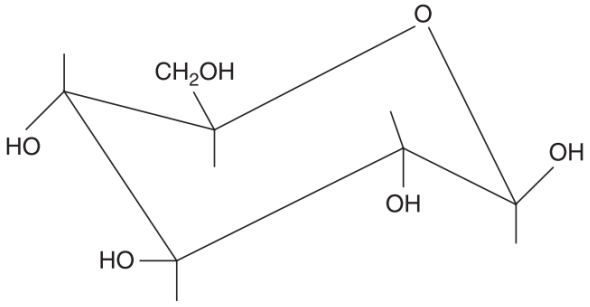

FIGURE 2.18: Chemical Structure of Glucose [35]

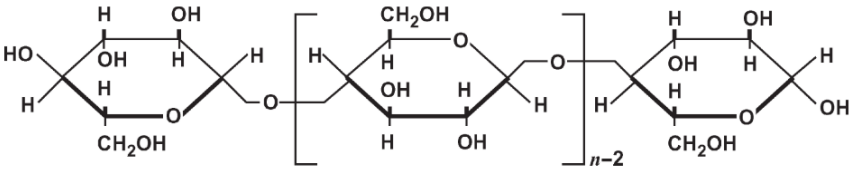

FIGURE 2.19: Chemical Structure of Cellulose Polymer [36]

Kraft paper has an initial DP value between 1100 and 1200, and mixed pulp cellulose has a higher initial DP value in the range of 1400 to 1600 [36]. Nonetheless, degradation factors such as thermal impact reduce the value of DP in the Kraft paper through the depolymerisation process [41]. Then when the DP value reaches the range of 100 to 200, the Kraft paper is considered the end of service life [41].

In the insulating paper's chemical structure, anhydroglucose units are connected via glycosidic bonds [41]. Within these compounds, the presence of multiple anhydroglucose rings results in the formation of two weak points, which are $C-O$ molecular bonds and glycosidic bonds [41]. In contrast to the hydrocarbon bonds in transformer oil, these bonds have lower thermal stability [41]. Thus, paper decomposition produces

CO, CO_2, hydrocarbon byproducts, water, and Furan compounds during thermal ageing [41].

The ageing process in Kraft paper and pressboard deteriorates the dielectric capability and mechanical strength together [41]. However, compared to the liquid dielectric, it is difficult to replace Kraft paper and pressboard from the power transformer, so condition monitoring for cellulose materials is vital for predicting the lifetime of the power transformer [41].

2.3.2 Mineral Oil

Transformer oil is a critical liquid insulator for oil-filled power transformers, similar to solid insulating materials [42]. Mainly, Kraft paper is impregnated with the transformer oil that fills the voids to remove the air gap [42]. This procedure can enhance the electrical insulation strength and improve heat dissipation capability by circulating oil in transformers [42].

The mineral oil is produced by refining collected hydrocarbons acquired from the distillation of petroleum crude stock [43]. The boiling range, type, and degree of refining process must be carefully selected for mineral oils to satisfy the specific requirements of a power transformer [43]. In the refining process, paraffin-based crude oil can be obtained through normal pressure, and naphthenic-based crude oil can be obtained from very low pressure [44]. Low pressure can lower the boiling range, which results in the separation of heavier molecules [44]. Usually, the refining process is implemented under 350°C to prevent thermal degradation [44].

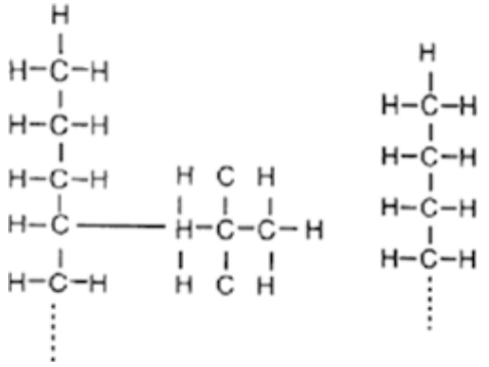

FIGURE 2.20: Chemical Structures of the Paraffinic Molecule [45]

Mainly, the mineral oil is produced from paraffinic-based crude oil or naphthenic-based crude oil, and these crude oils consist of hydrocarbons [46]. As shown in Figure 2.20, the straight-chain and branched-chain are two types of paraffinic molecules [44]. Unfortunately, paraffin-based oil has poor fluidity at low temperatures because it is easily crystallised [46]. Thus, paraffinic-based oil is not suitable for the power transformer in

a low-temperature environment [46]. Also, the limited solubility of paraffinic-based oil for water and oxidation products can lead to the precipitation of free water and sludge [45]. However, recently, isoparaffinic oil has regained attention due to its high purity and relatively high boiling point in synthetic hydrocarbon solvents.

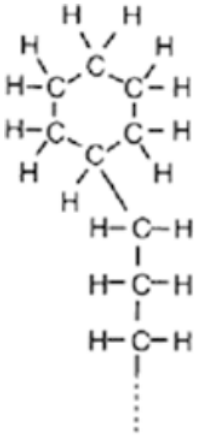

FIGURE 2.21: Chemical Structure of the Naphthenic Molecule [45]

Figure 2.21 depicts the chemical structure of the naphthenic molecule. Naphthenic-based oil consists of cyclic alkanes, and this ring structure has mostly 5-7 carbon atoms [44]. Unlike paraffinic-based oil, naphthenic-based oil has excellent lower temperature properties, so it is suitable as a transformer oil in the freezing environment (e.g. -40°C) [46]. Furthermore, at around 100°C, the naphthenic-based oil shows lower kinetic viscosity than the paraffinic-based oil, which indicates that the naphthenic-based oil has a better heat dissipation capability at high-temperature [46]. The naphthenic-based oil shows decent solubility that dissolves oil sludges produced by degradation factors such as high temperature, electric stresses, moisture, and metal catalysts [46]. This prevents oil sludges from accumulating on insulating materials, oil ducts, or cooling fins [46]. As a result, the naphthenic-based oil can inhibit local overheating that may be caused by sludges in the vicinity of the winding, so the longer service life of the power transformer can be expected [46]. Despite the various advantages of naphthenic-based oil, it is scarce because it consists of only about 2-3% of the total crude oil [46]. The paraffinic-based and naphthenic-based oils do not show a distinct difference in the dielectric properties [46].

Both paraffinic and naphthenic oils also include aromatic compounds [44]. Figure 2.22 describes the chemical structure of the aromatic molecule. Aromatic molecules typically contain an unsaturated benzene ring structure [45]. The physicochemical properties of aromatic molecules are significantly different from those of naphthenic molecules, but their dielectric constants are similar [44]. In aromatic molecules, the benzene rings partially contain double bonds, which make them more reactive than single bonds, so the solubility of these aromatic structures is the highest [47].

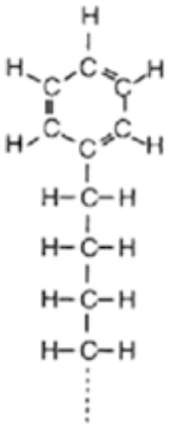

FIGURE 2.22: Chemical Structure of the Aromatic Molecule [45]

Aromatic compounds are classified as the most highly refined dielectric liquid for the power transformer [44]. Therefore, an adequate amount of aromatic compounds can improve the stability of the transformer oil during operation because most natural oxidation inhibitors are aromatic [44], [45]. However, if an excessive amount of aromatic compound is applied to the power transformer, it reduces the impulse strength and the dielectric performance of the oil [45]. Since each mineral oil is chemically and physically different, the mineral oil selection must be made according to the surrounding environmental conditions and the service purpose.

2.3.3 Natural Ester Liquid

Despite the excellent dielectric properties and relatively low costs, mineral oil has disadvantages such as high fire risk and low biodegradability. Also, since mineral oil is produced from a limited amount of crude oil, natural ester liquid is getting attention as an alternative. Natural ester liquid is the dielectric liquid and coolant produced from vegetable resources such as soybean, sunflower, and rapeseed [48], [49]. Figure 2.23 shows the biodegradability of different types of transformer oil. As well known, mineral oil is a toxic substance, and it has a low biodegradability, which is seriously harmful to the surrounding environment when the leakage occurs from the power transformer [49].

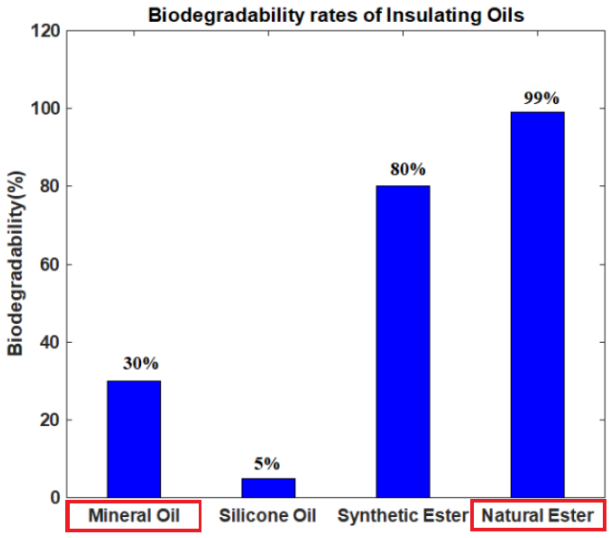

FIGURE 2.23: Biodegradability for Different Types of Transformer Oil [49]

However, natural ester liquid is an environmentally friendly oil with high biodegradability [49]. Mineral oil is always exposed to a fire hazard due to the low fire point (160°C), which requires additional fire safety equipment [42].

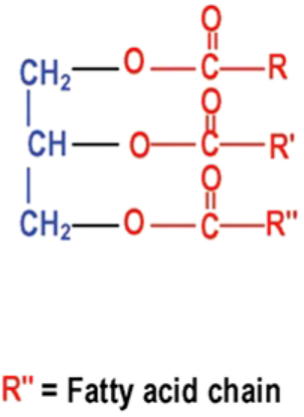

FIGURE 2.24: Chemical Structure of the Natural Ester (Triglyceride) [45]

Figure 2.24 illustrates the chemical structure of the natural ester [50]. The natural ester liquid is composed of a triglyceride structure, in which three fatty acids are attached to one glycerol [51]. However, the chemical and physical properties of the natural ester liquid are significantly affected by the degree of saturated fatty acids and unsaturated fatty acids in triglyceride [51]. When natural ester liquid contains a higher concentration of saturated fatty acids, it has a higher viscosity due to chemically high stability [51]. Conversely, when natural ester liquid contains a higher concentration of triple unsaturated fatty acids, which tend to have more oxidation, they have lower viscosity due to chemically low stability [49]. Thus, natural ester liquid, containing a high concentration of single unsaturated fatty acids, is appropriate as transformer oil [49]. Natural ester liquid has excellent moisture tolerance, which aids to extend the service life of

cellulose-based solid insulation [52]. As a highly polar molecule, water has a strong affinity for other polar molecules [53]. This is because mineral oil has non-polar properties since most polar substances are removed during the refining process, whereas natural ester liquid has polar properties due to the presence of ester linkages [47], [53]. Thus, these ester linkages can attract water molecules, whereas mineral oil faces difficulty in attracting these polar molecules [53]. At 23 °C, mineral oil can dissolve approximately 55ppm of water, while natural ester liquid can dissolve approximately 1100ppm of water [53].

Despite the advantages of natural ester liquids, several disadvantages still exist. First, it requires high production costs and is rapidly oxidised when exposed to air [54]. Second, although natural ester liquids are commercially available for high-voltage transformers (e.g. 420kV), their application is still limited to AC transformers [55]. Thus, their performance in HVDC power transformers is still inexperienced [54].

2.4 Space Charge Characteristics in Dielectrics

The rapid increase in energy demand has led to the necessity for HVDC transmission systems, and dielectric materials must meet special requirements under HVDC conditions for reliable and sustainable operation. Unfortunately, under DC conditions, space charges tend to accumulate in dielectric materials. This phenomenon causes local electric field enhancement as well as accelerated degradation of dielectric materials. This chapter discusses the principles of space charge dynamics, space charge measurement, and factors that affect space charge characteristics leading to degradation.

2.4.1 Overview of Space Charge in Dielectrics

When a high electric field is applied to dielectric materials, space charges are generated inside the materials, caused by charge injection from the electrodes or ionisation of impurities [56]. Notably, immobilised charge carriers within the dielectric material strengthen the electric field in specific regions, leading to deterioration and premature breakdown of dielectric materials [56].

A polarisation mechanism of space charges takes place in the dielectric material under the DC stress [57]. Bound charge carriers and free charge carriers are estimated to contribute to this mechanism [57]. The bound charge carriers mainly contribute fast and relaxing polarisations, while free charge carriers mainly contribute to migrating and space charge polarisations [57]. However, both bound and free charges still influence space charge accumulation [57]. Since many factors affect the space charge in dielectric materials, it is still difficult to accurately analyse space charge behaviours. Nevertheless, the bipolar charge transport (BCT) model aids in understanding better space charge dynamics.

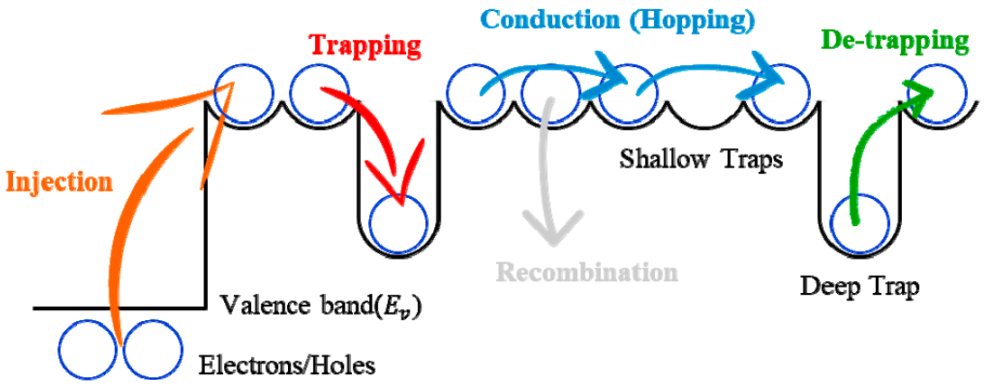

FIGURE 2.25: Bipolar Charge Transport (BCT) Model [58]

Figure 2.25 shows the process of the bipolar charge transport model. In the BCT model, there are five different charge transfer processes, which are injection, conduction, trapping, de-trapping, and charge recombination [58]. Then, four different charge carriers such as mobile electrons, mobile holes, trapped electrons, and trapped holes are involved in the charge transfer processes of the BCT model [58]. When the dielectric material is exposed to the DC electric field, charge injections occur between the electrode and dielectric [58]. Once charges are injected from the electrode, they tend to travel to the opposite electrode, which is called the conduction process based on the hopping mechanism [58]. The hopping mechanism indicates that mobile carriers have enough energy to pass by shallow traps [58]. However, some mobile carriers are caught in deep traps [58]. Some trapped charges may stay in deep traps or escape from deep traps to rejoin the conduction process [58]. Also, electrons and holes can be recombined, and these recombined neutrons do not contribute to the space charge dynamics due to the absence of charge carriers [58].

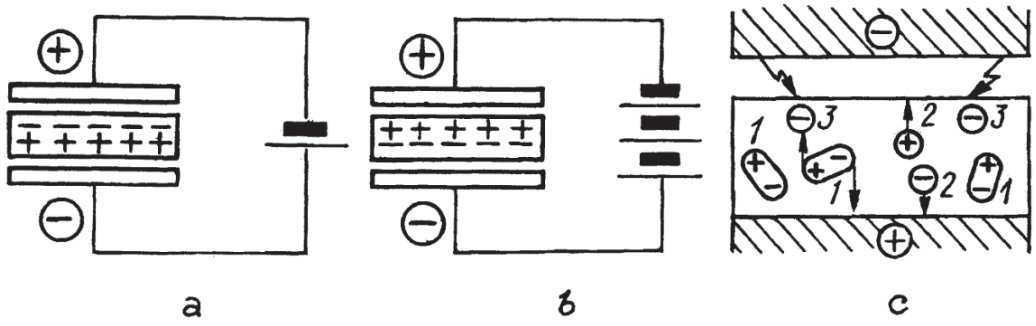

FIGURE 2.26: (a) Heterocharges, (b) Homocharges, and (c) Different Types of electric charges: 1- orienting and oriented dipoles, 2-shifted charges in a dielectric material, 3-injected charges from the electrode [59]

Figure 2.26 represents two different charges when the electric field is applied to the dielectrics. Heterocharges are produced by charge polarisation in the dielectric material, which is initiated by dipolar orientation, ionic polarisation, and space charge shift [59]. Also, charges with high mobility can be heterocharges, leading to positive charge accumulation near the cathode [57]. In contrast, homocharges occur due to the rapid charge injection of electrons from the cathode [57]. The charge injection increases the amount of charge in insulating materials [57]. Continuous homocharge injection increases the amount of charge inside the dielectric material, and injected homocharges tend to be accumulated in the vicinity of the electrode, which has the same polarity [57].

2.4.2 Space Charge Measurement

- Destructive Technique

The initial space charge measurement has been implemented through the destructive technique by using charge powders [60]. The process of this technique is that the dielectric material is initially prepared in the form of a flat plate, and the powder, which contains charge polarity, is placed on the dielectric material [60]. The powder is stuck to the surface charge of the dielectric for detecting charges [60]. In other words, lead oxide (PB_3O_3, red colour) powder is applied to verify positive charges, and sulphur (S, yellow-white colour) powder is applied to verify negative charges [60]. Combining the two-dimensional (2-D) results from each powder can provide the original three-dimensional (3-D) space charge profile [60]. However, this technique has apparent drawbacks in that the dielectric sample must be physically damaged by cutting, which affects the space charge distribution and provides only qualitative information [60]. Therefore, the non-destructive technique has been introduced to overcome the limitations of the destructive technique.

- Non-Destructive Technique (Pulsed-Electroacoustic Method)

There are several different types of non-destructive techniques, such as thermally stimulated current (TSC), pressure wave propagation (PWP), laser-induced pressure pulse (LIPP), and pulsed electroacoustic (PEA) methods. This thesis introduced the PEA method to acquire space charge profiles [61]. Tatsuo Takada introduced the Pulsed electroacoustic (PEA) method in 1987, and it is one of the representative non-destructive techniques for measuring space charge profile. The principle of the PEA method is based on the one-dimensional (1-D) Coulomb force law, and the overall diagram of the PEA method is described in Figure 2.27 [62].

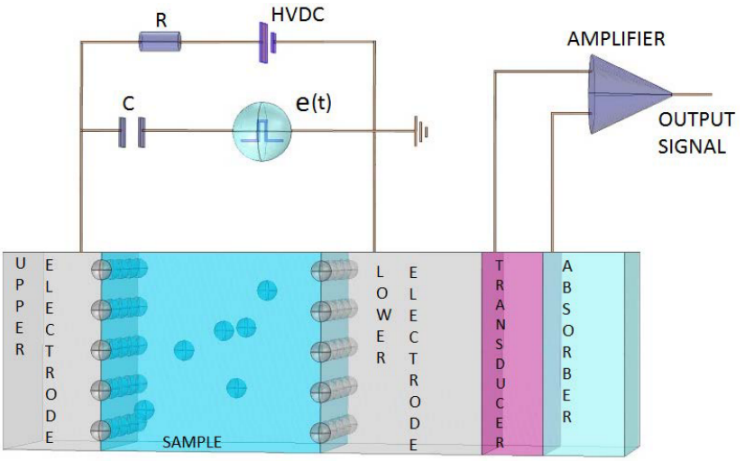

FIGURE 2.27: Overview of the PEA Method [62]

In general, the PEA method contains a HVDC supply, which can generate a high electric field on dielectric samples, and a pulse generator $e(t)$, which produces an acoustic wave via interaction with charges [62]. Then, the acoustic signal generated from charges is converted into a voltage signal in a piezoelectric transducer, which is based

on polyvinylidene fluoride (PVDF) [62]. In the final step, the voltage signal is amplified through the amplifier, and a PC receives the output voltage signal for data analysis [62].

The PEA method does not require any physical damages on dielectric materials. Also, unlike the destructive technique, the PEA method provides both quantitative and qualitative analysis. Since the PEA method is the primary technique for this research, further details will be discussed in Chapter 3.

2.4.3 Major Degradation Factors on Space Charge Characteristics

Paper and oil are widely used as the main dielectric materials in the HVDC power transformer. For high efficiency and reliability of the power transformer, a high level of dielectric performance must be maintained, but the degradation of the dielectric material is inevitable during the operation. Therefore, investigating the main degradation factors associated with space charges is essential for understanding the oil-impregnated paper insulation system.

The main degradation factors are as follows:

- Thermal Stress

The heat is generated during the transformer operation. The continuous thermal stress accelerates the degradation of cellulose materials such as paper and pressboard. As a result, the electrical, chemical and mechanical properties of cellulose materials are significantly affected [63]. In particular, thermal stress reduces the mechanical strength of the cellulose materials over time, as shown in Figure 2.28.

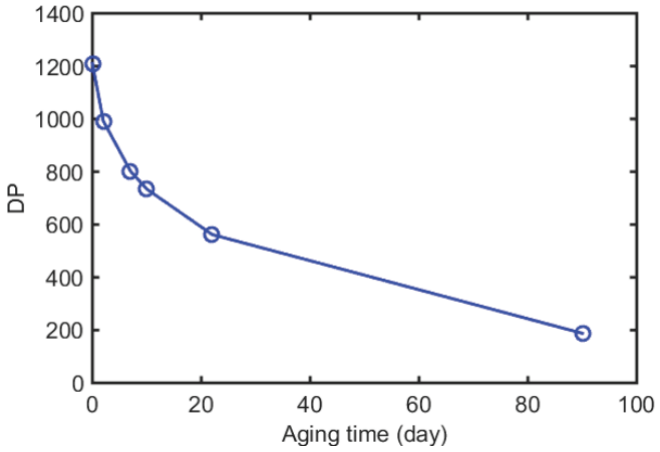

FIGURE 2.28: DP value of Insulating Paper with Aging Time (aged at 130°C) [64]

Cellulose is a chain of alpha-D-glucose units, and the number of monomer glucose units represents the degree of polymerisation (DP) and newly manufactured paper shows the number of DP typically between 1100 and 1600 [37]. Thermal ageing of cellulose includes various factors, which can reduce the DP via the depolymerisation process. These processes can occur through the breakage of linkages by hydrolytic decomposition and the breakup of the ring structure, resulting in the release of CO, CO2, and water [37]. Thermal ageing reduces the DP and mechanical strength of paper, resulting in increased brittleness and darker colours [37]. As a result, the DP value may rapidly decrease below 200, which is considered the end of service [65]. A lower DP

value indicates more mechanical deterioration of cellulose caused by heat, oxygen, water, and acids [65]. This generates polar by-products, elevating electrical conductivity, permittivity, and loss factor but weakening dielectric strength [65].

- Moisture

It is well known that the deterioration of the cellulose material is affected by the amount of oxygen or water during the power transformer operation. Moisture is the primary factor for the degradation of cellulose, and it contributes to reducing the mechanical strength by dissociating cellulose polymer chains [66]. Unfortunately, the moisture is generated as a by-product during the ageing process of cellulose, resulting in the high moisture concentration in the cellulose [66]. According to [67], as the moisture concentration increases, the space charges tend to penetrate deeper into the oil-impregnated paper as shown in Figure 2.29.

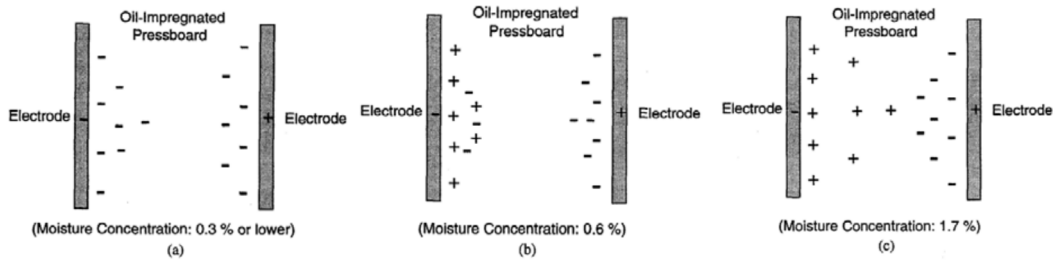

FIGURE 2.29: The Characteristic of Space Charge in Oil-Impregnated Pressboard (1mm) with Different Moisture Concentrations (steady-state condition) at DC 15kV/mm [67]

Thus, the moisture has a severe effect on the space charge formation, which results in electric field enhancement in a particular region as depicted in Figure 2.30 [67].

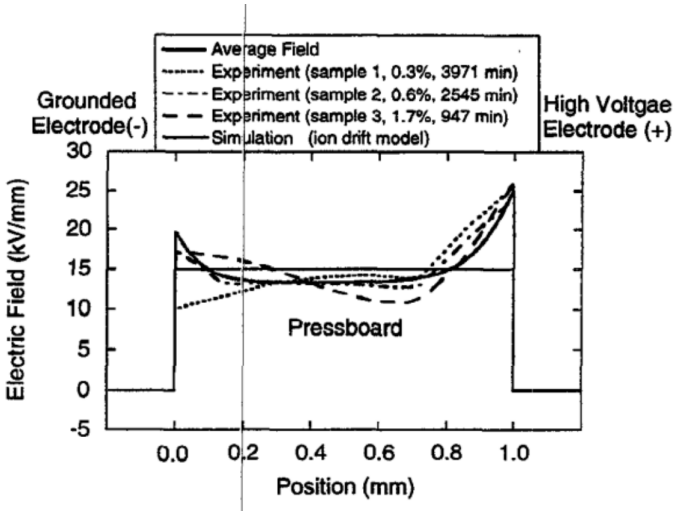

FIGURE 2.30: The Electric Field Distribution in Oil-Impregnated Pressboard (1mm) with Different Moisture Concentrations (steady-state condition) at DC 15kV/mm [67]

- Acidity

The acid hydrolysis also contributes to the insulating paper degradation mechanisms in the power transformer [68]. Oxidation, carboxylic acids, and water affect the degradation of cellulose insulating materials of the transformer [68]. The moisture catalyses the acid hydrolysis through the dissociation process in the transformer oil [68]. The insulating paper produces moisture during the transformer operation, so the synergy effect of the moisture and acid accelerates the ageing process of the insulation system [68]. Hydrolysis is catalysed exclusively by hydrogen ions from ionised acids, whereas non-ionised carboxylic acids do not contribute to the depolymerisation of cellulose [68]. Therefore, the concentration of H^+ rather than the neutralisation value or the total acid concentration is a significant contributor to increasing the transformer oil acidity [68]. The water contributes to an increase in the H^+ concentration through the ionisation of carboxylic acids in the transformer oil [68]. Low Molecular Weight Acids (LMAs) are more corrosive and hydrophilic, accelerating cellulose degradation compared to High Molecular Weight Acids (HMAs) [69]. This is because LMAs have higher reactivity and solubility, enhancing cellulose degradation more than HMAs [69]. Therefore, the LMA's concentration in the oil is the index closely related to a degradation of the cellulose insulation material.

2.4.4 Space Charge Characteristics of Mineral Oil-impregnated Paper

Currently, mineral oil-paper insulation systems have been used domestically in HVDC converter transformers. While studies on mineral oil-paper systems under DC conditions have been actively studied, studies on natural ester liquid-paper are still insufficient. This section explores existing studies on how various factors affect mineral oil-paper systems with respect to space charge characteristics.

- Effect of Applied Voltage

The strength of the applied voltage is one of the main factors affecting the space charge dynamics within the mineral-oil paper system. Figure 2.31 shows how the intensity of the different voltages affects the space charge dynamics of the three-layer mineral oil-impregnated paper. Tang et al. show that as the applied voltage increases, it is clear that more charges are injected into the bulk sample from both electrodes [70]. Furthermore, the increased voltage improves the charge's mobility, allowing the charges to penetrate deeper into the sample [70], [71].

Figure 2.32 represents the maximum induced charge density at both electrodes after removing DC voltage instantaneously. Under the condition that the sample thickness remains the same, this shows that as the applied voltage increases, the maximum charge

density peaks at the cathode and anode increase due to an increase in the amount of homocharge injection [70].

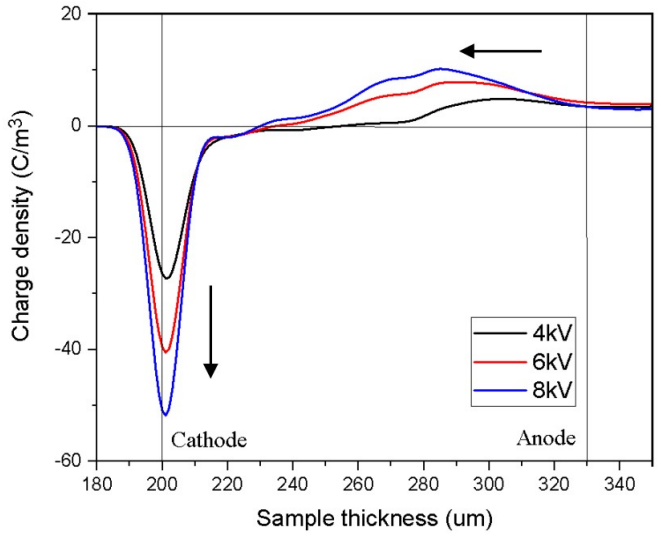

FIGURE 2.31: Effect of Applied DC Field on Space Charge Characteristics (Volts-on for 30 minutes at 20°C, three layers, 130 μm of total thickness) [70]

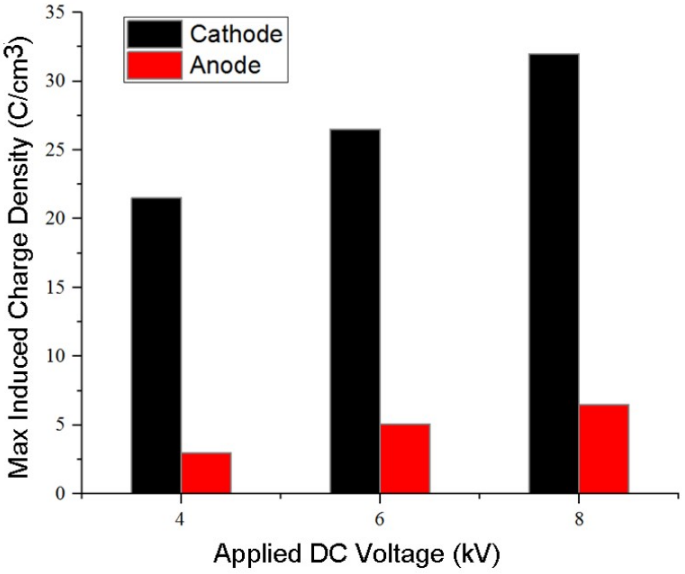

FIGURE 2.32: At 20 °C, the Maximum Induced Charge Density at Both Elctrodes after Instantaneous DC voltage off [70]

- Effect of Moisture

Moisture is the biggest factor in shortening the life of oil-paper insulation systems and most of the moisture is dissolved in oil or absorbed by solid insulating materials. Zhou

et al. explored how different moisture levels affect spatial charge dynamics in oil-paper insulation systems [72]. Different moisture levels were achieved through moisture control of cellulose in [72].

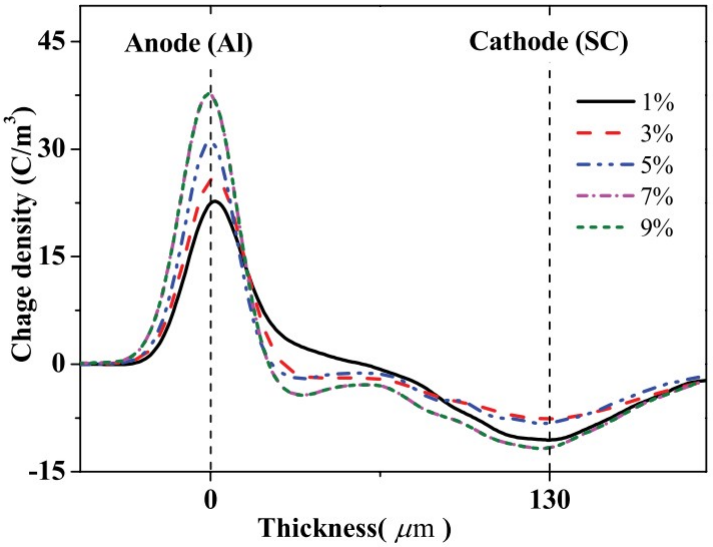

FIGURE 2.33: Space Charge Characteristics of Mineral Oil-impregnated Paper (130 μm) with Different Moisture Levels under 10kV/mm for 30 minutes [72]

In [72], the mineral oil-impregnated papers with five different moisture levels (1%, 3%, 5%, 7%, and 9 %) were measured with the PEA method as shown in Figure 2.33. The result showed that as the moisture content of the paper increased, the amount of space charge injected into the sample increased as well. It is believed that the increase in moisture may have contributed to the increased mobility of the charge [72]. In other words, the increased mobility of the charge due to moisture helped the negative charges travel from the cathode to the anode. As a result, it was shown that when moisture exceeded 3%, hetero charges began to accumulate near the anode. In addition, since the mineral oil-paper insulation system is considered a liquid-solid dielectric, the ionisation process is also likely to have influenced space charge accumulation [72].

- Effect of Thermal Ageing

Thermal ageing is one of the main factors that degrade the oil-paper insulation system. Thermal stress degrades the electrical, chemical, and mechanical characteristics of oil-paper insulation systems. Zou at el. studied the space charge characteristics of mineral oil-impregnated paper (160μm of thickness) regarding the effect of thermal ageing [73]. Thermal ageing for samples was accelerated for 0, 25, and 55 days at 130 °C in [73].

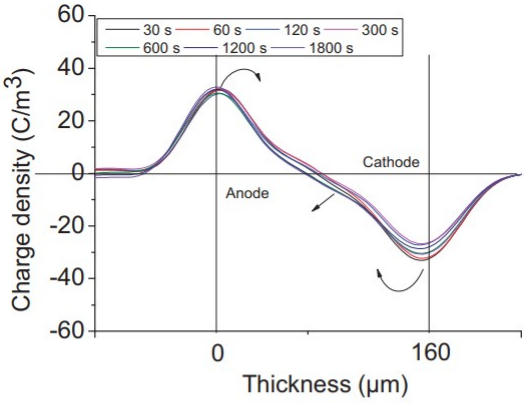

(a) sample aged for 0 day

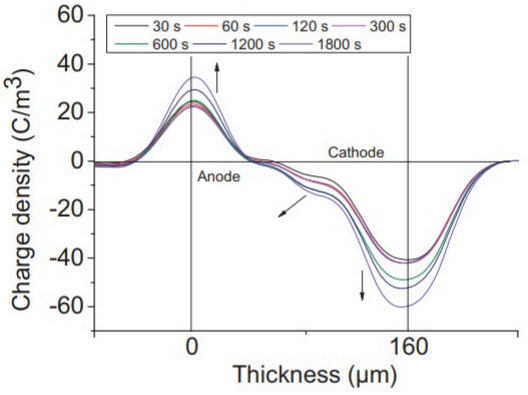

(b) sample aged for 25 days

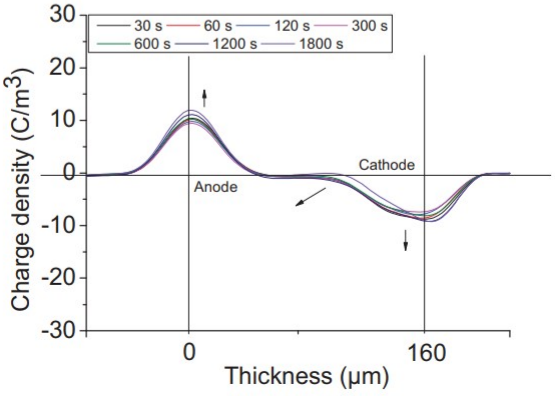

(c) sample aged 55 day

FIGURE 2.34: Space Charge Characteristics of Mineral Oil-impregnated Paper (160 μm) with Different Thermal Ageing Periods under 15kV/mm [73]

Figure 2.34 depicts space charge characteristics of mineral oil-impregnated paper with different thermal ageing times under 15kV/mm. All three samples showed that negative charges were injected from the cathode when the voltage was applied [73]. However, when the sample was thermally aged for 25 days, comparing day 0 and day 55, the negative charges shifted more clearly to the bulk of the sample [73]. Additionally,

[73] explained why no distinct charges were found in the centre of the thermally aged sample for 55 days. Zou at el. argued that it is possible that the negative and positive charges, shifted from both electrodes, were neutralised by recombining with each other [73]. In addition, according to [72], due to the impact of thermal ageing, the threshold voltage of the mineral oil-paper sample decreased, which resulted in more charge injection as shown in Figure 2.35. Figure 2.35. Additionally, the peak value of charge density at the anode decreased due to decreased threshold voltage [72].

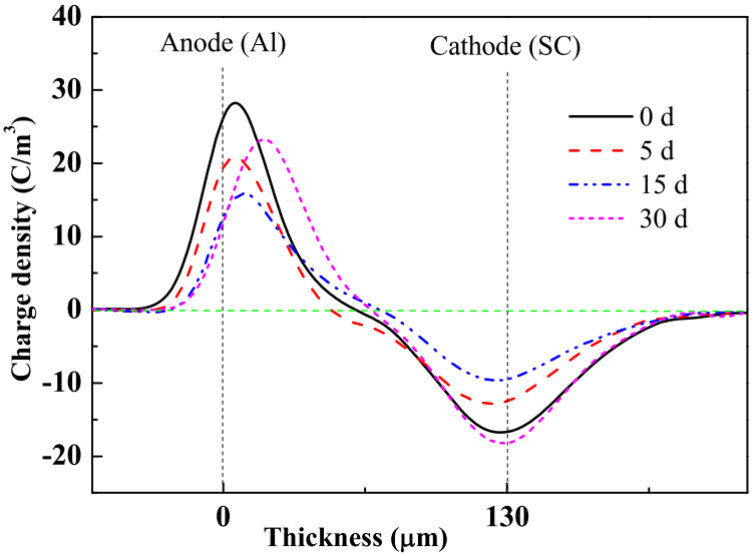

FIGURE 2.35: Space Charge Characteristics of Mineral Oil-impregnated Paper (130 μm) with Different Thermal Ageing Periods under 10kV/mm [72]

Nevertheless, very complex factors such as chemical, physical, and electrical properties are still linked to the thermal ageing of oil-paper insulation systems, and it is difficult to find clear reasons for how they affect space charge properties. Therefore, further research is still required for better understanding.

2.5 Summary

The comprehensive review of existing literature in this chapter has examined HVDC technology, HVDC converter transformer, insulation system of HVDC converter transformer, and space charge characteristics in dielectrics. This chapter looked at different perspectives, theories, and existing experimental studies to give a complete view of the topic.

HVDC technology enables more efficient long-distance power transmission than HVAC systems. For the sustainable operation of HVDC power transmission, HVDC converter

transformers play a crucial role. However, the performance of HVDC technology heavily relies on an electrical insulation system, making the choice of appropriate electrical insulating materials a significant consideration.

Mineral oil has served in HVDC converter transformers for its outstanding dielectric performance and heat transfer capabilities. However, intrinsic weaknesses like limited biodegradability and high flammability still exist. Thus, natural ester liquid is considered a potential substitute to replace mineral oil in HVDC converter transformers, but research on space charge dynamics for natural ester liquid remains insufficient.

Especially, the double layer of natural ester liquid and natural ester liquid-impregnated paper has not been explored yet. Therefore, this thesis investigated the space charge dynamics of the double layer of natural ester liquid and natural ester liquid-impregnated paper by comparing it with mineral oil.

Space charge profiles were measured for a single layer of natural ester liquid-impregnated paper under the impacts of moisture and thermal ageing, respectively. Furthermore, space charge measurements were conducted for the double layer of natural ester liquid-impregnated paper under the influence of moisture. Finally, polarity reversal effects were applied to the double layer of natural ester liquid-impregnated paper for space charge measurements.

Chapter 3

Methodology

3.1 DC Conductivity Test

Conductivity determines the conduction current density of the dielectric material according to the applied electric field [74]. The relationship between conductivity and current density can be expressed as Ohm's Law in Equation 3.1.

$$J = \sigma E \tag{3.1}$$

where J is the surface current density (A/m^2), σ is the conductivity (S/m), E is the electric field (V/m).

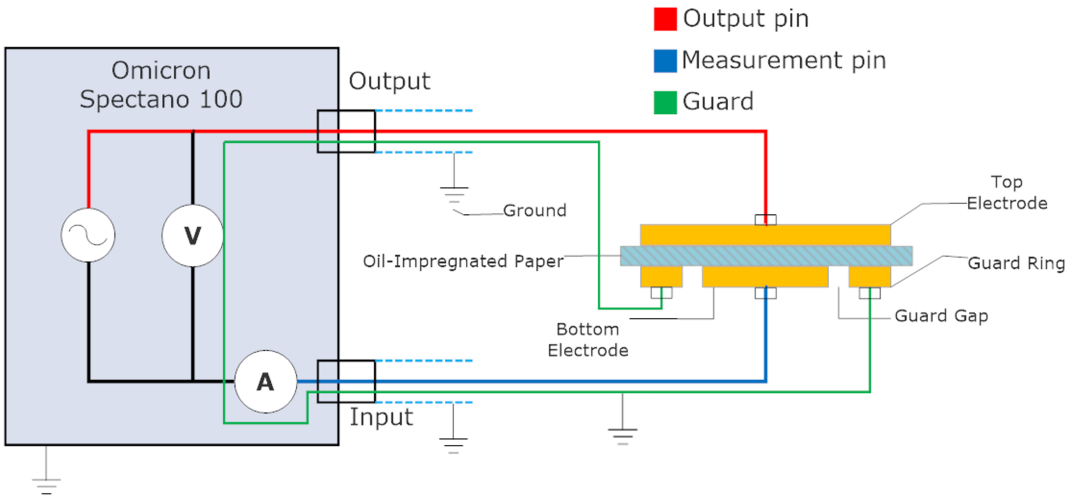

FIGURE 3.1: Connection Diagram for DC Conductivity Measurement

Typically, the dielectric material maintains a low conductivity because the molecules remain intact under the applied electric field [74]. Nonetheless, degradation factors such as water and thermal ageing raise the conductivity of the dielectric material, which

affects the charge transport [74]. the DC conductivity of the dielectric material dominates in low-frequency regions. Thus, the Omicron Spectano 100 has been introduced to measure quasi-dc conductivity. Figure 3.1 illustrates the connection diagram for dc conductivity measurement. The quasi-DC conductivity process indicates that when charge carriers dominate the dielectric material, the dielectric response gradually increases as the frequency decreases.

The conductivity $\sigma(\omega)$ based on the frequency can be expressed as Equation 3.2 [75].

$$\sigma(\omega) = \sigma_{dc} + A\omega^{s} \tag{3.2}$$

where A is constant, $0 < s < 1$. It shows that the conductivity linearly increases as the frequency increases, but dc conductivity σ_{dc} becomes the dominant factor in the low-frequency range [75]. The interfacial polarisation contributes that when $s \simeq 1$, the conductivity $\sigma(\omega)$ based on the frequency has a similar value to DC conductivity σ_{dc} ($\sigma(\omega) \simeq \sigma_{dc}$), which means that the imaginary part of the dielectric permittivity has a slope of -1 at the low-frequency range [76].

The bottom electrode consists of a guard gap and a guard ring that minimises noises from the leakage current. The diameter of the bottom electrode is 30 mm, and the guard gap is 1 mm. Omicron Spectano 100 provides both frequency domain spectroscopy (FDC) and polarisation depolarisation current method (PDC). In particular, the PDC method is much faster than FDC in the low-frequency range. The PDC method has been introduced to measure the dc conductivity of the oil-impregnated paper. Spectano Analyzer software has been used to control the sweeping frequency and the applied voltage. The sweeping frequency from $1.0mHz$ to 99 mHz has been applied, based on 10 sampling points/decade. Then, 200 V_{peak} DC has been applied for the DC conductivity measurement. For the single-layer investigation, the experiment involved measuring a 200 µm thickness $(E = 1kV/mm)$ of oil-impregnated paper. For the double-layer experiment, a 250 µm thickness $(E = 0.8kV/mm)$ of oil-impregnated paper was measured for the DC conductivity.

3.2 Karl Fischer Titrator

As well known, moisture is one of the undesirable substances that reduce the dielectric strength of the HVDC power transformer. The moisture level in the HVDC power transformer is one of the critical indicators for condition monitoring. Karl Fischer titration is the most common technique to verify the moisture contents in the solution. The chemical principle of Karl Fischer titration is based on the reaction between the water

and the oxidation of sulphur dioxide by iodine: $I_2 + 2H_2O + SO_2 \rightarrow 2HI + H_2SO_4$ [77]. Figure 3.2 illustrates the structure of the Karl Fischer Titrator. HVDC power transformer should maintain a low moisture level, so a coulometric titrator is appropriate to analyse the low moisture contents in the solution.

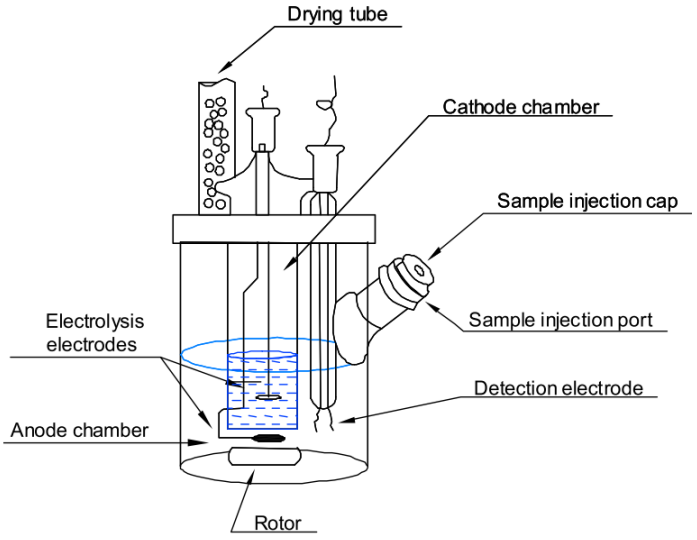

FIGURE 3.2: Karl Fischer Titrator

Then, generated iodine is consumed for water titration. During the titration process, two detector electrodes detect the constant current [77]. The amount of current required to produce iodine to reach the endpoint is measured to calculate the amount of water in the sample solution [77]. Aquamax KF Coulometric titrator has been introduced to verify the moisture contents in the transformer oil. 1 ml of transformer oil has been injected through the sample injection port to verify the amount of moisture in the transformer oil. Then, the result has been presented in ppm according to Equation 3.3.

$$\text{Moisture Content (ppm)} = \frac{\text{Mass of Moisture } (\mu \text{ g})}{\text{Mass of Transformer Oil (g)}} \tag{3.3}$$

3.3 Pulsed Electroacoustic (PEA) Methods

Oil and paper are the vital dielectric materials in HVDC converter transformers. The dielectric performance depends not only on electrical, chemical, and mechanical stresses but also on space charges. Under DC stresses, the space charge accumulation is a prominent feature, and the space charge packet distorts the electric field in the oil-impregnated paper, which contributes to accelerating degradation. Since the understanding of space charge characteristics is directly related to the performance of the oil-impregnated paper, non-destructive methods have been developed to acquire the space charge profiles. The pulsed electroacoustic (PEA) method is one of the most

popular non-destructive measurements. This section discusses the details of the PEA method.

3.3.1 Principle of the PEA Method

The PEA method is based on the propagation of acoustic waves generated from charges in the dielectric as shown in Figure 3.3 [62], [78]. In the PEA method, an electrical pulse $e_p(t)$ is applied to the dielectric sample [60]. Then, charges $p(z)$ in the dielectric sample are vibrated, and it produces acoustic waves [60]. Finally, a piezoelectric transducer detects the propagation of acoustic waves by converting them to electrical signals [60].

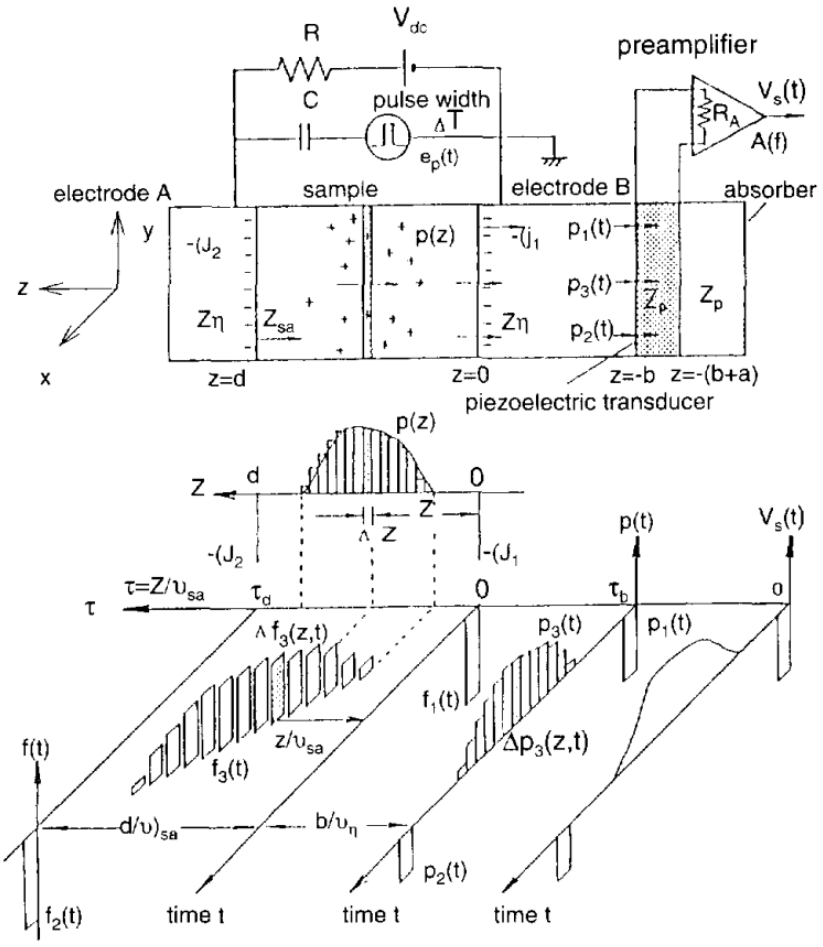

FIGURE 3.3: The PEA Method [78]

However, obtaining data from the PEA method must meet the following conditions:

- Pulse Generation of Acoustic Wave

The width of the pulsed electric field ΔT_p should be much shorter than the pulse width of the acoustic wave ΔT_s that propagates through the sample as described in Equation 3.4 [78], [79].

$$\Delta T_p << \Delta T_s = \frac{d}{v_{sa}} \tag{3.4}$$

where d is the thickness of the dielectric sample and v_{sa} is the acoustic velocity in the dielectric sample. When a significant narrow pulse voltage is applied to the dielectric sample, surface charges generate the identical shape of the narrow pulse acoustic wave [79]. Acoustic waves have the same shape of the acoustic wave generated from the surface charges, and it also has an acoustic delay corresponding to the thickness of the dielectric sample [79]. Thus, the space charge profiles can be obtained from the acoustic waves generated from space charges [79]. Besides, the acoustic impedance must be matched between the HVDC electrode and the dielectric sample by setting a piece of conducting impedance matching material, as shown in Equation. 3.5 [79].

$$Z_{sa} = Z_{bs} \tag{3.5}$$

where Z_{sa} is the acoustic impedance on the sample side, and Z_{bs} is the acoustic impedance on the electrode side. According to [79], the acoustic wave signal can be expressed as Equation 3.6.

$$\begin{aligned} p(t) =& \frac{Z_{Al}}{Z_{sa}+Z_{Al}}\sigma(0)e_p(t) \\ &+ \frac{2Z_{Al}}{Z_{sa}+Z_{Al}}\frac{1}{2}v_{sa}\int_0^\infty \rho(\tau)e_p(t-\tau)d\tau \\ &+ \frac{2Z_{Al}}{Z_{sa}+Z_{Al}}\frac{Z_{sa}}{Z_{ba}+Z_{sa}}\sigma(d)e_p(t-\frac{d}{v_{sa}}) \end{aligned} \tag{3.6}$$

where Z_{Al} is the acoustic impedance of the ground electrode, $\sigma(0)$ is the surface charge at the ground electrode, $\sigma(d)$ is the surface charge at the HVDC electrode. The first component in Equation 3.6 is for surface charge $\sigma(0)$ on the ground electrode, and $Z_{Al}/(Z_{sa}+Z_{Al})$ is the transmission ratio [79]. The second component is for space charge $\rho(z)$, and it represents the acoustic wave is produced from charges in the dielectric sample, which propagates through the ground electrode [79]. In the second component, the generation ratio of the acoustic wave is $Z_{sa}/(Z_{sa}+Z_{sa}) = \frac{1}{2}$ in the dielectric sample, and $2Z_{Al}/(Z_{sa}+Z_{Al})$ represents the transmission ratio at the interface of the dielectric sample and the ground electrode. Thus, total transmission ratio is $Z_{Al}/(Z_{sa}+Z_{Al})$ in the second component. The third component is for the surface charge $\sigma(d)$, and it represents that the acoustic wave is produced at the interface of the dielectric sample and HVDC electrode [79]. The generation ratio is The generation ratio for the third component at the interface of the sample and the HV electrode

is $Z_{sa}/(Z_{ba}+Z_{sa})$. The generation ratio equals $\frac{1}{2}$ when Z_{sa} matches Z_{ba}. . At the interface between the sample and the ground electrode, the transmission ratio equals $2Z_{Al}/(Z_{sa}+Z_{Al})$. Equation 3.6 indicates $Z_{sa} = Z_{bs}$, indicating matching material equivalence, thus generating a total ratio of $Z_Al/(Z_{sa}+Z_{Al})$ for each acoustic wave component.

Thus, Equation 3.6 can be simplified as described in Equation 3.7.

$$p(t) = \frac{Z_{Al}}{Z_{sa}+Z_{Al}}\left[\sigma(0)e_p(t) + v_{sa}\int_0^\infty \rho(\tau)e_p(t-\tau)d\tau + \sigma(d)e_p(t-\frac{d}{v_{sa}})\right] \tag{3.7}$$

Equation 3.7 is based on the time domain, so with Fourier transform, the equation based on the frequency domain can be acquired as shown in Equation 3.8.

$$P(f) = \frac{Z_{Al}}{Z_{sa}+Z_{Al}}v_{sa}\Delta\tau E(f)\left[\frac{\sigma(0)}{v_{sa}\Delta\tau} + R(f) + \frac{\sigma(d)}{v_{sa}\Delta\tau}exp(-i2\pi f\frac{d}{v_{sa}})\right] \tag{3.8}$$

where $\Delta\tau$ is the sampling time, which decides the sampling interval distance $v_{sa}\Delta\tau$, $R(f)$ represents the Fourier transform of $\rho(t)$ [79].

- Detecting Pulsed Acoustic Wave

The pulsed acoustic wave $p(t)$ is detected at a piezoelectric transducer on the ground electrode, where the acoustic wave is converted into a charge signal $q(t)$ associated with space charge distribution [79]. According to [79], Equation 3.9 is the charge signal in the time domain, and Equation 3.10 is the charge signal in the frequency domain.

$$q(t) = \frac{2Z_p}{Z_{Al}+Z_p}\frac{v_p}{b}\int_0^\infty h(\tau)p(t-\tau)d\tau \tag{3.9}$$

where $h(\tau)$ is the transmission function for a piezoelectric transducer.

$$Q(f) = \frac{2Z_p}{Z_{Al}+Z_p}\frac{v_{p\Delta\tau}}{b}H(f)P(f) \tag{3.10}$$

where $Q(f)$, $H(f)$, and $P(f)$ are the charge signal, transmission function, and acoustic wave respectively in frequency domain, Z_p represents the acoustic impedance of the piezoelectric transducer. The signal reflection can be prevented by matching the acoustic impedance between the piezoelectric transducer and the rear electrode [79].

For example, if PVDF(polyvinylidene fluoride)-β is used for a piezoelectric transducer, a material with the same acoustic impedance as PVDF-β must be used [79].

TABLE 3.1: Different Types of Piezoelectric Transducers [80]

Material	**Acoustic Velocity** $v[m/s]$	**Acoustic Impedance** $Z[kg/m^2sec]$
$LiNbO_3$	7360	34.4×10^6
$PZT-4$	4600	34.5×10^6
$PVDF-\alpha$	2260	4.0×10^6
$PVDF-\beta$	2260	4.0×10^6

Table 3.1 shows the different types of piezoelectric transducers according to acoustic velocity and impedance. Polymer piezoelectric transducer such as PVDF is more popular than ceramic piezoelectric transducer due to higher piezo capability, wide frequency range, a broad dynamic response, and relatively lower acoustic impedance [81]. Additionally, the polymer piezoelectric transducer is optically clear and flexible, and it is easy to shape physically [81].

- Space Charge Distribution from the PEA Method

As mentioned earlier, the acoustic waves from space charges are detected by a piezoelectric transducer, and they are transformed into charge signals [79]. According to [79], the output voltage signal in the frequency domain can be expressed in Equation 3.11.

$$V(f) = S(f)\left[\frac{\sigma(0)}{v_{sa}\Delta\tau} + R(f) + \frac{\sigma(d)}{v_{sa}\Delta\tau}exp\left(\frac{-i2\pi fd}{v_{sa}}\right)\right] \tag{3.11}$$

where $S(f)$ is the system function. In Equation 3.11, the surface charge at the ground electrode ($z = 0$) is expressed in the first component, and the space charge in the dielectric sample ($0 < z < d$) is expressed in the second component. The third component represents the surface charge at the HVDC electrode ($z = d$). The system function $S(f)$ can be represented as Equation 3.12 according to [79].

$$S(f) = \frac{W(f)H(f)}{C_p}\frac{2Z_p}{Z_{Al+Z_p}}\frac{Z_{Al}}{Z_{sa}+Z_{Al}}\frac{v_{sa}v_p\Delta\tau^2}{b}E(f) \tag{3.12}$$

where $W(f)$ is the Fourier transform of the transfer function of the detection circuit $w(t)$, C_p $[F/m^2]$ represents the capacitance of the piezoelectric transducer. When $S(f)$

is known, the space charge distribution can be acquired in the time domain or position domain $\rho(z = v_{sa}\tau)$ by inverse Fourier transform. To acquire $S(f)$, a DC voltage V_{dc} is applied to induce surface charges in the dielectric sample [79]. It is essential to apply low and short V_{dc}, consequently reducing E_{dc} impact to prevent space charge formation in the dielectric. When pulse voltage is applied, surface charges ($\sigma(0)$ and $\sigma(d)$) can be obtained, and only surface charge signal $V_0(t)$ responding to $\sigma_0(0)$ is necessary for the calibration [79]. $V_0(t)$ of the time domain can be transferred as $V_0(f)$ of the frequency domain as shown in Equation 3.13.

$$V_0(f) = \frac{S(f)\sigma_0(0)}{v_{sa}\Delta\tau} \tag{3.13}$$

$\sigma_0(0)$ can be expressed as shown in Equation 3.14.

$$\sigma_0(0) = \varepsilon_0\varepsilon_r\frac{V_{dc}}{d} \tag{3.14}$$

where $\varepsilon = \varepsilon_0\varepsilon_r$ is the permittivity, ε_0 is the vacuum permittivity, ε_r is the relative permittivity. Thus, when permittivity ε and thickness d of the dielectric sample are known, the charge distribution $\frac{V(f)}{V_0(f)}$ in the frequency domain can be obtained as shown in Equation 3.15.

$$\frac{V(f)}{V_0(f)} = \frac{\frac{\sigma(0)}{v_{sa}\Delta\tau} + R(f) + \frac{\sigma(d)}{v_{sa}\Delta\tau}exp\left(-i2\pi f\frac{d}{v_{sa}}\right)}{\varepsilon_0\varepsilon_r\frac{V_{dc}}{d}\frac{1}{v_{sa}\Delta\tau}} \tag{3.15}$$

Thus, Equation 3.15 with inverse Fourier transform can be converted into the function for the space charge distribution $\rho(z = v_{sa}\tau)$ in the position domain [79].

3.3.2 Experimental Setup of the PEA Method

Figure 3.4 shows the experimental setup of the PEA method for space charge measurement. In the PEA method, a flat shape of the dielectric sample is placed between the ground electrode and the high-voltage electrode. A semi-conductive layer is placed between the dielectric sample and the high-voltage electrode to improve acoustic impedance matching. Additionally, the proper mechanical pressure is applied in order to maintain tight contact between the dielectric sample and electrodes. 20kV/mm of DC electric field is applied to the oil-impregnated paper sample for 60 minutes respectively to obtain the space charge profiles. Then, the DC voltage is completely removed for 60 minutes in order to investigate the space charge dissipation. Every test should

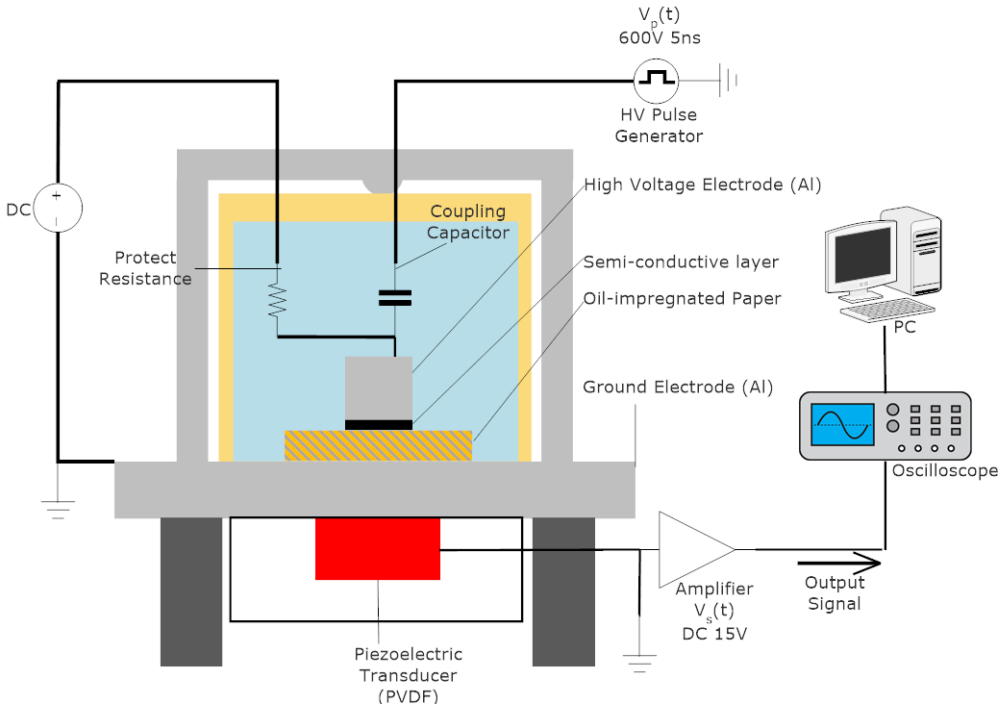

FIGURE 3.4: Physical Overview of the PEA Method

be carried out with the new sample in order to avoid the pre-stressed effect on charge formation in the oil-impregnated paper.

3.4 DC Breakdown Test

To measure DC breakdown, each electrode was equipped with a diameter of 35 mm ball bearings to secure the oil-impregnated paper. Mineral oil-impregnated paper and natural ester liquid-impregnated paper were in mineral oil and natural ester liquid, respectively for DC breakdown measurement. A sample with a thickness of 100 μm was subjected to an applied ramp rate of 500 V/s. 20 different points on each sample were assessed for +DC breakdown measurement.

3.5 Acids Number Measurements

The acidity of the oil was measured via titration in accordance with ASTM D-974. To determine the acidity of aged natural ester liquid and mineral oil, a titration solvent was prepared by mixing 49.5ml of isopropyl alcohol and 0.5ml of water. Then, 0.25g of 1-naphtholbenzein was placed in a 25ml titration solvent to prepare the indicator solution. Afterwards, 1ml of aged oil, 50ml of titration solution, and 0.25ml of indicator solution were mixed. Then, the KOH solution, which is a mixture of 0.3g of potassium

hydroxide, 0.5g of barium hydroxide, and 300ml of isopropyl alcohol, has slowly added until the colour goes from orange to a stable green.

3.6 Degree of Polymerisation Measurements

According to ASTM D4243, the DP of thermally aged natural ester liquid-impregnated paper and mineral oil-impregnated paper was measured. 15mg of thermally aged natural ester liquid-impregnated paper or mineral oil-impregnated paper was placed into distilled water, which was sonicated for 10 minutes to disperse and fully wet. Afterwards, the solution was placed into a sealed glass bottle and stirred magnetically for 20 minutes at room temperature. After adding 10ml of bis(ethylenediamine) copper (II) hydroxide solution, the mixture was stirred for at least 4 hours at room temperature. Then, the solution for DP measurement was deposited into a viscometer tube and placed into a viscometer bath at 20 °C. After allowing the temperature to stabilise for at least 30 minutes, five viscosity measurements were taken, and the DP was calculated according to the standard.

3.7 Sample Preparations

3.7.1 Sample Information

The Kraft papers with 100 μm and 250 μm of thickness have been applied to this research. Diala S3 ZX-IG has been used as mineral oil from Shell company. Then, the Midel eN 1204 has been used natural ester liquid from the Midel company. Table 3.2 provides more information regarding transformer oils

3.7.2 Sample Preparation for Impact of Moisture on Single Layer Oil-Paper

The Kraft paper with 100 µm of thickness was applied to this research. Figure 3.5 illustrates the sample preparation to investigate how moisture affects the transformer oil-impregnated paper and study the difference between natural ester liquid and mineral oil. Kraft paper is hygroscopic, making it easy to absorb moisture. Thus, the moisture content can be controlled using Kraft paper. Each Kraft paper is 5cm in diameter and 100µm in thickness.

To eliminate moisture, Kraft paper was heated in a fan-assisted oven at 130°C for 3 hours. After removing Kraft paper from a fan-assisted oven, it was weighed on an analytical balance. Table 3.5 illustrates the weight of Kraft paper with different moisture contents.

TABLE 3.2: Transformer Oil Information [82][83]

	Diala S3 ZX-IG	**Midel eN 1204**
Flash Point (°C)	136 (ISO 2719)	315 (ISO 2592)
Fire Point (°C)	-	350 (ISO 2592)
Pour Point (°C)	-57 (ISO 3016)	-31 (ISO 3016)
Density at 20°C (g/cm^3)	0.88 (ISO 3675)	0.92 (ISO 3675)
Viscosity at 40°C (mm^2/s)	8.0 (ISO 3104)	37 (ISO 3104)
Breakdown Voltage (kV)	70 (2.5mm gap, IEC 60156)	75 (2.5mm gap, IEC 60156)
Relative Permittivity	2.2	3.1
Biodegradability (%)	≤10	≥90

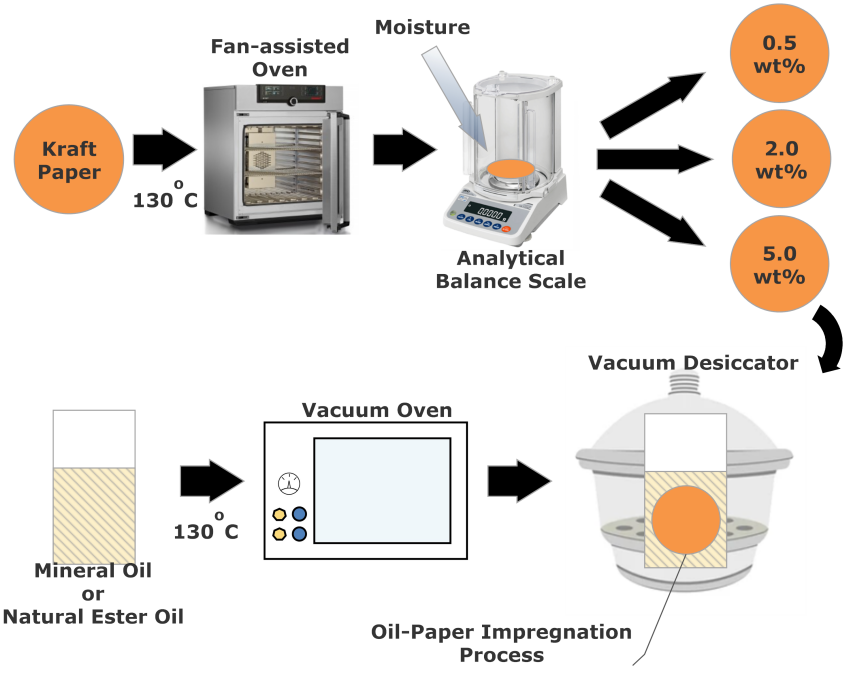

FIGURE 3.5: Sample Preparation regarding the Impact of Moisture

The moisture level in the HVDC power transformers should be dried as much as possible to avoid the effects of moisture. The moisture content of the cellulose in a new transformer is around 0.5wt%, and it is predicted to increase over the transformer's lifetime steadily [84]. According to IEC 60422, less than 2.0wt% of the moisture content in transformers is a dry state; 2.0wt%-5.0wt% of the moisture content is considered moderately wet, and over 5.0wt% of the moisture content is an extremely wet state

TABLE 3.3: Weight of Kraft Paper with Different Moisture Contents

Weight of Paper Before absorbing Moisture (g)	Weight of Paper After Absorbing Moisture (g)	Moisture Contents (wt%)
0.1176	0.1182	0.50
0.1218	0.1244	2.01
0.1180	0.1241	5.00

[7]. Thus, Kraft papers with 0.5wt%, 2.0wt%, and 5.0wt% of moisture were prepared, respectively.

Natural ester liquid and mineral oil were placed in the vacuum oven for 3 hours at 130°C to reduce moisture. Then, Kraft papers with different moisture contents were impregnated with degassed mineral oil and natural ester liquid for 24 hours, respectively. The mass-weight ratio between transformer oil and Kraft paper is 10:1 for the oil-paper impregnation process.

- **Moisture Contents**

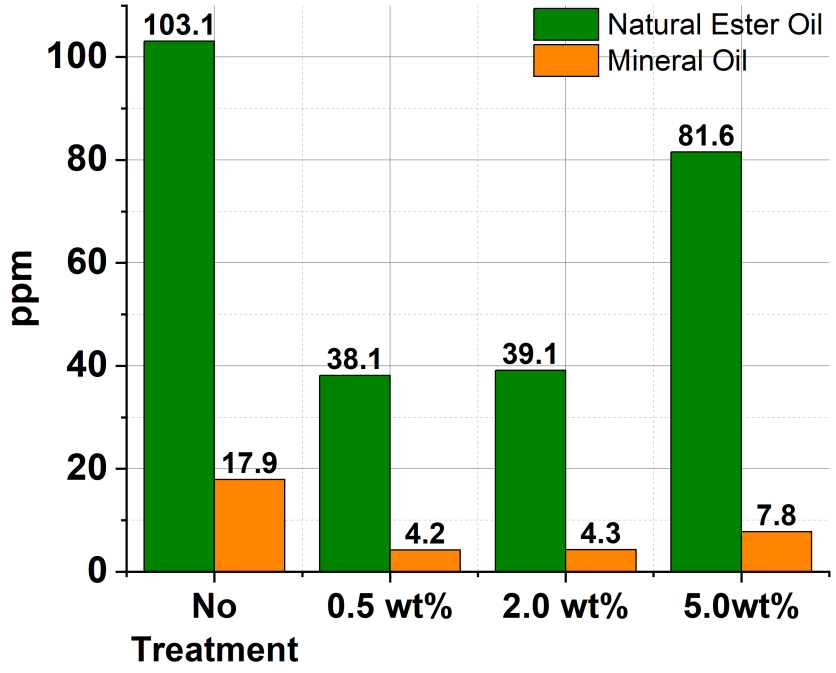

FIGURE 3.6: Moisture Contents (ppm) in Natural Ester Liquid and Mineral Oil with Different Moisture wt% in Kraft Paper

Figure 3.6 represents how different moisture contents in Kraft papers affected the natural ester liquid and mineral oil, respectively. 1mL of natural ester liquid and mineral oil

was added to the Karl Fischer titrator at room temperature (20°C) to examine the moisture level. Kraft paper with different moisture levels (0.5wt%, 2.0wt%, and 5.0wt%) was impregnated with the degassed natural ester liquid and mineral oil, respectively.

The natural ester liquid without any treatments had 103.1 ppm of moisture. When Kraft paper contained 0.5wt% of the moisture, considered a dry state, and was impregnated with the natural ester liquid, the moisture level in the oil was about 38.1 ppm. After Kraft paper with 2.0wt% of moisture contents was impregnated with the natural ester liquid, it showed 39.1 ppm. 2.0 wt% of moisture in Kraft paper did not significantly influence the increase in moisture in the natural ester liquid and mineral oil because 2.0wt% of moisture in Kraft paper was still considered as low as 0.5wt%. However, when Kraft paper with 5.0wt% of moisture was impregnated with degassed natural ester liquid, the moisture content in the natural ester liquid was much higher (81.58ppm) than samples with 0.5wt% and 2.0wt%. The mineral oil without treatment had 17.93 ppm of moisture content. When the degassed mineral oil was impregnated with Kraft paper, which contained 0.5wt% of moisture, it showed 4.2 ppm. When Kraft paper had 2.0wt% of moisture content, the mineral oil had 4.3 ppm. However, after the Kraft paper, which contained extremely high moisture content (5.0wt%), was impregnated with the mineral oil, 7.8 ppm of the moisture level was observed.

Kraft paper is a hygroscopic material that absorbs moisture readily. In the oil-paper insulation system, water is mainly absorbed by cellulose, so it is essential to keep cellulose dry [36]. However, although the Kraft paper had 5.0wt%, mineral oil rarely removed cellulose's moisture due to its hydrophobic characteristics [84]. On the other hand, like cellulose, natural ester liquid is a hydrophilic liquid [84]. Hence, when the cellulose contained 5.0wt% of moisture, the natural ester liquid absorbed more water (81.6 ppm) from the cellulose than mineral oil.

Triglycerides of natural oil react with water through hydrolysis, which results in long-chain fatty acids [85]. This process consumes dissolved water in natural ester liquid [85]. As a result, it moves extra water from the paper to the natural ester liquid to keep the equilibrium [85]. This characteristic of the natural ester liquid keeps the cellulose dry, and it can delay the degradation of the cellulose that may occur due to moisture.

3.7.3 Sample Preparation for Impact of Thermal Ageing on Single Layer Oil-Paper

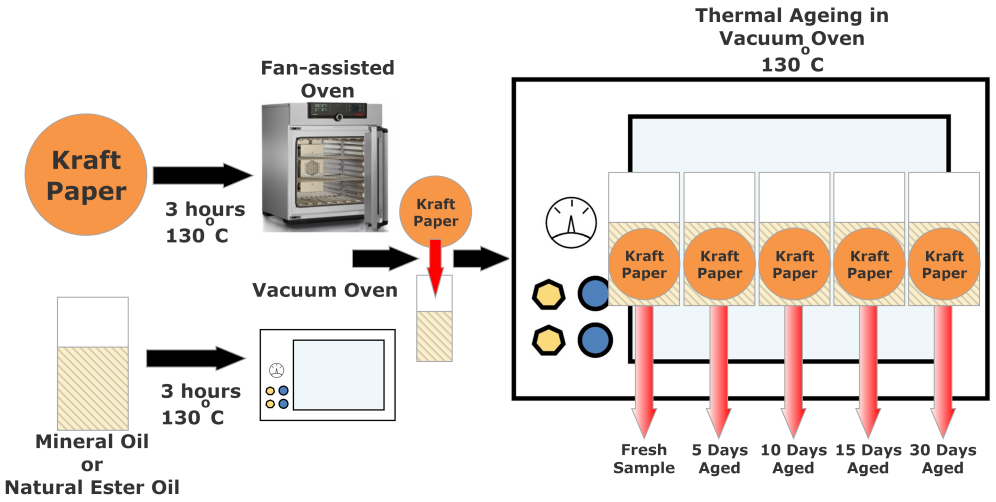

FIGURE 3.7: Sample Preparation regarding the Impact of Thermal Ageing

Figure 3.7 depicts the methodology for investigating how thermal ageing degrades transformer oil-impregnated paper by comparing natural ester liquid and mineral oil. The Kraft papers were placed in the fan-assisted oven, whilst the transformer oils (natural ester liquid and mineral oil) were placed in the vacuum oven for 3 hours at 130°C. This reduced the amount of water in Kraft paper and transformer oils to minimise the influence of moisture. Then, the degassed Kraft papers were respectively impregnated with degassed natural ester liquid and mineral oil for 24 hours in a vacuum oven. Afterwards, samples were thermally aged by heating them to 130°C in a vacuum oven [86]. When each sample attained the specified ageing durations (0 days, 5 days, 10 days, 15 days, and 30 days), it was removed from the vacuum oven for the rest of the measurements.

Thermal ageing of the samples was conducted in a vacuum oven for safety reasons. While transformers typically operate between 60 and 90°C, a temperature of 130°C was applied to accelerate the ageing process, causing the evaporation of the dielectric liquid. Hence, the use of a vacuum oven was essential to ensure complete isolation of the thermal ageing process from the atmosphere for safety.

As seen in Figure 3.8, as thermal ageing progressed, the colour of natural ester and mineral oils became darker compared to fresh oils. 1mL of oil was added to Aquamax Karl Fischer titrator to monitor the changes in moisture in fresh and aged natural ester liquid and mineral oil, as shown in Table **??**.

Throughout thermal ageing, natural ester liquids maintained moisture concentrations between 31.48 and 39.33 ppm, whereas mineral oils had moisture concentrations between 5.23 and 6.96 ppm.

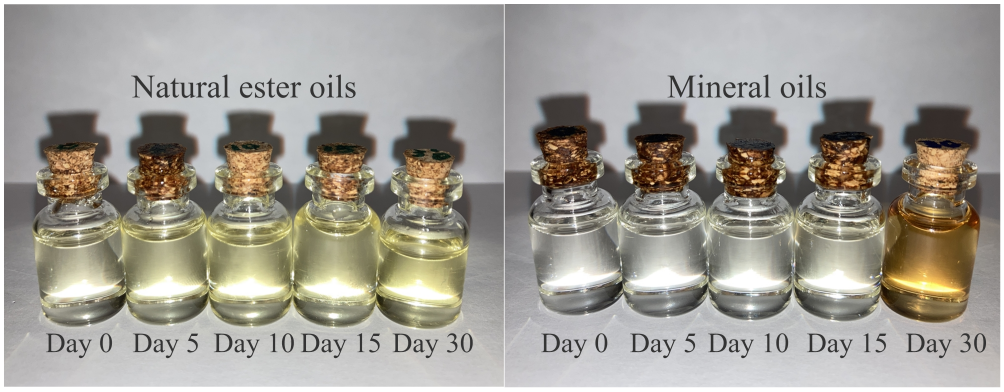

FIGURE 3.8: Discolouration of Natural Ester Liquid and Mineral Oil during Thermal Ageing

TABLE 3.4: Moisture Concentrations in Natural Ester Liquids and Mineral Oils during Thermal Ageing

Ageing Time (days)	Moisture Concentrations in natural ester liquid (ppm)	Moisture Concentrations in Mineral Oil (ppm)
Day 0	32.27	6.43
Day 5	33.91	6.96
Day 10	31.48	5.9
Day 15	37.48	5.23
Day 30	39.33	6.26

3.7.4 Sample Preparation for Impact of Moisture on Double Layer Oil-Paper

In this study, Kraft papers with 100 µm and 250 µm of thickness were used. This sample preparation method is identical to section 3.7.2.

Kraft papers with 12 cm of diameter and 250 µm of thickness were prepared for space charge measurement. In addition, Kraft papers with 5 cm of diameter and 100 µm of thickness were prepared for DC breakdown measurement. Table 3.5 illustrates the weight measurements of Kraft paper under different levels of moisture content.

The configuration of a double layer comprising of oil and paper, which was utilised in this study to measure space charge, is presented in Figure 3.9. Polytetrafluoroethylene (PTFE) ring with 250μm of thickness was placed on the ground electrode. Then, a drop of transformer oil (mineral oil or natural ester liquid) was placed at the centre of the PTFE ring. Afterwards, mineral or natural ester liquid-impregnated paper was then placed on the oil gap, and the high-voltage electrode with appropriate mechanical pressure was placed. When the dielectric liquid was placed at the oil gap, the air bubble was minimised to reduce the effect of partial discharges. A semiconducting layer

TABLE 3.5: Weight of Kraft Paper with Different Moisture Contents

Weight of Paper Before absorbing Moisture (g)	Weight of Paper After Absorbing Moisture (g)	Moisture Contents (wt%)
Kraft Paper (Thickness: 100μm)		
0.1176	0.1182	0.50
0.1175	0.1198	2.00
0.1180	0.1241	5.00
Kraft Paper (Thickness: 250μm)		
3.2910	3.3070	0.50
3.3000	3.3660	2.01
3.3000	3.4650	5.00

was introduced between the HV electrode and oil-impregnated paper to improve the acoustic matching impedance.

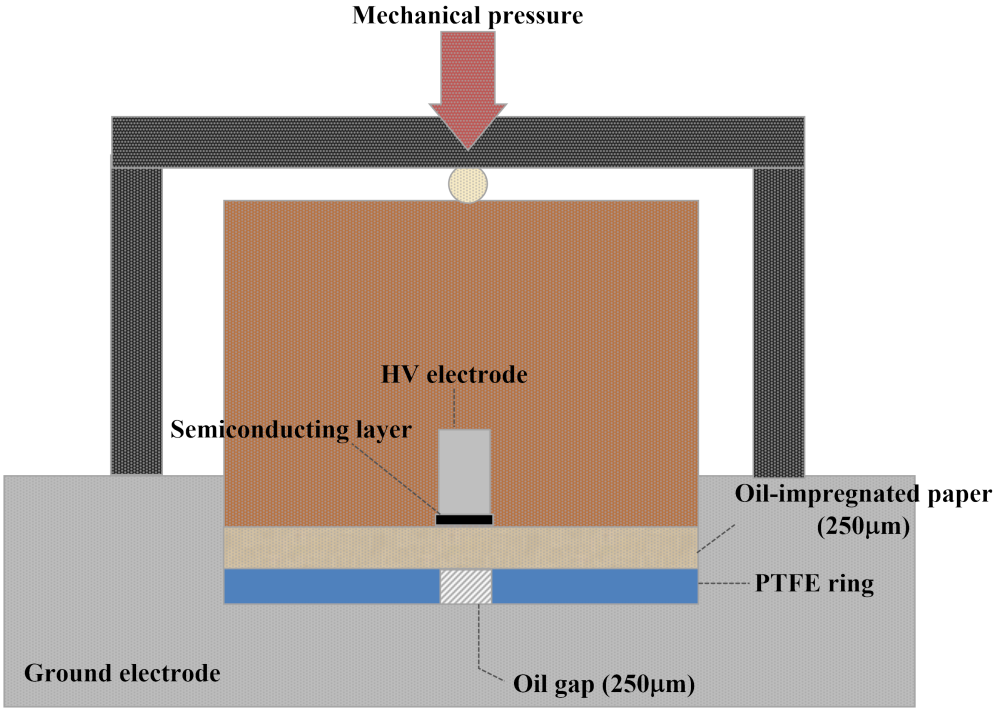

FIGURE 3.9: Double Layer Configuration of Oil and Paper for Space Charge Measurement

The sample was exposed to a DC electric field of 20kV/mm for 60 minutes to investigate the space charge characteristics. Afterwards, the voltage was entirely removed to measure the space charge decay over the following 60 minutes.

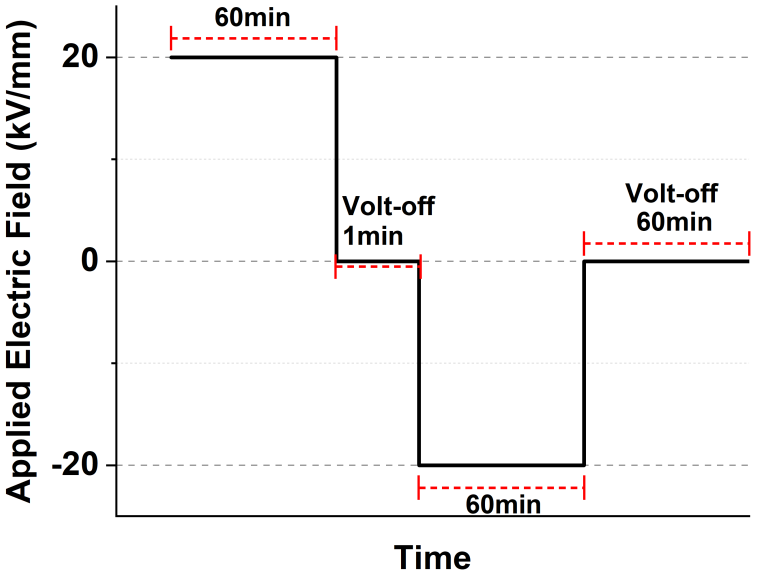

FIGURE 3.10: Voltage Application for Polarity Reversal Effect

Studies were also conducted on the polar reversal effect after investigating a single polarity. In this case, 20 kV/mm of (+) polarity was applied to the sample during the initial 60 minutes as shown in Figure 3.10. After that, the voltage supplier was cut off for one minute [87]. Then, 20 kV/mm of (-) polarity was applied to the sample for an additional 60 minutes. As a final step, the space charge decay was measured for 60 minutes after the voltage supplier was completely removed.

- **Moisture Contents**

Figure 3.11 depicts the impact of varying moisture levels in kraft papers (250 μm of thickness) on natural ester liquid and mineral oil. Before and after the oil-impregnation procedure, the moisture content of both oils was evaluated. Results indicated that the natural ester liquid contained more moisture than the mineral oil at all levels of paper moisture measured. As the moisture content of the paper increased, the difference in moisture content between the two oils also increased.

For instance, when the paper moisture was 0.5wt%, the natural ester liquid had a moisture content of 39.8ppm, while the mineral oil had a moisture content of 6.8ppm. At 2.0wt% paper moisture, the natural ester liquid contained 106.7ppm of moisture while the mineral oil contained 11.2ppm of moisture. Additionally, when the Kraft paper is in extremely wet condition (5.0wt%), the natural ester liquid had a moisture content of 254.1ppm, whereas the mineral oil had a moisture content of 23.9ppm.

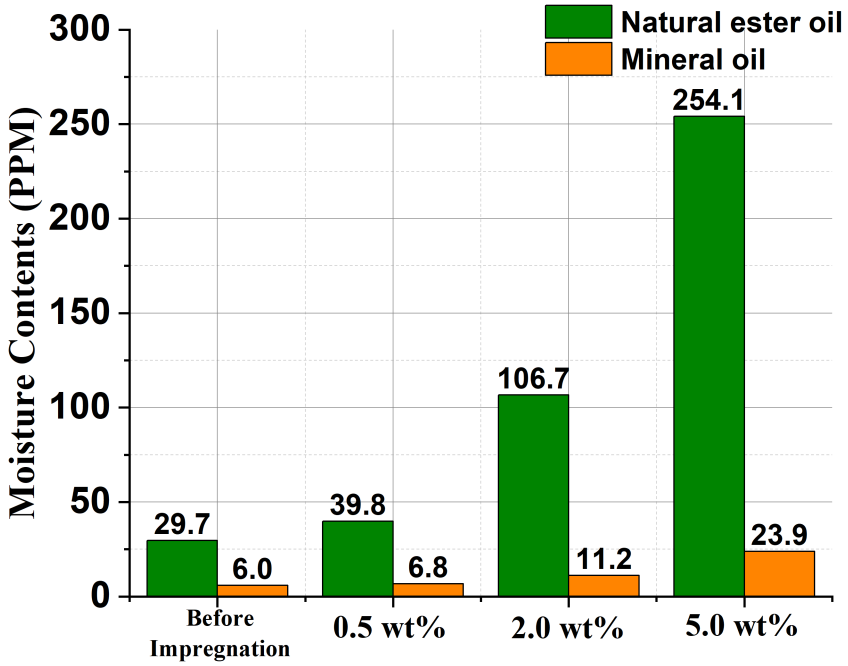

FIGURE 3.11: Moisture Content Comparison between Natural Ester Liquid and Mineral Oil after Oil-Paper Impregnation Process

Mineral and natural oils are both used for insulation and cooling, but their chemical structures are noticeably different. The natural ester has a greater water solubility because its chemical structure polarises its molecule, and the polar molecule attracts substances [88]. Therefore, as the moisture content of Kraft paper increases, the hydrophilic nature of natural ester liquid causes it to absorb moisture from the paper. On the other hand, mineral oil exhibits hydrophobic properties due to its non-polar nature. Thus, even as the moisture content of Kraft paper increases, mineral oil repels the moisture, causing it to remain on the paper [88].

These results indicate significant implications for the design and operation of transformers. Particularly, by absorbing moisture during transformer operation, the results show that natural ester liquid is more efficient than mineral oil at maintaining the paper's dryness.

Chapter 4

Space Charge Characteristics of Natural ester Liquid-impregnated Paper with Different Moisture Contents

4.1 Research Motivation

As previously discussed, the HVDC power transformer is highly dependent on its insulation system. Mineral oil has been used predominantly as the dielectric liquid for the HVDC power transformer. However, the high fire risk, low biodegradability, and scarcity of mineral oil have required an alternative to compensate for these weaknesses.

Moisture is one of the most undesirable substances in the oil-paper insulation system [46]. Cellulose is a hygroscopic material, so it must be maintained to be dry. However, moisture is produced by the oxidative process and the degradation of the molecular chain once oil-paper insulation systems get aged over many years [36].

During the ageing process, the furfural and acid contents in the dielectric liquid are affected by the moisture level [46]. Thus, the high moisture level can accelerate the degradation of the oil-paper insulation system, drastically lowering the insulation system's breakdown strength and reducing the transformer's life [89]. Also, moisture aids the depth of charge penetration into the dielectric materials, which may cause higher electric field distortion in the oil-paper system.

Different chemical structures between natural ester liquid and mineral oil may cause other impacts on dielectric properties. Therefore, further information is still needed

about the natural ester liquid whether it is applicable to the HVDC apparatus. This section mainly focused on how different moisture levels affect the space charge dynamics of natural ester liquid-impregnated paper in comparison to mineral oil-impregnated paper.

4.2 DC Conductivity

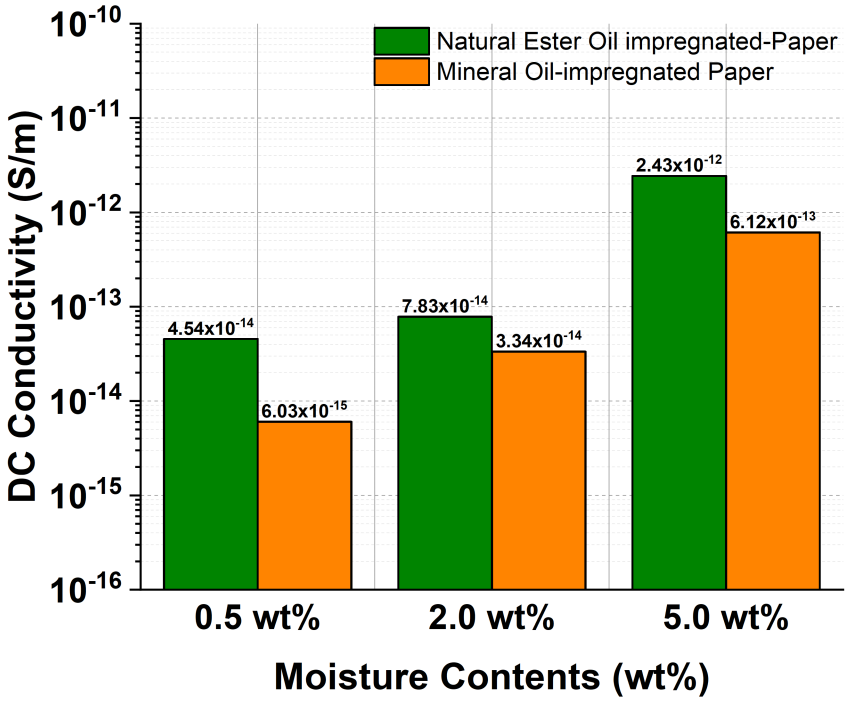

FIGURE 4.1: DC Conductivity with Different Moisture Contents

200 V_{dc} was applied for the quasi-dc conductivity measurement. The quasi-dc conductivity takes place in the low-frequency range. Figure 4.1 represents that as the amount of moisture increased, the dc conductivity of both natural ester liquid-impregnated paper and mineral oil-impregnated paper also increased. The dc conductivity of the natural ester liquid-impregnated paper was 4.54×10^{-14} S/m (at 0.5wt%), 7.84×10^{-14} S/m (at 2.0wt%), and 2.43×10^{-12} S/m (at 5.0wt%). Then, the dc conductivity of the mineral oil-impregnated paper showed 6.03×10^{-15} S/m (at 0.5wt%), 3.34×10^{-14} S/m (at 2.0wt%), and 6.12×10^{-13} S/m (at 5.0wt%).

The result illustrated that the dc conductivity of the natural ester liquid-impregnated paper always had a higher value than the mineral oil-impregnated paper for the same moisture contents due to a greater affinity of natural ester liquid for water. From 0.5 wt% to 5.0wt% of moisture contents, the dc conductivity of the natural ester liquid-impregnated paper increased by 53.53 times. However, the dc conductivity of mineral oil-impregn- ated paper increased by 101.5 times from 0.5wt% to 5.0wt% of moisture contents. Unlike natural ester liquid, the hydrophobic characteristic of mineral oil forces the moisture to stay in the cellulose. This phenomenon increased the dc conductivity of mineral oil-impregnated paper at a faster rate than that of the natural ester liquid-impregnated paper with the increase of moisture.

4.3 Space Charge Characteristics

Under dc conditions, space charges can be injected into oil-impregnated papers. Accumulated charges can enhance the electric field in specific regions [67]. Also, it may accelerate the degradation process of the insulation system.

Figure 4.2 represents space charge characteristics of the natural ester liquid-impregnated paper and mineral oil-impregnated paper with different moisture contents. The electric stress can lower the potential barrier between electrodes and oil-impregnated paper. As a result, obvious homocharges are injected from both electrodes when a dc electric field is applied. For dry natural ester liquid-impregnated paper (0.5wt%), negative charge injections occurred when the dc field was applied. Then, these negative charges were accumulated initially, but the number of negative charges in the middle of the paper decreased over time due to a possible recombination process. For dry mineral oil-impregnated paper (0.5wt%), negative charges also travelled to the middle of the paper after the dc field was applied. After that, these negative charges were trapped and accumulated in the middle of the paper. However, a relatively lower amount of negative charges were injected in the mineral oil-impregnated paper than in the natural ester liquid-impregnated paper.

When the natural ester liquid-impregnated paper was moderately wet (2.0wt%), more negative charges were injected from the cathode than in the dry state. Also, positive charges travelled from the anode to the middle of the paper because of the higher moisture content. Then, these positive charges started to be accumulated in the middle of the paper at 60 minutes. When the moisture content was 2.0wt%, similar space charge characteristics were observed in the mineral oil-impregnated paper.

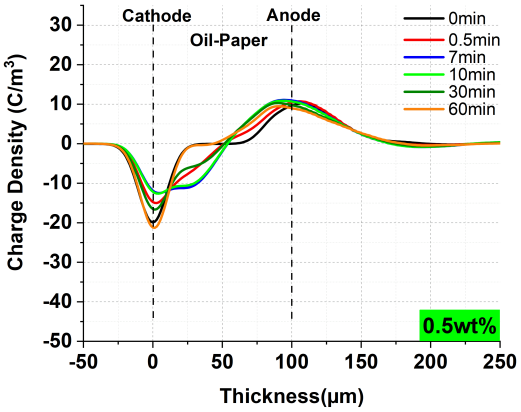

(A) 0.5wt% (Natural Ester Liquid-Paper)

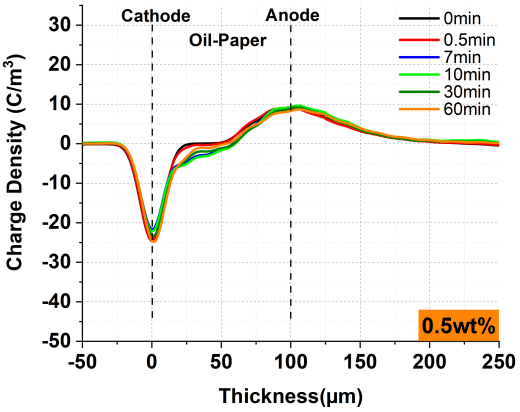

(D) 0.5wt% (Mineral Oil-Paper)

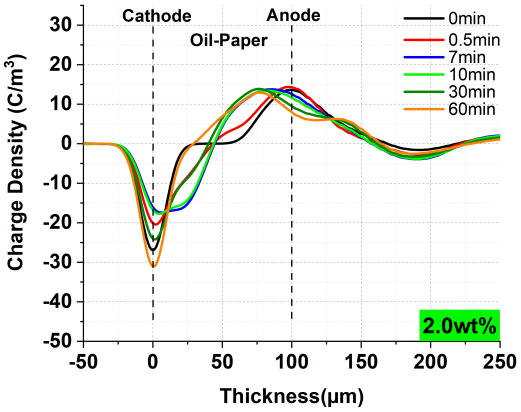

(B) 2.0wt% (Natural Ester Liquid-Paper)

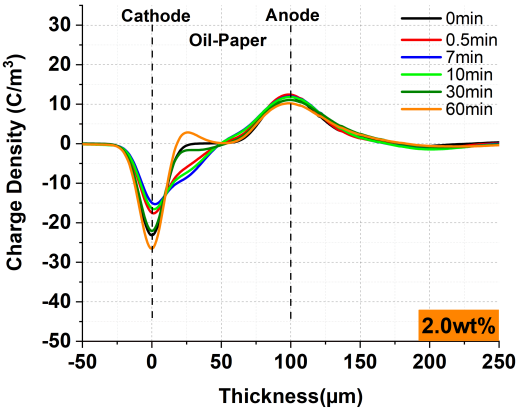

(E) 2.0wt% (Mineral Oil-Paper)

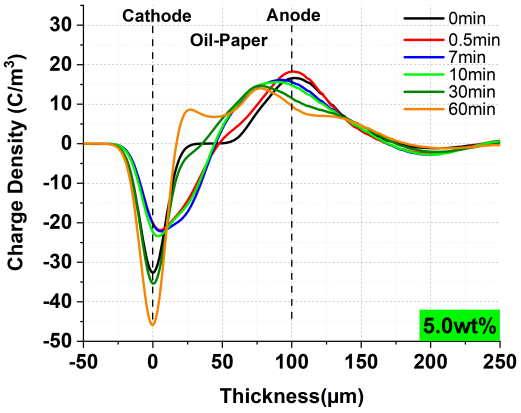

(C) 5.0wt% (Natural Ester Liquid-Paper)

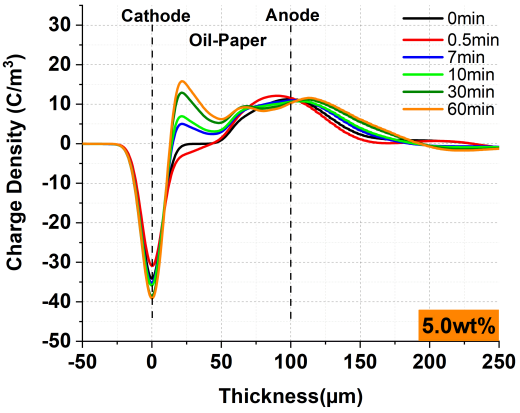

(F) 5.0wt% (Mineral Oil-Paper)

FIGURE 4.2: Space Charge Characteristics of the Natural Ester Liquid-impregnated Paper, (A), (B), and (C), and the Mineral oil-impregnated Paper,(D), (E), and (F), with Different Moisture Contents

However, the difference is that the increase in water caused the higher mobility of positive charges in the mineral oil-impregnated paper, resulting in forming heterocharges

in the vicinity of the cathode at 60 minutes.

In extremely wet conditions (5.0wt%), the largest amount of heterocharges in the natural ester liquid-impregnated paper was formed in the vicinity of the cathode at 60 minutes. These heterocharges induced negative charges on the cathode, resulting in the highest negative charge peak (45 C/m^3). On the other hand, natural ester liquid-impregnated papers with 0.5wt% and 2.0wt% of moisture had 22 C/m^3 and 30 C/m^3 of negative charge peaks, respectively. When the mineral oil-impregnated paper was extremely wet (5.0wt%), it also showed the largest amount of heterocharges near the cathode, causing the highest negative peak (38 C/m^3). However, 0.5wt% and 2.0wt% of mineral oil-impregnated papers showed 25 C/m^3 and 27 C/m^3 of negative peaks, respectively.

The difference between the natural ester liquid-impregnated paper and mineral oil-impregnated paper was that the mineral oil impregnated-paper caused faster heterocharge formation near the cathode than natural ester liquid-impregnated paper in an extremely wet condition. This is probably because mineral oil's hydrophobic properties make water stay in the cellulose, creating more paths for charges, which travel freely in the mineral oil-impregnated paper. The moisture content of Kraft paper has a major effect on space charge properties, while mineral oil and natural ester liquid also have some effect on it. Mineral oil, in other words, repels moisture into the paper, but natural ester liquid absorbs moisture from the paper. As a result, once the Kraft paper contains a high moisture content, it may give better mobility to charges, allowing them to travel more easily to the opposite electrode in the mineral oil-impregnated paper.

High moisture levels in oil-impregnated papers are undesirable because they form heterocharges, which induce charges near the electrodes. Then, heterocharges likely cause an enhanced electric field in a specific region. With a moisture content of 5%, both charges and moisture play a significant role in space charge dynamics. Free charges respond to electric fields, while water's ionisation affects these characteristics.

However, when the moisture content in the Kraft paper is low, the properties of transformer oil are an important consideration in terms of space charge characteristics [90]. Even though the natural ester liquid was degassed, the polar nature of the natural ester liquid attracted a more considerable amount of moisture than mineral oil, causing the higher dc conductivity in the natural ester liquid-impregnated paper [49]. Then, it resulted that when the natural ester liquid-impregnated paper had a lower moisture level, it showed a higher amount of negative charges injected from the cathode than the mineral oil-impregnated paper.

4.4 Total Charge Amount

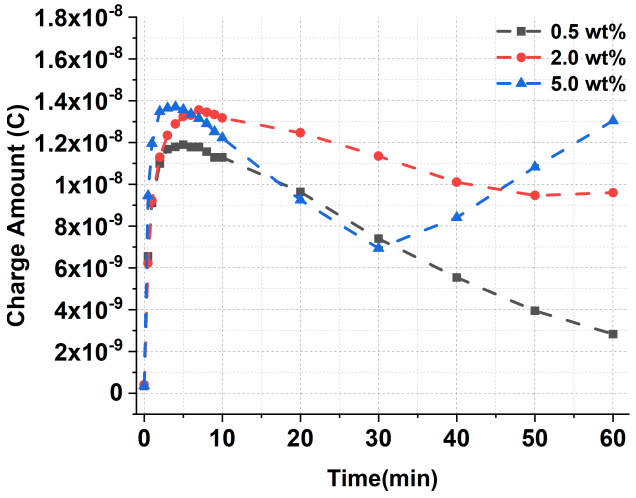

(A) Natural Ester Liquid-impregnated Paper

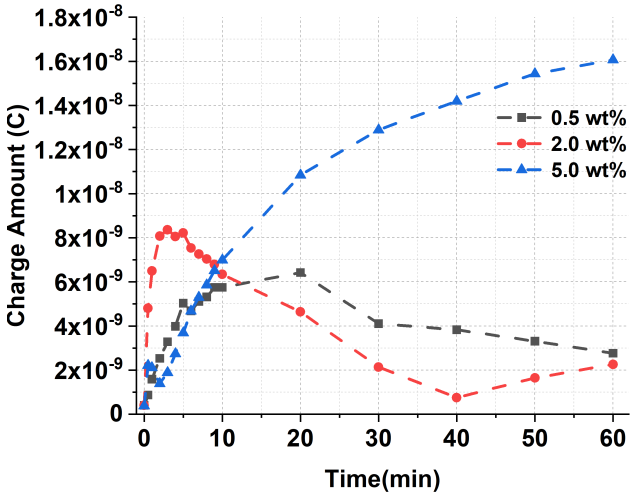

(B) Mineral Oil-impregnated Paper

FIGURE 4.3: The Total Amount of Charge with Different Moisture Contents

Figure 4.3 represents the total amount of charges in both oil-impregnated papers with different moisture contents for 60 minutes. The charge density at both electrodes was excluded in order to investigate the moisture impacts on space charge characteristics. As a result, the results only included charge density in the oil-impregnated paper. The total amount of charges can be calculated based on Equation 4.1 [91].

$$\int_0^d |\rho| \cdot S dx \tag{4.1}$$

where, Q_{total} is the total amount of charge, d is the thickness of the sample, ρ is the charge density, S is the area of the electrode. For natural ester liquid-impregnated papers, as moisture increased, the total amount of charges increased together. For 0.5wt% and 2.0wt% of moisture contents in the natural ester liquid paper, the largest total amount of charges occurred within 10 minutes. After that, it kept decreasing over time due to possibly recombination effects. For 5.0wt% of moisture content in the natural ester liquid-impregnated paper, the largest total amount of charges also took place within 10 minutes. Then, it kept decreasing until 30 minutes due to possibly recombination effects.

However, from 30 to 60 minutes, the total amount of charges increased again since the heterocharges were formed near the cathode. For 0.5wt%, 2.0wt%, and 5.0wt% of moisture contents, the largest total amount of charges in the natural ester liquid-impregnated paper were $1.19 \times 10^{-8} C/m^3$, $1.36 \times 10^{-8} C/m^3$, and $1.37 \times 10^{-8} C/m^3$, respectively. This indicates that the largest total amount of charges in the natural ester liquid-impregnated paper increased about 1.15 times in the extremely wet state compared to the dry state.

When the cellulose contained 0.5wt% of moisture content, the total amount of charges in the mineral oil-impregnated paper increased during the first 20 minutes. Then, it kept decreasing due to the recombination effect until it reached $2.76 \times 10^{-9} C/m^3$ of the total amount of charges for 60 minutes. For 2.0wt% of moisture content, the total amount charges in the mineral oil-impregnated paper sharply increased from $4.6 \times 10^{-10} C/m^3$ to $8.36 \times 10^{-9} C/m^3$ for the first 4 minutes. Then, it kept decreasing up to 40 minutes due to recombination effects. After that, it slightly increased again due to heterocharge formation near the cathode.

For 5.0wt% of moisture contents, the total amount of charges kept increasing over time because of fast heterocharge formation near the cathode and positive charge accumulation in the middle of the paper. As a result, the largest total amount of charges $(1.61 \times 10^{-8} C/m^3)$ in the mineral oil-impregnated paper was formed at 60 minutes. Also, it indicates that the largest total amount of charges in the mineral oil-impregnated paper increased about 2.5 times in the extremely wet state compared to the dry state. The result from space charge profiles shows that the higher moisture in oil-impregnated papers contributed to forming heterocharges, which increased the negative charge peak at the cathode.

4.5 Electric Field Distortion

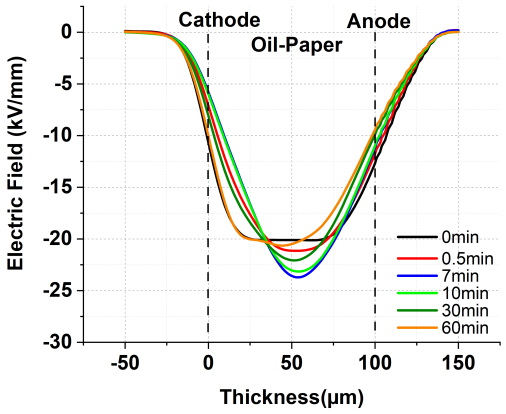

(A) 0.5wt% (Natural Ester Liquid-Paper)

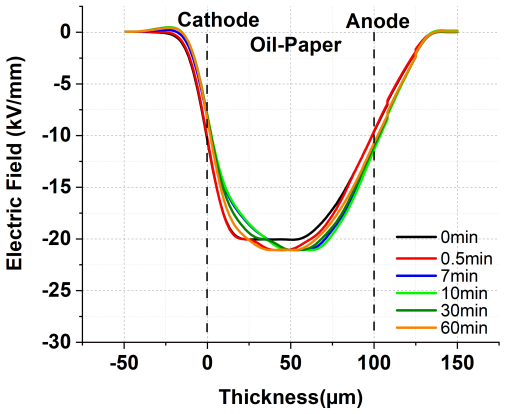

(D) 0.5wt% (Mineral Oil-Paper)

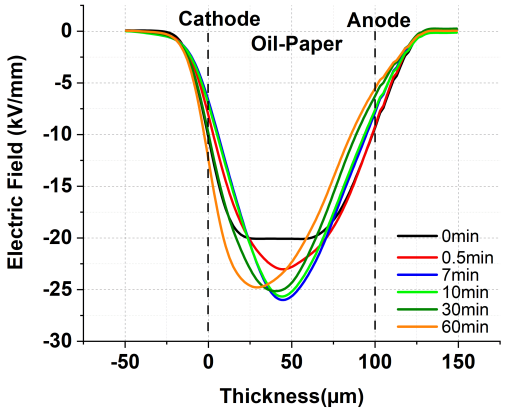

(B) 2.0wt% (Natural Ester Liquid-Paper)

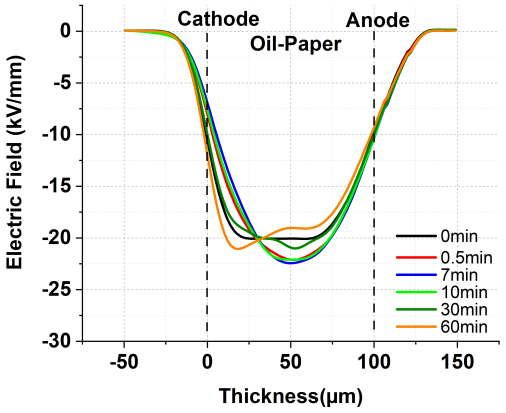

(E) 2.0wt% (Mineral Oil-Paper)

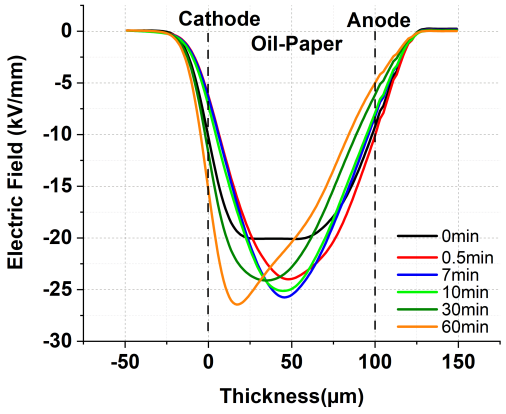

(C) 5.0wt% (Natural Ester Liquid-Paper)

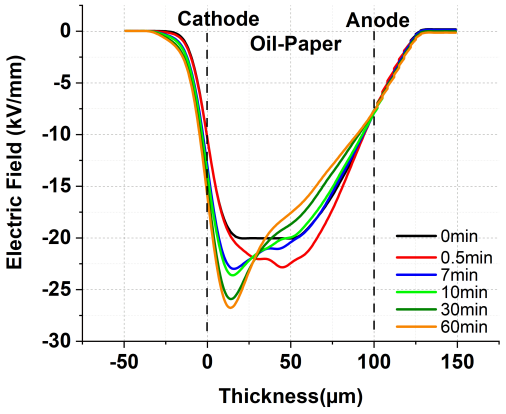

(F) 5.0wt% (Mineral Oil-Paper)

FIGURE 4.4: Electric Field Distribution of the Natural Ester Liquid-impregnated Paper, (A), (B), and (C), and the Mineral oil-impregnated Paper,(D), (E), and (F), with Different Moisture Contents

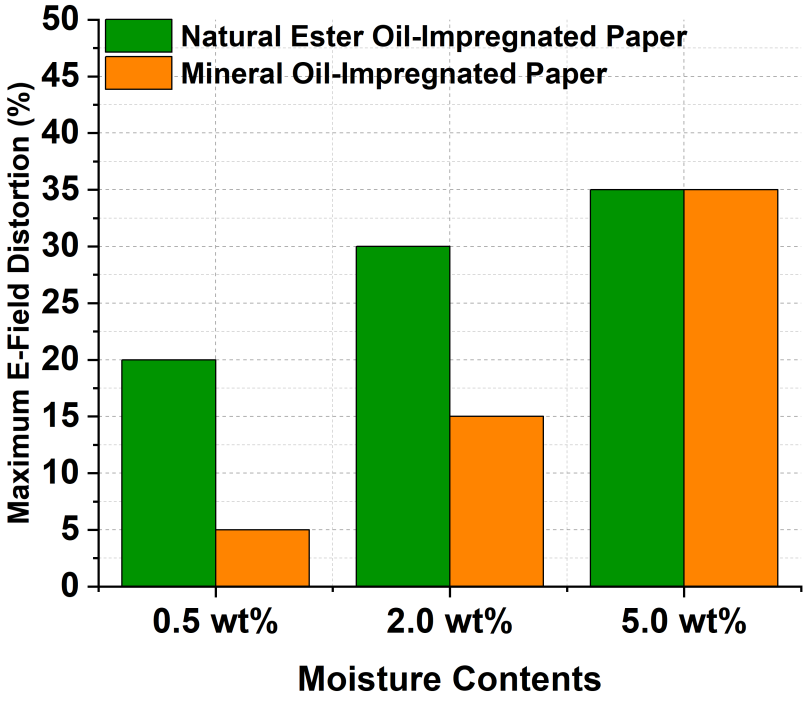

FIGURE 4.5: Electric Field Distortion Rate with Different Moisture Contents

Under dc conditions, space charges can accumulate in the oil-paper insulation system, causing electric field enhancement in the specific region, which can accelerate the degradation of the insulation system. Figure 4.4 represents electric field distributions and Figure 4.5 shows maximum electric field distortion rates with different moisture contents in the natural ester liquid-impregnated paper and the mineral oil-impregnated paper. The maximum electric field distortion was calculated based on Equation 4.2.

$$\Delta E = \frac{E_{max} - E_{applied}}{E_{applied}} \times 100(\%) \tag{4.2}$$

Regarding 0.5wt% and 2.0wt% of moisture contents, the natural ester liquid-impregnated paper had 20% and 30% of the maximum electric field distortion rates. On the other hand, the mineral oil-impregnated paper showed 5% and 15% of the maximum electric field distortion rate for 0.5wt% and 2.0wt% of moisture contents. This represents that when the moisture level is low in Kraft papers, the electric field distortion rate in the natural ester liquid-impregnated paper was greater than that in the mineral oil-impregnated paper because of its higher moisture content in the natural ester liquid. However, when the moisture content was 5.0wt% in Kraft papers, the maximum electric field distortion rate was 35% for both oil-impregnated papers. In terms of electric field enhancement, mineral oil-impregnated paper is more sensitive to water than natural ester liquid-impregnated paper.

4.6 Space Charge Decay

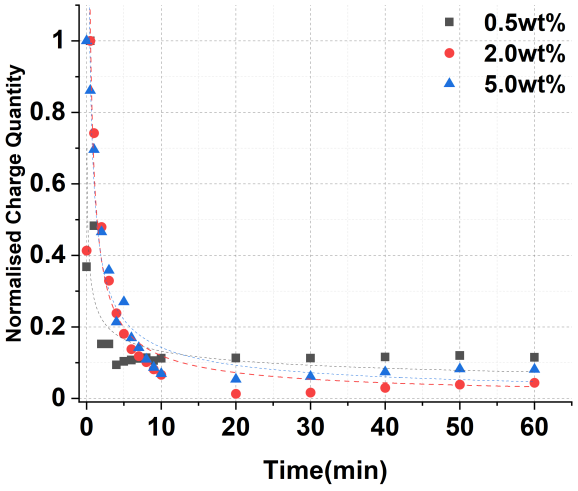

(A) Natural Ester Liquid-impregnated Paper

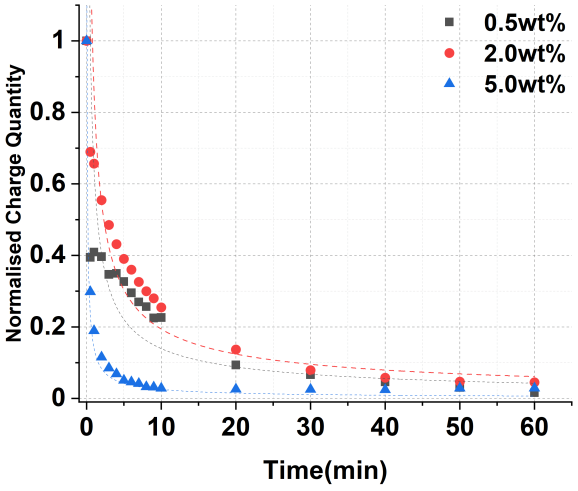

(B) Mineral oil-impregnated Paper

FIGURE 4.6: Total Charge Decay with Different Moisture Contents

The space charge decay for the natural ester liquid-impregnated paper and the mineral oil-impregnated paper was depicted in Figure 4.6. After removing the dc voltage, the space charge decay was observed for 60 minutes.

Most charges dissipated quickly within the first 10 minutes for the natural ester liquid-impregnated paper. The natural ester liquid had a greater polarity, which attracted more water. Thus, the higher the polarity, the higher the dc conductivity, which led to that charges can easily escape from traps in the natural ester liquid-impregnated

paper [70]. As a result, fast charge dissipation occurred in the natural ester liquid-impregnated paper.

The mineral oil-impregnated paper showed that when Kraft paper had 0.5 wt% and 2.0wt% of moisture contents, it took about 30 minutes to dissipate most charges. However, when the moisture level was high (5.0wt%), the mineral oil-impregnated paper showed that most charges were dissipated within the first 10 minutes. When the moisture contents were low (0.5wt% and 2.0wt%), the rate of charge dissipation was slower in the mineral oil-impregnated paper than in the natural ester liquid-impregnated paper.

4.7 Discussion

Unlike a dielectric liquid, cellulose in the HVDC converter transformer is not easily accessible. Thus, it is crucial to investigate the difference between natural ester liquid-impregnated paper and mineral oil-impregnated paper regarding the impact of moisture. As shown above, moisture significantly affects the space charge dynamics of the natural ester liquid-impregnated paper and the mineral oil-impregnated paper. When the moisture increases, charges are more likely to have higher mobility [92]. In other words, the increase in moisture facilitates charges to penetrate deeper into the oil-impregnated paper [92].

When the moisture level was low, fewer charges were injected into the mineral oil-impregnated paper than the natural ester liquid-impregnated paper. As a result, the mineral oil-impregnated paper showed only 5% of the maximum electric field distortion, while 20% of the maximum electric field distortion rate occurred in the natural ester liquid-impregnated paper. In a dry state, although the influence of moisture was subtle, a relatively larger amount of moisture in natural ester liquid aided that more charges were injected into cellulose than mineral oil. When the moisture level was moderately wet (2.0wt%), it showed a slight heterocharge accumulation in the mineral oil-impregnated paper due to increased mobility of charges, while natural ester liquid-impregnated paper did not show the heterocharge accumulation for 60 minutes.

When cellulose was extremely wet (5.0wt%), a significant difference was observed between the natural ester and mineral oils. natural ester liquid tends to absorb the water due to its high polarity, which produces fatty acids, as shown in Figure 4.7, so this characteristic leads natural ester liquid to have a great affinity for moisture [93].

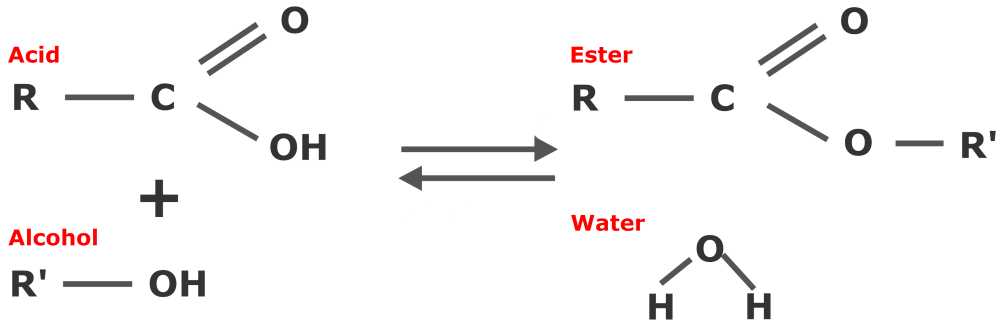

FIGURE 4.7: Esterification Process of the Ester-based Fluid

Therefore, when cellulose contains a high moisture level, natural ester liquid captivates the water from the cellulose. On the other hand, mineral oil has a hydrophobic property, so when cellulose has a high moisture level, mineral oil forces water to stay in the cellulose. As a result, if the moisture level is high, the mineral oil-impregnated paper is more affected by water than the natural ester liquid-impregnated paper. Thus, the mineral oil-impregnated paper forms faster heterocharge accumulations under high moisture level conditions than the natural ester liquid-impregnated paper. In addition, the mineral oil-impregnated paper showed a lower maximum electric field distortion rate under low moisture level conditions (0.5wt% and 2.0wt%). However, when cellulose contained a high moisture level (5.0wt%), the same maximum electric field distortion rate was observed in both oil-impregnated papers. This indicates that the great affinity for moisture in the natural ester liquid can be advantageous when the cellulose contains high moisture content. On the other hand, space charge characteristics in the mineral oil-impregnated paper were more susceptible to moisture than in the natural ester liquid-impregnated paper.

After the applied voltage was removed, the space charge decay for both natural ester liquid-impregnated paper and mineral oil-impregnated paper was observed. The decay process can be influenced by the charging time and the number of deep traps in the sample [94]. Furthermore, the sample's dc conductivity is the major factor influencing charge decay [95].

In dry conditions (0.5wt%), it seems that the oil properties, rather than moisture, mainly influenced both the natural ester liquid-impregnated paper and the mineral oil-impregnated paper in terms of space charge decay. However, when the moisture content of the Kraft paper increases, the interaction of oil and moisture appears to be strongly involved in space charge decay. In common, even though both oil-impregnated papers accumulated more charges with 5.0wt% of moisture compared to 2.0 wt% during the volts-on process, most charges were dissipated more quickly. The higher conductivity caused by higher moisture levels is thought to improve charge mobility [95].

The difference is that if a large amount of moisture is present in the Kraft paper, some moisture can be absorbed by natural ester liquid due to the hydrolysis interaction between natural ester liquid and moisture. This characteristic resulted in only a slight increase in the rate of charge dissipation of the natural ester liquid-impregnated paper at 5.0wt% moisture compared to 2.0 wt% moisture. On the other hand, there is no hydrolysis process between mineral oil and moisture. Therefore, when the Kraft paper contained 5.0wt% of moisture, most of the moisture remained in the Kraft paper. As a result, the rate of charge dissipation in the mineral oil-impregnated paper increased significantly compared to the condition with 2.0 wt% moisture.

4.8 Summary

Moisture is one of the most undesirable substances in the oil-paper insulation system [46]. Cellulose is a hygroscopic material, so it must be maintained to be dry. natural ester liquids are made up of triglycerides, whereas mineral oils are made up of hydrocarbon chains. Thus, as moisture contents varied in the paper, natural ester and mineral oils showed some differences regarding reaction with the moisture.

As the moisture in the paper increased, the moisture moved from the paper to the natural ester liquid, which is due to the hydrophilic nature of the natural ester liquid. On the other hand, the hydrophobic nature of mineral oil prevented moisture from travelling from the paper to the oil.

As the amount of moisture in the paper increased, heterocharges began to accumulate near the cathode. However, natural ester liquid delayed the accumulation of heterocharges compared to mineral oil.

Lastly, the mineral oil-impregnated paper had a slow charge dissipation rate when it was dry, but it became faster as the moisture increased. However, natural ester liquid-impregnated paper showed a fast charge dissipation rate regardless of moisture.

Chapter 5

Influence of Thermal Ageing on Space Charge Characteristics of natural ester liquid-impregnated Paper

5.1 Research Motivation

Natural ester liquid is one of the most promising candidates to replace mineral oils for HVDC converter transformers. They are produced from plentiful renewable resources, such as soybean and rapeseed, which are fully biodegradable [51]. Furthermore, natural ester liquid has a relatively higher flash and fire point (above 300°C) than mineral oil, reducing fire risk significantly [51].

Transformer oil and cellulose are subject to electrical, mechanical, and thermal stresses and degrade over time during the operation of transformers [96]. When transformers are exposed to long-term thermal stress, cellulose can become brittle and might break away from the transformer winding, causing sludge to accumulate [96]. Additionally, due to thermal ageing, water can be created as a by-product, and local carbonisation of the paper can increase conductivity, leading to overheating and conductor failures [96].

natural ester liquids are resilient to fire, easily biodegradable, and devoid of corrosive sulphur compounds [97]. In addition, it has been verified that ester-based fluids improve the lifespan of cellulose insulation, offering additional advantages to transformers. Even so, further information is still required regarding the dielectric performance of natural ester liquid through DC electric fields, as ester oils are predominantly used

in distribution transformers [97]. By comparing with the mineral oil-impregnated paper, this chapter explores how thermal ageing affected the space charge characteristics of the natural ester liquid-impregnated paper.

5.2 Acidity

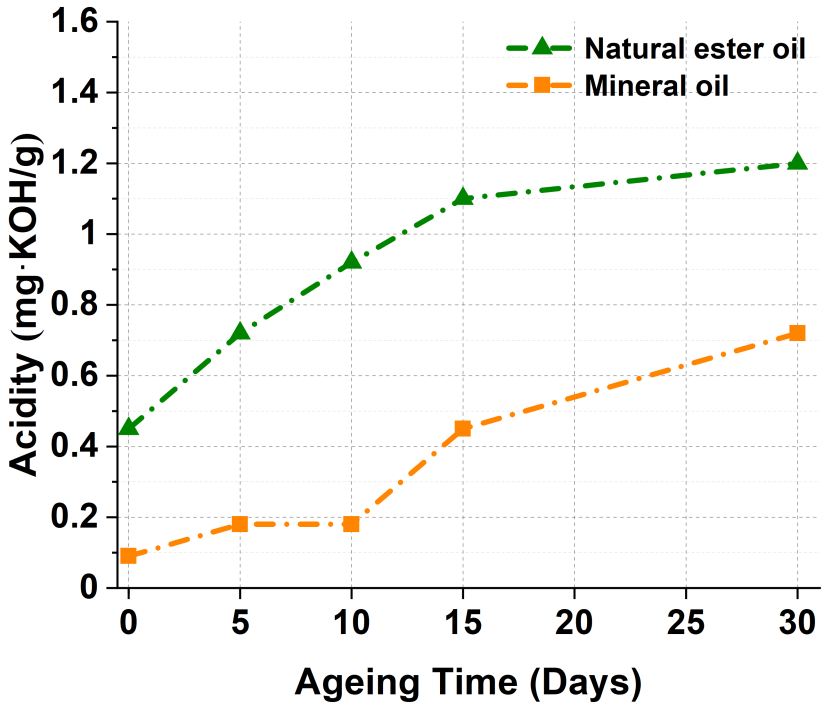

FIGURE 5.1: Acidity of Natural Ester Liquid and Mineral Oil during Thermal Ageing

Aged insulating paper and oil in transformers produce acids as by-products [12]. It is well known that low molecular acids (LMAs) in a transformer can accelerate the deterioration of an oil-paper insulation system [98]. natural ester liquid and mineral oil may have different chemical stability during thermal ageing due to their different properties [98].

Figure 5.1 represents the acidity of natural ester liquid and mineral oil during thermal ageing. As thermal ageing progressed, acid levels increased in both natural ester liquid and mineral oil. The acid level of natural ester liquid was considerably higher than that of mineral oil throughout thermal ageing. natural ester liquid increased from 0.45 mg·KOH/g to 1.2 mg·KOH/g, while mineral oil increased from 0.09 mg·KOH/g to 0.72 mg·KOH/g during 30 days of thermal ageing.

natural ester liquid has a triglyceride structure consisting of three fatty acids connected to a glycerol molecule [51]. Therefore, through hydrolysis, the water interacts with the triglycerides composing the natural ester to generate long-chain fatty acids [85]. In contrast, mineral oil mainly yields carboxylic acids through the oxidation of mineral oil or hydrolysis of Kraft paper during thermal ageing [99]. Unsaturated double bonds

of fatty acids frequently undergo several active reactions, such as oxidation, which reduces the oxidation stability of natural ester liquid [93]. Eliminating a hydrogen atom from the methylene group adjacent to a double bond can readily generate free radicals. Peroxy radicals are created when free radicals react quickly with oxygen. Then, the oxidation process can be furthered when the peroxy radical attacks other lipid molecules, removing a hydrogen atom to create hydroperoxide and another free radical [93]. Consequently, unsaturated double bonds and the hydrolysis process in natural ester liquid produce more acids than in mineral oil. Nevertheless, natural ester liquid mostly creates high molecular weight acids (HMA), whereas mineral oil primarily produces low molecular weight acids (LMA) [62].

Due to the lack of aggression and solubility in HMAs, they do not significantly contribute to the degradation of Kraft paper [99]. On the other hand, LMAs are more hydrophilic and corrosive and absorbed by Kraft paper, accelerating cellulose degradation [99]. During thermal ageing, natural ester liquid mainly produces HMAs, which are not aggressive, but natural ester liquid still produces more acids compared to mineral oil. Even though HMAs from natural ester liquid are beneficial, they still have some impact on dielectric properties [100]. Thus, it is crucial to understand how the space charge characteristics of natural ester liquid-impregnated paper are affected by the acidity that occurs during thermal ageing.

5.3 Degree of Polymerisation

Cellulose consists of alpha-D-glucose units, and the degree of polymerisation (DP) is measured by the number of monomer glucose units, which for new paper might range from 1100 to 1600 [37]. However, after drying and oil impregnation, the DP number may decrease by 10% of its initial value [37]. Thermal ageing is a primary factor that reduces the DP via depolymerisation. When cellulose is depolymerised, the linkages are broken through hydrolytic decomposition and ring structure breakdown, which produces by-products such as CO, CO2, and water [37]. By lowering the DP, cellulose's mechanical strength is consequently diminished. Therefore, it is crucial to comprehend how different effects of natural ester liquid and mineral oil on cellulose's mechanical strength during thermal ageing.

The degree of polymerisation of natural ester liquid-impregnated paper and mineral oil-impregnated paper with different thermal ageing times is depicted in Figure 5.2. The DP of both oil-impregnated papers gradually decreased as thermal ageing progressed. The DP of natural ester liquid-impregnated paper decreased from 1111 to 633, whilst the DP of paper with mineral oil-impregnated paper reduced from 1015 to 447. The results indicated that natural ester liquid had a slower rate of cellulose degradation than mineral oil.

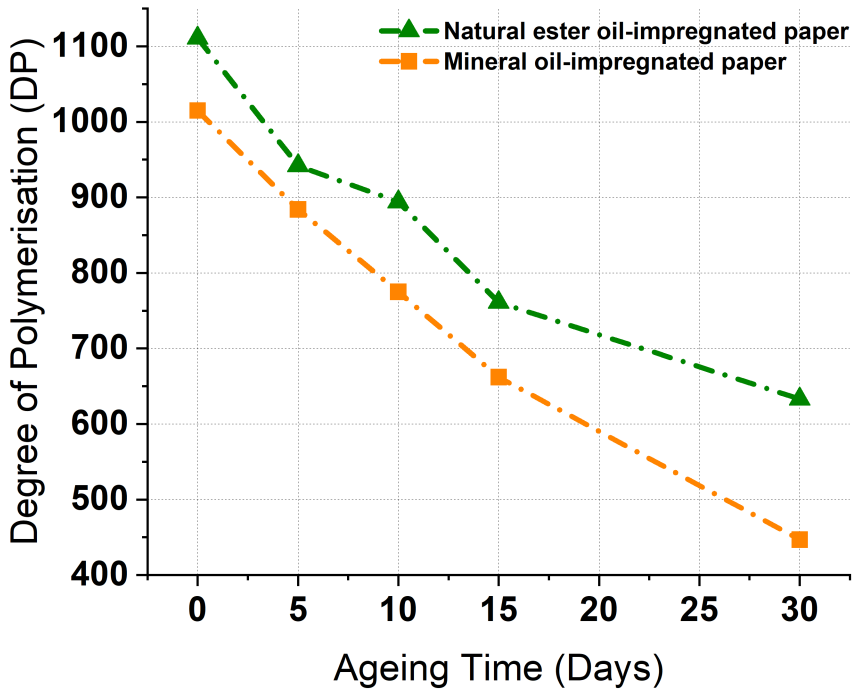

FIGURE 5.2: Degree of Polymerisation of Natural Ester Liquid-impregnated Paper and Mineral Oil-impregnated Paper during Thermal Ageing

Cellulose hydrolysis during thermal ageing produces acids and water, contributing to cellulose degradation acceleration [101]. As a result, the natural ester liquid may be able to dissolve more water, which generates more long-chain fatty acids [100]. Consequently, paper with natural ester liquid may be drier than paper with mineral oil during thermal ageing. Moreover, unlike mineral oil, acids generated from natural ester liquid are not aggressive towards cellulose. These effects may result in a slower degradation process for paper impregnated with natural ester liquid.

Clearly, there are still many other factors to consider when analysing cellulose's mechanical strength during thermal ageing. However, according to the results, natural ester liquid can protect cellulose more effectively than mineral oil as it absorbs more water and produces non-aggressive acids.

5.4 DC conductivity

Figure 5.3 shows that the DC conductivity of both the natural ester liquid-impregnated paper and mineral oil-impregnated paper increased as thermal ageing progressed. During 30 days of thermal ageing, the DC conductivity of the natural ester liquid increased from 3.14×10^{-14} S/m to $3.6 \times 10^{-13} S/m$, whilst the mineral oil-impregnated paper

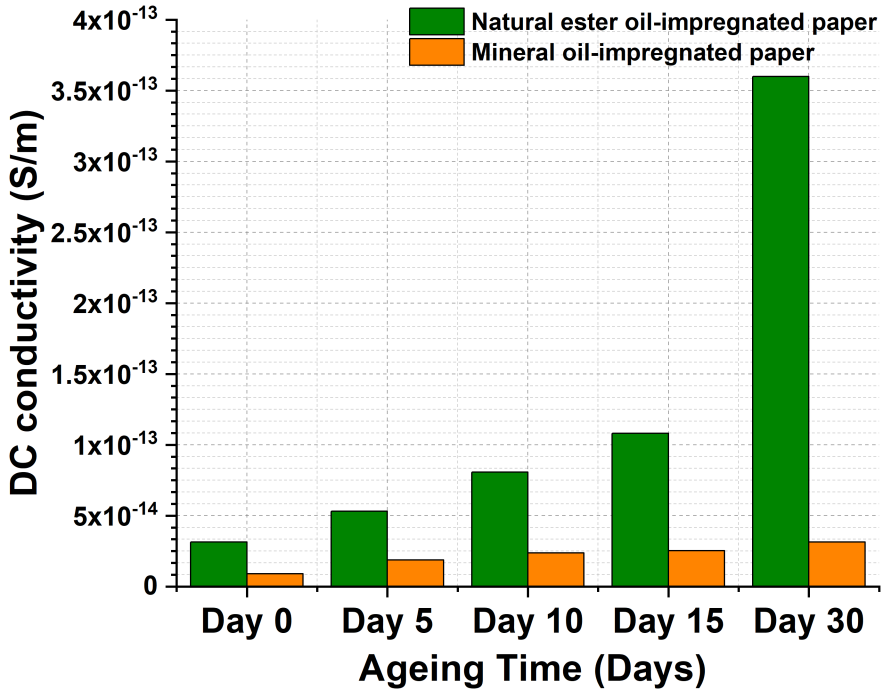

FIGURE 5.3: DC Conductivity with Different Thermal Ageing Times

showed that dc conductivity increased from $8.96 \times 10^{-15} S/m$ to $3.14 \times 10^{-14} S/m$. The results found that the DC conductivity of the natural ester liquid-impregnated paper was much higher than that of the mineral oil-impregnated paper under thermal ageing conditions. The DC conductivity of the natural ester liquid-impregnated paper rose 11.46 times from its initial state to day 30. However, after 30 days of thermal ageing, the DC conductivity of mineral oil-impregnated paper increased by only 3.5 times.

The water solubility of natural ester liquid is significantly greater than that of mineral oil. In other words, natural ester liquid interacts with water more vigorously during the thermal ageing period and creates more fatty acids than mineral oil. Consequently, this hydrophilic characteristic and the production of a greater amount of acid can improve the mobility of charges, resulting in a significantly greater increase in the DC conductivity for the natural ester liquid-impregnated paper under thermal ageing conditions.

5.5 Space Charge Characteristics

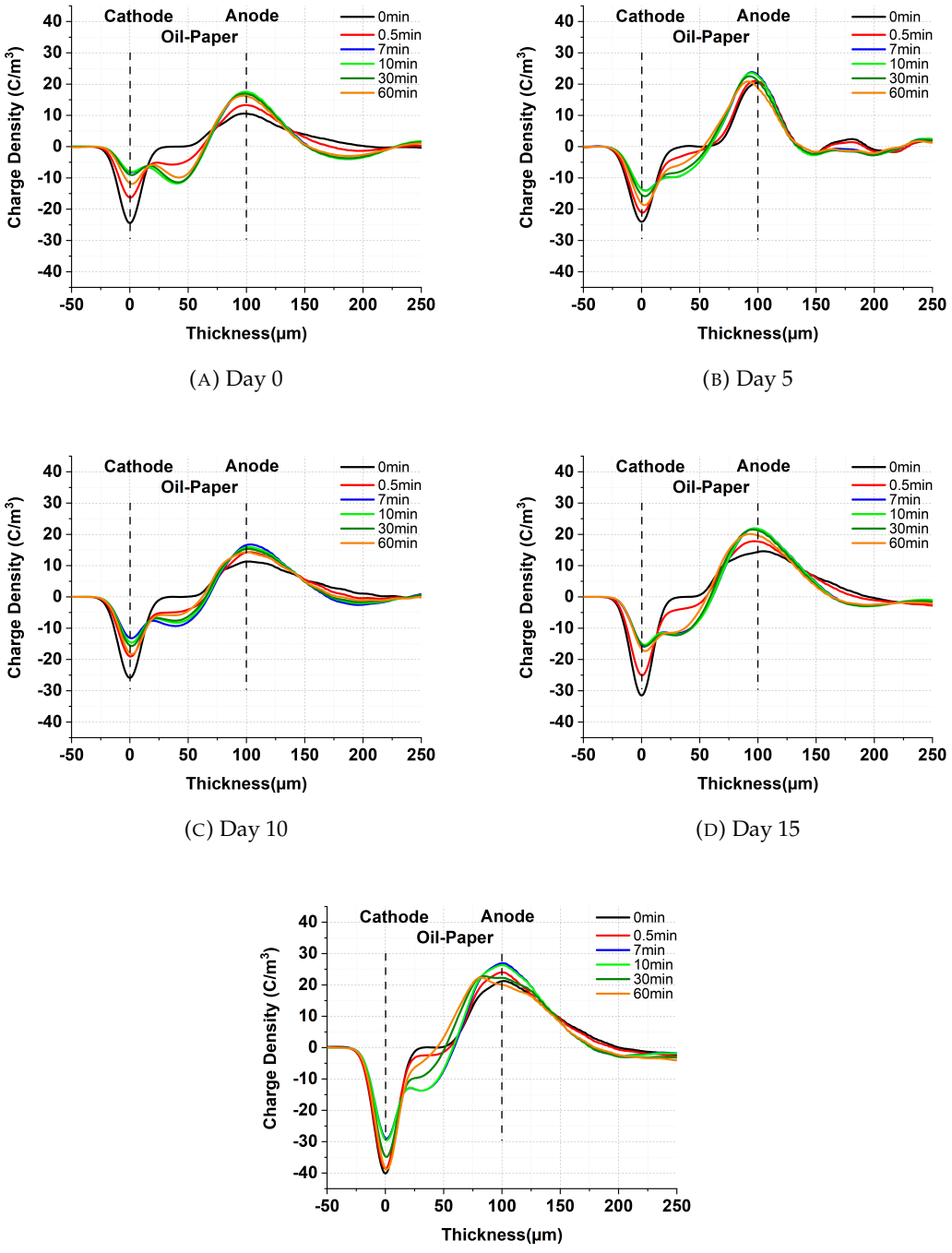

(A) Day 0

(B) Day 5

(C) Day 10

(D) Day 15

(E) Day 30

FIGURE 5.4: Space Charge Characteristics of Natural Ester Liquid-impregnated Paper during Thermal Ageing

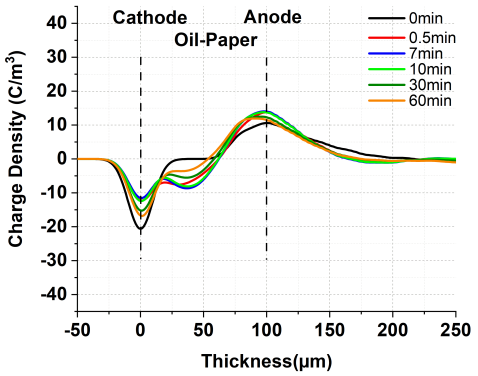

(A) Day 0

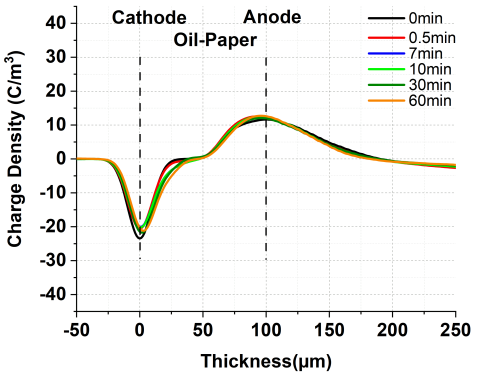

(B) Day 5

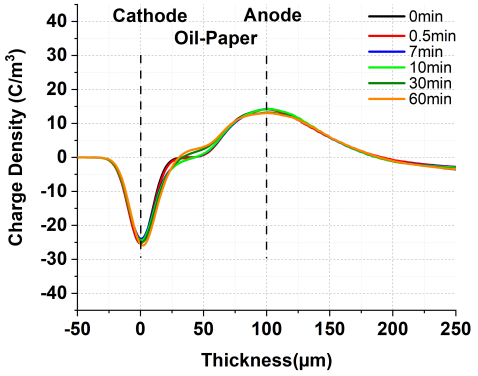

(C) Day 10

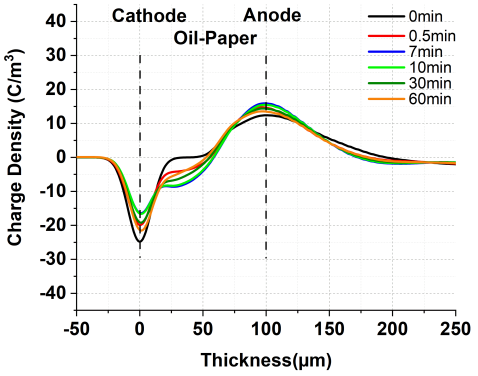

(D) Day 15

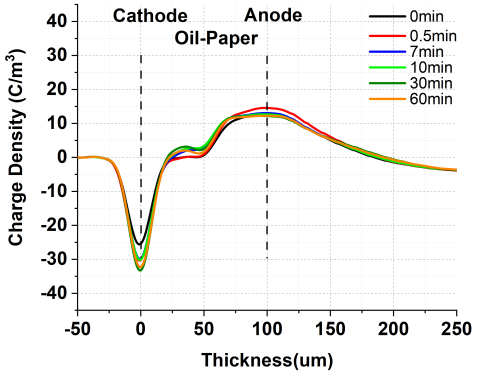

(E) Day 30

FIGURE 5.5: Space Charge Characteristics of Mineral oil-impregnated Paper during Thermal Ageing

Space charge accumulation has been identified as a critical challenge in dielectric materials under DC conditions [91]. The presence of space charge enhances the local electric field, causing dielectric materials to degrade or possibly breakdown prematurely [91].

Figure 5.4 and Figure 5.5 represent space charge characteristics of natural ester liquid-impregnated paper and mineral oil-impregnated paper under thermal ageing conditions. After applying DC voltage, the electric potential barrier between electrodes and oil-impregnated paper lowered. Therefore, when DC voltage was supplied, obvious homocharges were injected from electrodes into oil-impregnated papers.

In Figure 5.4 (A), when the natural ester liquid-impregnated paper was in its fresh condition, negative charges were injected into it, and these charges eventually accumulated in the middle of the sample. This reduced the peak charge density near the cathode, whereas the negative charge accumulated in the middle, which induced positive charges, thereby increasing the peak charge density near the anode. After 5 and 10 days of thermal ageing in Figure 5.4(B) and (C), the space charge characteristics of the natural ester liquid-impregnated paper were similar to the fresh condition. Nonetheless, after 15 days, as shown in Figure 5.4 (D) and (E), more negative charges penetrated into the middle of the natural ester liquid-impregnated paper. Because of the increased charge mobility, more negative charges were injected from the cathode, and more positive charges were injected from the anode when thermal ageing reached 30 days. Due to the recombination effect between negative and positive charges in the middle of the natural ester liquid-impregnated paper, negative charges gradually decreased over time, while the positive charge accumulated in the middle. As a result, the positive charges that accumulated in the middle of the natural ester liquid-impregnated paper induced negative charges adjacent to a cathode, increasing the cathode's peak charge density.

Like fresh natural ester liquid-impregnated paper, when a DC voltage was applied, negative charges were injected and accumulated in the middle of the fresh mineral oil paper-impregnated paper, as shown in Figure 5.5 (A). However, when thermal ageing reached 5 and 10 days in Figure 5.5 (B) and (C), it was observed that fewer negative charges were injected into the middle of the mineral oil-impregnated paper as compared to the fresh condition. As thermal deterioration progresses, this leads to loss of moisture retention as cellulose loses fibre flexibility [102]. Therefore, it is believed that fewer negative charges were injected during the deterioration period of 5 and 10 days due to the lower amount of moisture in the cellulose than in the fresh condition. However, the loss of water retention of cellulose may increase brittleness, which causes a decrease in mechanical strength [91]. As the ageing period reached 15 days, as shown in Figure 5.5 (D), negative charges were injected again into the middle of the mineral oil-impregnated paper with increased acidity. When the thermal deterioration period reached 30 days in Figure 5.5 (E), the high acidity increased the charge mobility, resulting in the positive charge from the anode accumulated in the middle of the mineral oil-impregnated paper. Consequently, positive charges accumulated in the middle of the paper, inducing negative charges near the cathode, and increasing the peak charge density of the cathode.

Moisture is the most hazardous by-product regarding transformer operation, but when the cellulose is in the dry state, the properties of transformer oil are the most crucial factor for space charge properties during the ageing period. According to the results, the generation of fatty acids due to the water affinity of the natural ester liquid led to an increase in conductivity and more space charge accumulation in the natural ester liquid-impregnated paper during thermal ageing.

5.6 Total Charge Amount

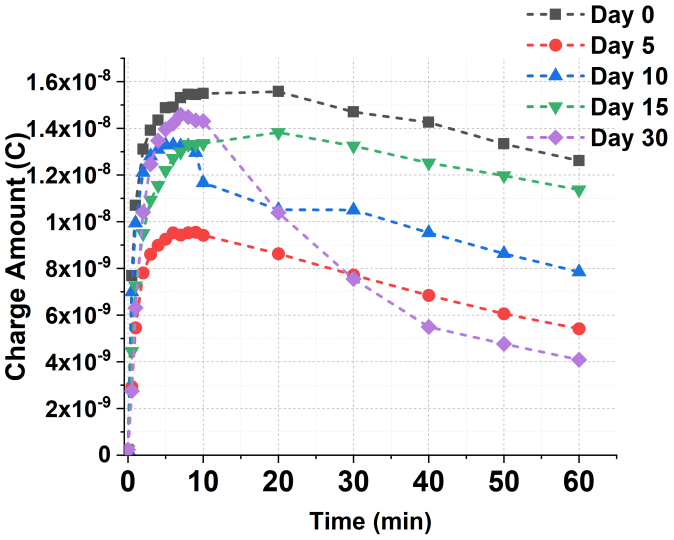

(A) Natural Ester Liquid-impregnated Paper

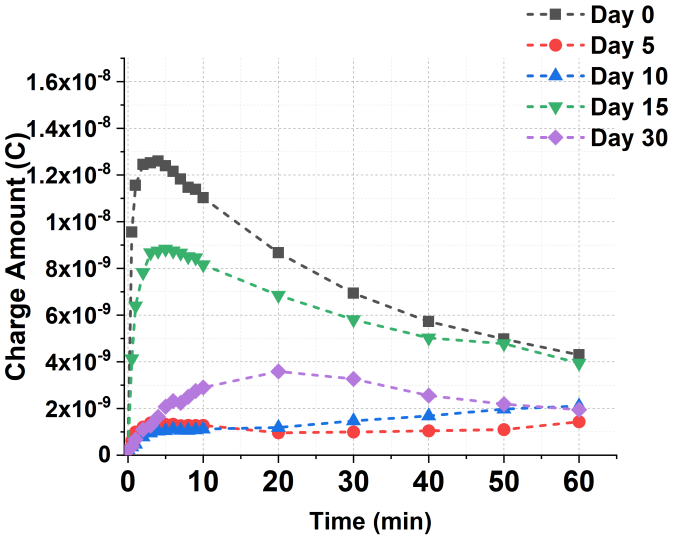

(B) Mineral Oil-impregnated Paper

FIGURE 5.6: Total Amount of Charge during Thermal Ageing

Fiure 5.6 depicts the total charges in the natural ester liquid-impregnated paper and mineral oil-impregnated paper for 60 minutes with different thermal ageing periods. To observe the impact of thermal ageing on space charge accumulation in the sample, the charge density at electrodes was exempted.

Both oil-impregnated papers had the largest amount of charges when they were in a fresh state and a smaller amount of charges accumulated after thermal ageing. Then, the total amount of charge accumulated in the natural ester liquid-impregnated paper gradually increased as thermal ageing progressed. However, when the mineral oil-impregnated paper reached 15 days of thermal ageing, the total charges rose due to increased acidity. The recombination effect reduced the total amount of charges after 30 days, but positive charges began to accumulate in the middle of the mineral oil-impregnated paper due to the increased acidity and DC conductivity.

5.7 Space Charge Decay

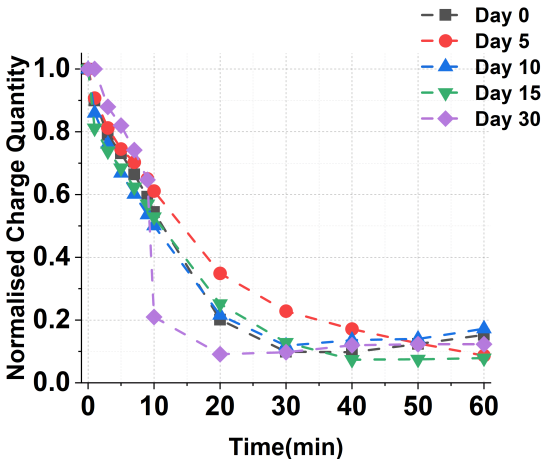

(A) Natural Ester Liquid-impregnated Paper

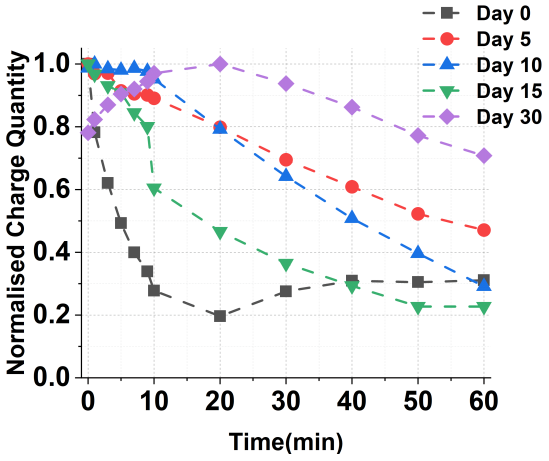

(B) Mineral Oil-impregnated Paper

FIGURE 5.7: Space Charge Decay (Normalised Charge Quantity)

Figure 5.7 shows space charge decay between natural ester liquid-impregnated paper and mineral oil-impregnated paper under thermal ageing conditions. During thermal ageing, the natural ester liquid-impregnated papers exhibited faster charge decay rates than the mineral oil-impregnated papers. Due to the presence of polar ester groups in its chemical structure, the hydrophilic nature of natural ester liquid can create extra charge transport pathways, which can make it easier to move charges. This can lead to a reduction in charge-trapping properties and an increment in charge mobility, eventually leading to a faster charge decay.

Therefore, natural ester liquids are probably better suited for high-voltage applications, which require rapid charge decay to mitigate space charge accumulation, such as the polarity reversal effect.

5.8 Electric Field Distortion

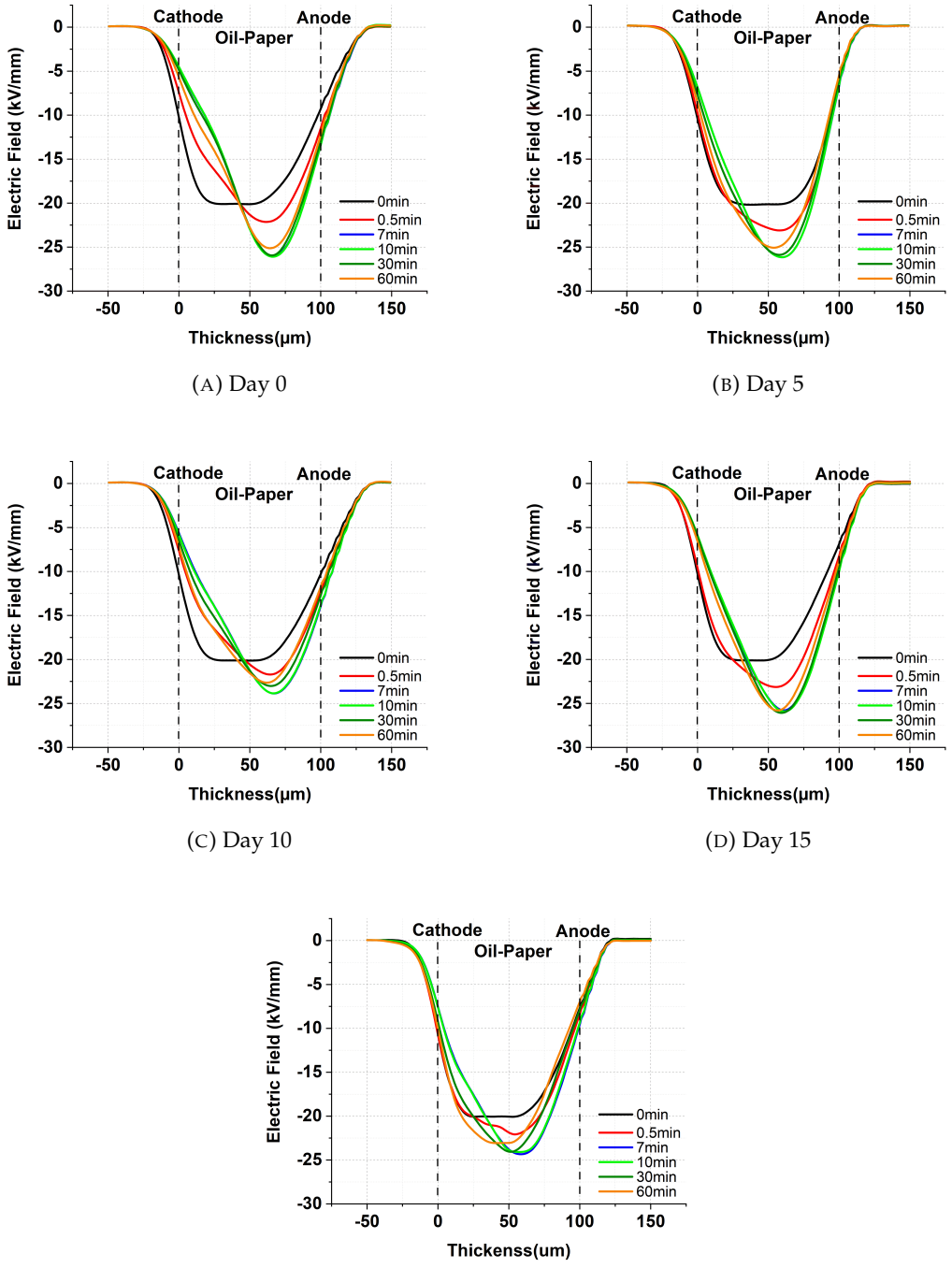

(A) Day 0

(B) Day 5

(C) Day 10

(D) Day 15

(E) Day 30

FIGURE 5.8: Electric Field Distributions of Natural Ester Liquid-impregnated Paper during Thermal Ageing

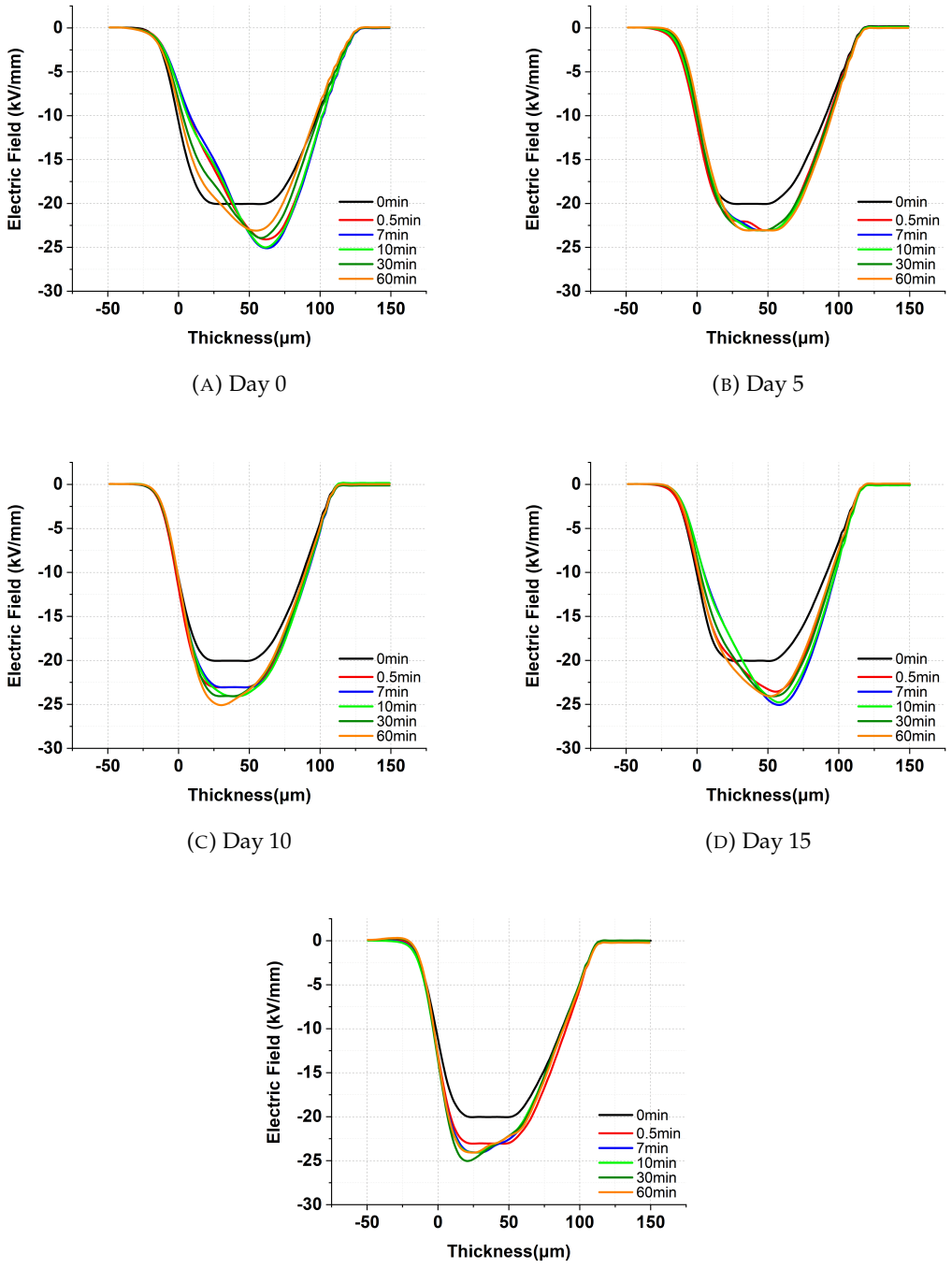

(A) Day 0

(B) Day 5

(C) Day 10

(D) Day 15

(E) Day 30

FIGURE 5.9: Electric Field Distributions of Mineral Oil-impregnated Paper during Thermal Ageing

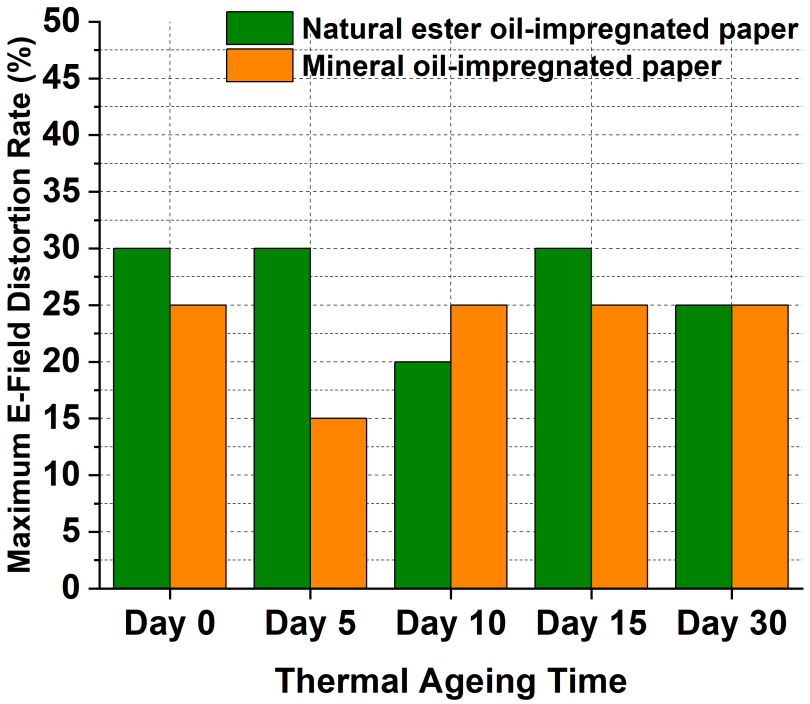

FIGURE 5.10: Electric Field Distortion Rate in Oil-impregnated Papers under Thermal Ageing Conditions

The space charge accumulation can enhance the electric field in specific areas of the oil-paper insulation system, hence accelerating its deterioration. Figure 5.8 and Figure 5.9 represent electric field distributions of natural ester liquid-impregnated paper and mineral oil-impregnated paper during thermal ageing, respectively. Figure 5.10 illustrates maximum electric field distortion rates in oil-impregnated papers under thermal ageing conditions.

During the 30-day thermal ageing period, natural ester liquid-impregnated papers had a maximum field distortion of 20-30%, while mineral oil-impregnated papers had a maximum field distortion of 15-25%. Compared with the fresh condition, when the thermal ageing period reached 30 days, the maximum electric field distortion rate of the natural ester liquid-impregnated paper was reduced by 5%, and the mineral oil-impregnated paper had the same maximum electric field distortion rate as the fresh condition. Eventually, when the thermal ageing reached 30 days, they had the same maximum field distortion.

5.9 DC breakdown

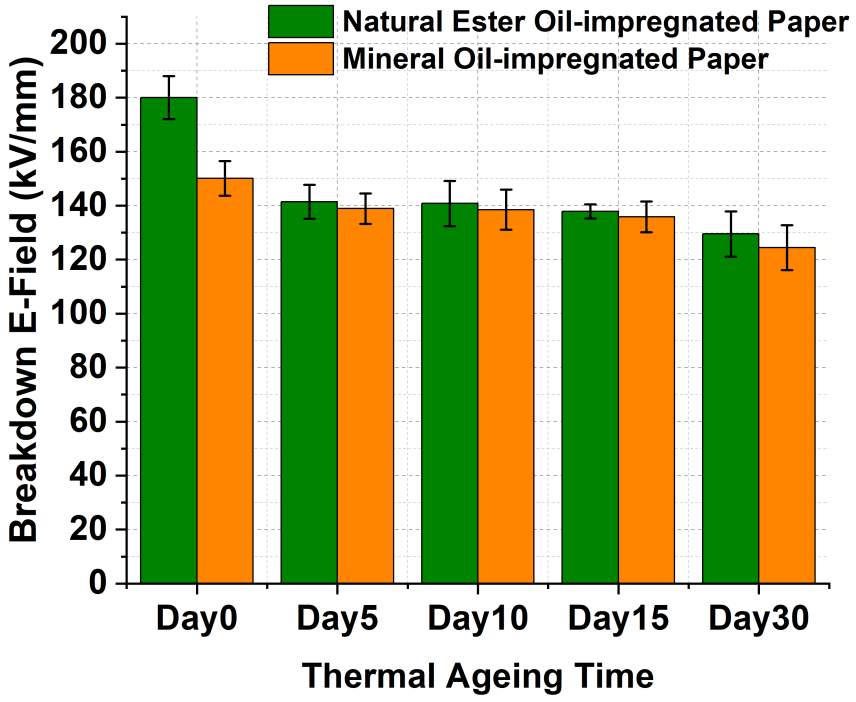

FIGURE 5.11: DC Breakdown Voltages of Oil-impregnated Papers during Thermal Ageing

Fig. 12 describes the DC breakdown voltages of the natural ester liquid-impregnated paper and mineral oil-impregnated paper. The DC breakdown voltage of the fresh natural ester liquid-impregnated paper was 180.4 kV/mm, and after 5 days of thermal ageing, it was 141.4 kV/mm. After that, the DC breakdown voltage decreased slightly until a thermal ageing period of 30 days was reached.

However, the fresh mineral oil-impregnated paper has a DC breakdown voltage of 151.0 kV/mm. Afterwards, the dc breakdown voltage of the mineral oil-impregnated paper slightly reduced as the thermal ageing process progressed. It was shown that the natural ester liquid-impregnated paper had a higher DC breakdown voltage than the mineral oil-impregnated paper during thermal ageing. As the DP decreased due to thermal ageing, the DC breakdown voltage of natural ester liquid-impregnated paper and mineral oil-impregnated paper was also reduced. Apart from the initial drop, the electrical strength of both oil-impregnated papers was slightly affected by further thermal ageing.

The observed slight decrease in DC breakdown strength does not strongly correlate with the mechanical loss of the paper during thermal ageing. It is likely that by-products of thermal ageing mainly influence DC breakdown rather than mechanical loss, suggesting a subtle impact of thermal ageing on dielectric performance.

5.10 Discussion

It is widely acknowledged that natural ester liquids have much higher water affinity than mineral oils. Therefore, natural ester liquids react with water to produce significantly more fatty acids than mineral oils as thermal ageing progresses.

Chemical ageing is another mechanism of ageing in Kraft paper. Kraft paper is composed of cellulose fibres, lignin, and other substances [36]. These materials have the potential to react with external chemicals like acids over time, which could result in a reduction in mechanical strength and an increase in electrical conductivity [103]. Thus, even though the total amount of space charge in the mineral oil impregnated-paper was less than that of natural ester liquid-impregnated paper during thermal ageing, the DC breakdown strength was lower due to mechanical loss, which was harmed by LMA [103]. However, although the natural ester liquid-impregnated paper produced a larger amount of acids than the mineral oil-impregnated paper, most acids produced by natural ester liquid were HMA, which was not harmful to Kraft paper. The higher dielectric constant of the natural ester liquid tends to have higher polarisability, which makes it a better solvent for polar and ionic compounds, so natural ester liquid tends to absorb more polar compounds from Kraft paper compared to mineral oil [97]. Therefore, this possibly helps the natural ester liquid aids to have higher breakdown strength of Kraft paper than mineral oil.

Although the amount of accumulated charge initially decreased due to a reduction of water retention in the natural ester liquid-impregnated paper as thermal ageing progressed, the total charge amount increased again along with the increase in acidity. In comparison to mineral oil, natural ester liquid exhibits a significantly lower ionisation potential, as demonstrated by [104]. Hence, natural ester liquid requires a lower voltage to produce a substantial number of electrons than mineral oil. The ester group's greater ability to attract electrons may result in a greater impact on itself than the alkane in mineral oil, accelerating the transition from slow to fast charge injections [104]. As a result, natural ester liquid generates a greater number of electrons and positive ions. During the thermal ageing period, even though more charges accumulated in the natural ester liquid-impregnated paper than in the mineral oil-impregnated paper, the DC breakdown voltage was found to be greater in the natural ester liquid-impregnated paper. Under DC conditions, conductivity becomes more critical, so regarding the natural

ester liquid, higher conductivity may be beneficial for achieving a more uniform electric field distribution. Therefore, the point of electric stress tends to shift from liquid to solid when Kraft paper is impregnated with mineral oil [97].

However, when Kraft paper is impregnated with natural ester liquid, the point of electric stress tends to shift from a solid to a liquid, which partly explains why the oil-impregnated paper has a higher breakdown strength [97]. Nevertheless, both oil-impregnated papers that were subjected to thermal ageing did not suffer a significant reduction in their electrical strength. In addition, it demonstrated that natural ester liquid has a slower DP reduction in cellulose than mineral oil, suggesting that it may provide a longer service life for cellulose.

Therefore, if the HVDC transformer is well sealed from moisture, natural ester liquid has a remarkably high potential to replace mineral oil.

5.11 Summary

To assess the reliability and sustainability of natural ester liquid, it is essential to have a thermal ageing experiment to evaluate how the natural ester liquid acts in the long term under high-temperature conditions. During thermal ageing, the acidity of both oils increased. Even though the acidity in natural ester liquid was higher than that in mineral oil during thermal ageing, the breakdown strength of the natural ester liquid-impregnated paper was higher than that of the mineral oil-impregnated paper. During thermal ageing, mineral oil mainly produces LMA, so it may accelerate the mechanical loss of the paper, which can reduce the breakdown strength.

Under thermal ageing conditions, the natural ester liquid-impregnated paper showed greater charges than the mineral oil-impregnated paper. This is probably because the lower ionisation level of the natural ester liquid contributed to the faster charge injection than the mineral oil. During thermal ageing, the DC breakdown strength of the natural ester liquid-impregnated paper and mineral oil-impregnated decreased slightly compared to the fresh condition. However, both oil-impregnated papers did not show a significant drop in DC breakdown. On the other hand, the DP number of both oil-impregnated papers decreased remarkably. This may indicate that thermal ageing is more likely to impact physiochemical properties rather than dielectric properties.

Chapter 6

Impact of Moisture on Space Charge Characteristics of Multilayer of Natural Ester Liquid-impregnated Paper

6.1 Research Motivation

HVDC converter transformers are essential equipment to maintain reliable and sustainable HVDC power transmission systems. Insulation is a vital part of the HVDC converter transformer, and it is required that the insulation system achieves the desired performance and reliability criteria. Oil-paper insulation systems are complex components of fluids and solids [105]. Therefore, the injection, transport, accumulation, and discharge characteristics regarding space charge between liquid and solid insulating materials are still unclear [105].

Often, a wide oil gap is applied for effective heat dissipation by circulating dielectric liquid in the HVDC converter transformer [105]. Nonetheless, interfaces serve as extra electrical barriers between transformer oil and cellulose in HVDC converter transformers, allowing space charge to accumulate [106]. The discontinuity between two different materials at the interface could be considered deep traps for charges [106]. Hence, it is vital to investigate the effect of multilayers on space charge dynamics.

In this study, the impacts of moisture on the space charge characteristics of double-layer natural ester liquid-impregnated paper were examined and compared to those of mineral oil-impregnated paper.

6.2 DC Conductivity

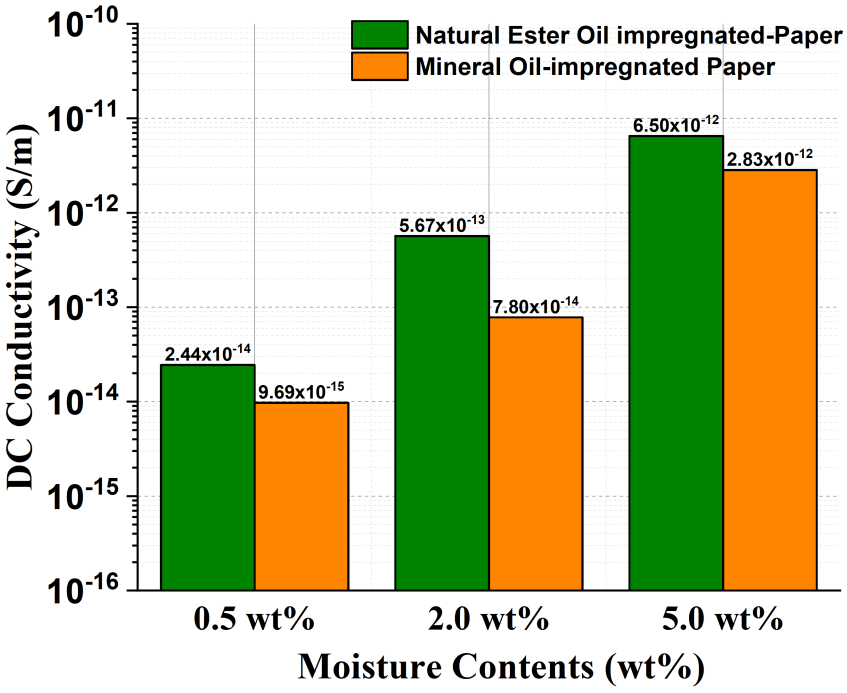

FIGURE 6.1: DC Conductivity of the Natural Ester Liquid-impregnated Paper and Mineral Oil-impregnated Paper with Different Moisture Contents (250μm of Thickness)

Moisture is an undesirable by-product of transformer operation that causes a rapid decrease in dielectric strength and has a significant impact on the transformer's lifespan [107]. This is because H+ and OH- dissociation in water increases the conductivity, leading to the accumulation of more space charge in the insulating material [92], [107]. As a result, in contrast to the AC field distribution, the DC field stress in HVDC converter transformers is heavily influenced by the conductivity of the cellulose and insulating liquid-based material [107].

The DC conductivity of natural ester liquid-impregnated paper and mineral oil-impregnated paper with different moisture contents is illustrated in Figure 5. The results demonstrated that the natural ester liquid-impregnated paper had a higher DC conductivity than the mineral oil-impregnated paper regardless of moisture content levels. Specifically, the DC conductivity of natural ester liquid-impregnated paper was $2.44 \times 10^{-14} S/m, 5.67 \times 10^{-13} S/m$, and $6.50 \times 10^{-12} S/m$ at 0.5wt%, 2.0wt%, and 5.0wt%, respectively. On the other hand, the mineral oil-impregnated paper showed $9.69 \times 10^{-15} S/m, 7.80 \times 10^{-14} S/m$, and $2.83 \times 10^{-12} S/m$ at the same moisture content level.

As the moisture content rose from 0.5 to 5.0wt%, the DC conductivity of natural ester liquid-impregnated paper increased by 266.39 times. However, under the same conditions, the DC conductivity increased 294.79 times for the mineral oil-impregnated paper. This shows that although the natural ester liquid-impregnated paper showed a higher DC conductivity, the rate of increase in the DC conductivity with increasing water content was faster in the mineral oil-impregnated paper. Ionisation is one of the main components of conduction in oil-paper insulation systems [107]. According to the results, the hydrophobic characteristic of the mineral oil enables moisture to be kept in the paper, which contributes to a faster rate of DC conductivity rises due to increased ionisation of the water.

6.3 Space Charge Characteristics

HVDC converter transformers rely heavily on the efficiency of their insulation system, which is generally made up of oil and cellulose. When space charge accumulates in the insulation system, it may affect its electrical properties significantly, and it can lead to failure and premature breakdown.

Consequently, an understanding of space charge characteristics is necessary for assessing the insulating properties of oil-paper systems.

Figure 6.2 and Figure 6.3 show the space charge characteristics of natural ester liquid-impregnated paper and mineral oil-impregnated paper with an oil gap, respectively, at different moisture contents. When a DC voltage was applied, the electric potential barrier between the electrodes and the sample decreased. This caused homocharges to be injected from both electrodes into the sample. The increase in moisture in an oil-paper insulation system creates more electrical pathways, which facilitates the penetration of more charges deeper into the sample. In addition, charges accumulate at the interface due to the discontinuity of the dielectric properties between the oil gap and the paper [106].

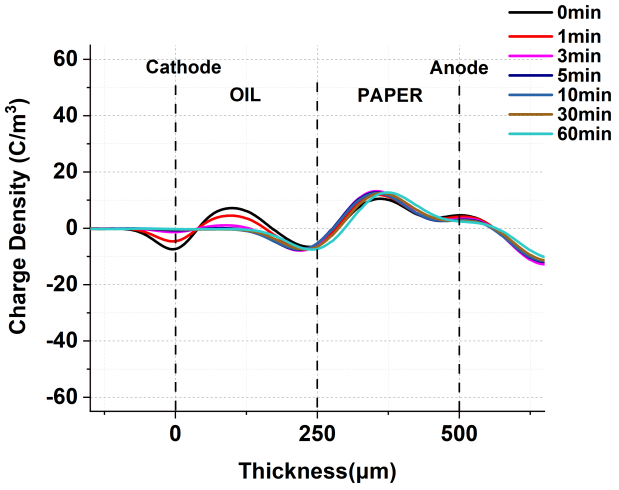

(A)

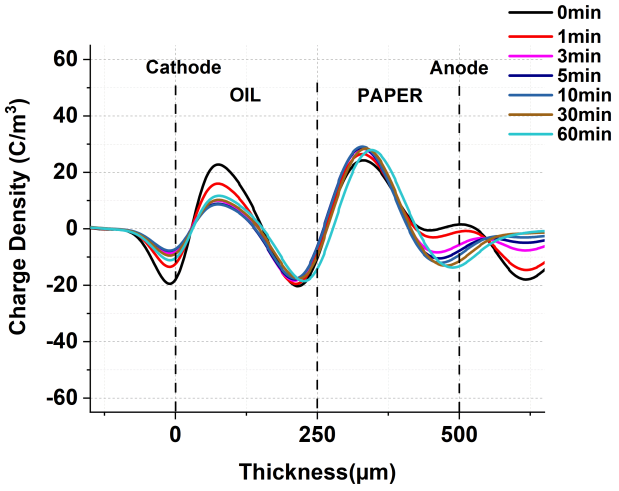

(B)

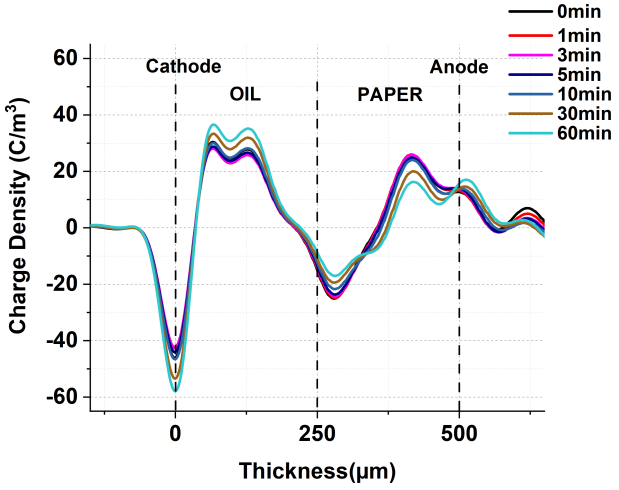

(C)

FIGURE 6.2: Space Charge Characteristics of Double Layers of Natural Ester Liquid and the Natural Ester liquid-impregnated Paper with Different Moisture Contents (A) 0.5 wt%, (B) 2.0 wt%, and (C) 5.0 wt%

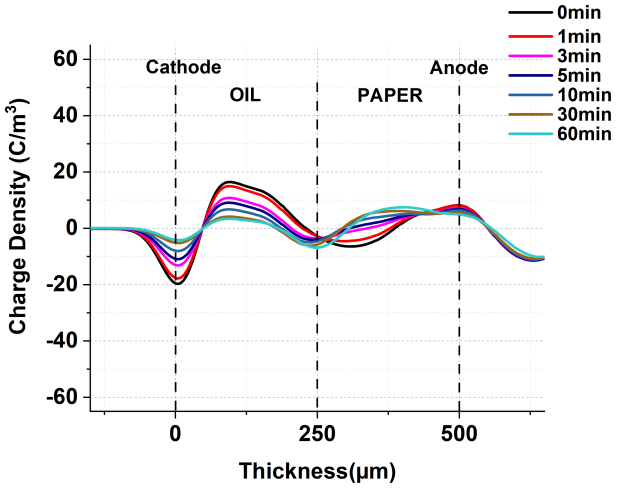

(A)

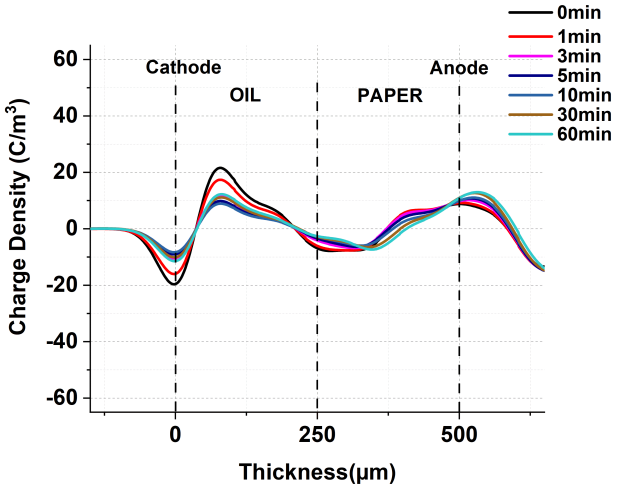

(B)

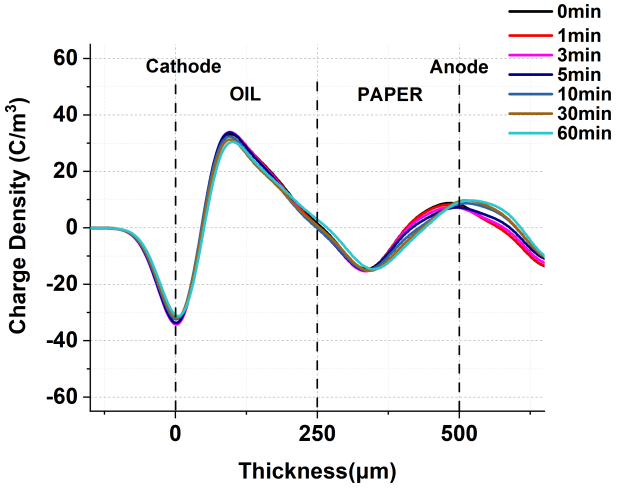

(C)

FIGURE 6.3: Space Charge Characteristics of Double Layers of Mineral Oil and the Mineral Oil-impregnated Paper with Different Moisture Contents (A) 0.5 wt%, (B) 2.0 wt%, and (C) 5.0 wt%

At a moisture content of 0.5wt% in the double layer of natural ester liquid-impregnated paper, obvious charges were injected from both electrodes. Ionisation energy represents the minimum energy needed to detach a loosely bound electron from one mole of a neutral gaseous atom [108]. The high electric field causes ionisation in the liquid dielectric, initiating the motion of ions that generates current within the liquid [108]. Therefore, a low ionisation energy of natural ester liquid can cause heterocharges between the cathode and the natural ester liquid gap. Therefore, when negative charges were generated near the cathode, they tended to recombine with heterocharges, causing the charge peak at the cathode to diminish over time. At a moisture content of 2.0wt% in the double layer of the natural ester liquid-impregnated paper, there was an increase in both positive and negative charge injection from the electrodes. Thus, it was observed that larger amounts of positive and negative charges accumulate at the oil-paper interface. At a moisture level of 2.0wt%, the recombination effect caused the charge peak value at the cathode to decrease over time, as was observed at a moisture level of 0.5wt%. Even though recombination effects were observed, after 60 minutes, heterocharges remained between the oil and cathode. When the paper has a moisture level of 5.0wt%, positive charges accumulate significantly near the cathode due to the ionisation effect and high DC conductivity. Due to the hydrophilic properties of the natural ester liquid, more water was transferred from the paper to the oil. As a result, the high level of moisture in the natural ester liquid created more electrical paths, which increased the mobility of charges significantly.

When the double layer mineral oil-impregnated paper contained 0.5wt% of water, the charge peak value at the cathode in the oil decreased over time due to the recombination effect, similar to the case of natural ester liquid. However, because the difference in permittivity between mineral oil and paper was greater than that between natural ester liquid and paper, this most likely resulted in a larger amount of charge accumulation in mineral oil, initially [109].

Consequently, it implies that the mineral oil-paper insulation system has a less uniformly distributed electric field than the natural ester liquid-paper insulation system. With a 2.0wt% moisture content, the double layer mineral oil-impregnated paper showed a higher initial accumulation of heterocharges in the oil due to moisture effects. In addition, the charge peak value near the anode progressively increased as more negative charges accumulated at the interface between the natural ester liquid and paper. Under extremely high moisture conditions of 5.0 wt%, a significant amount of heterocharges were observed to accumulate between the oil and cathode in double layer mineral oil-impregnated paper, similar to the pattern observed in natural ester liquid. In comparison to the 0.5wt% and 2.0wt% moisture conditions, the increased conductivity enabled more efficient charge movement, resulting in a greater charge peak value at the cathode.

Under the conditions of 0.5wt% and 2.0wt% moisture, the natural ester liquid-paper system showed that the charges were predominantly concentrated on the paper, whereas the mineral oil-paper system demonstrated that the charges were mainly concentrated on the oil. However, in an extremely high moisture environment of 5.0wt%, both samples showed that the charges were mainly concentrated in the oil.

Regarding the interface, the permittivity difference between the natural ester liquid and paper is relatively lower than between mineral oil and paper. The mismatch in permittivity between materials at the interface influences the accumulation and distribution of space charges [109]. Therefore, as moisture increases, more heterocharges in the paper can be found in the mineral oil-paper system. However, the natural ester liquid effectively inhibited the accumulation of heterocharges near the anode.

6.4 Total Charge Amount

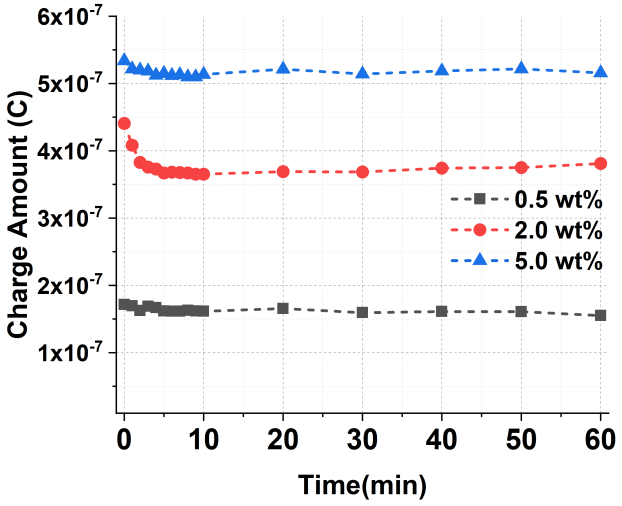

(A)

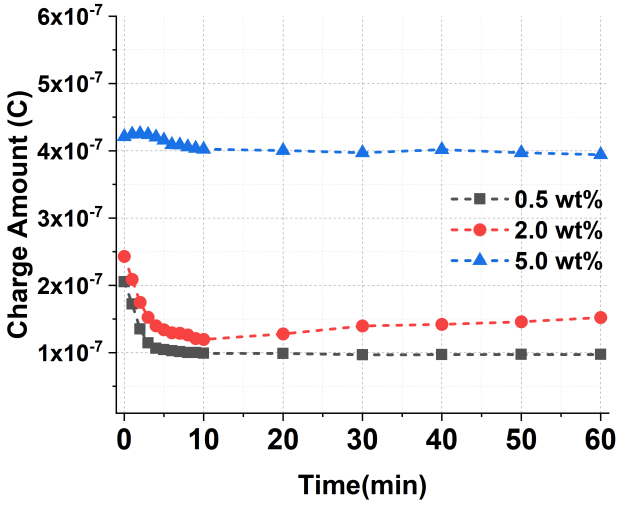

(B)

FIGURE 6.4: Total Amount of Charge with Different Moisture Contents (A) Double Layer of Natural Ester Liquid and Natural Ester Liquid-impregnated Paper (B) Double Layer of Mineral Oil and Mineral Oil-impregnated Paper

Figure 6.4 depicts the total charges in double layer natural ester liquid-impregnated paper and mineral oil-impregnated paper for 60 minutes with different moisture contents. In order to investigate the impact of moisture on space charge accumulation, the charge density at electrodes was excluded for the analysis. The total charge was calculated using Equation 4.1, with initial negative charges neutralising positive charges through recombination.

As the moisture level increased from 0.5wt% to 5.0wt%, the total amount of charge in both samples increased. Regarding all moisture levels, the double layer natural ester liquid-impregnated paper exhibited a larger amount of charge than the double layer mineral oil-impregnated paper. At 60 minutes, the charge amount of the double layer natural ester-impregnated paper increased by 3.32 times from $1.55 \times 10^{-7}C$ to $5.15 \times 10^{-7}C$. On the other hand, the double layer mineral oil-impregnated paper increased by 4.04 times from $9.73 \times 10^{-8}C$ to $3.94 \times 10^{-7}C$. This shows that the mineral oil-paper insulation system is more susceptible to moisture than the natural ester liquid-paper insulation system.

6.5 Electric Field Distortion

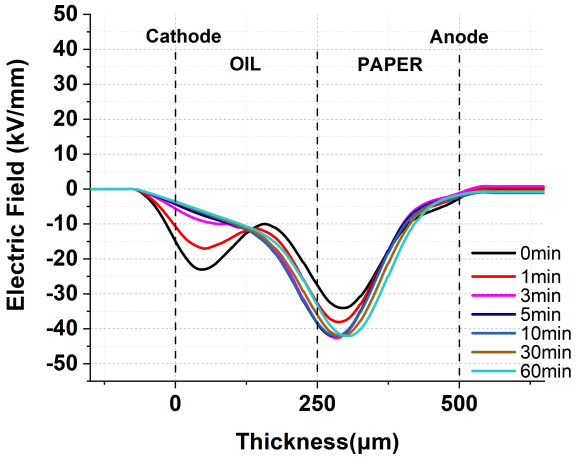

(A)

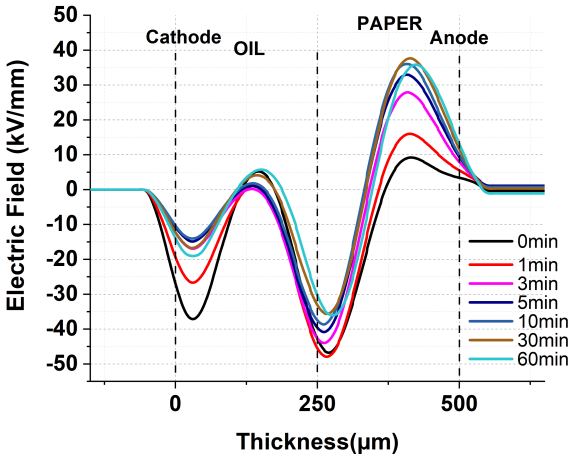

(B)

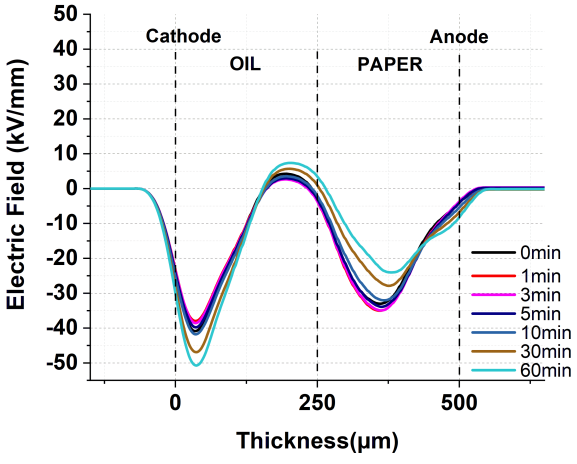

(C)

FIGURE 6.5: Electric Field distributions of Double Layers of Natural Ester Liquid and the Natural Ester Liquid-impregnated Paper with Different Moisture Contents (A) 0.5 wt%, (B) 2.0 wt%, and (C) 5.0 wt%

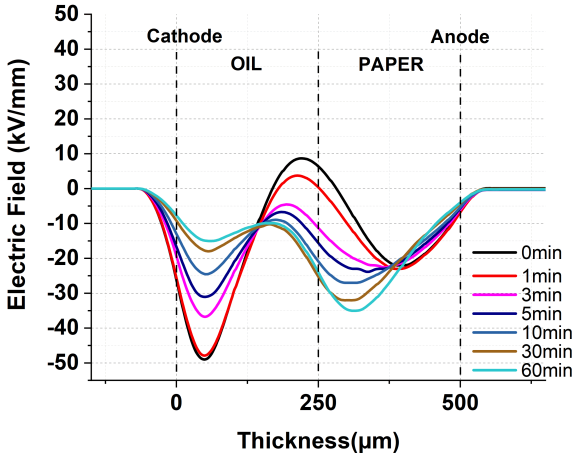

(A)

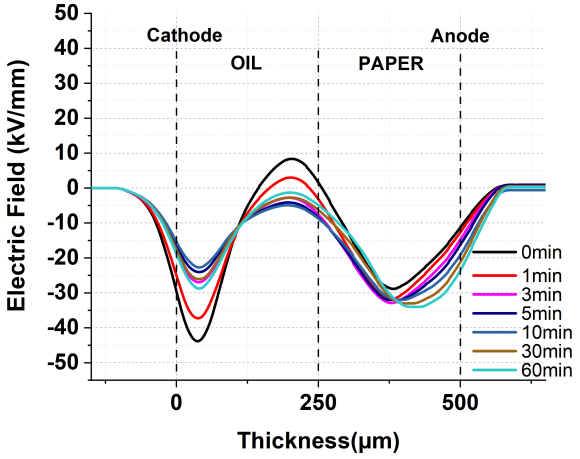

(B)

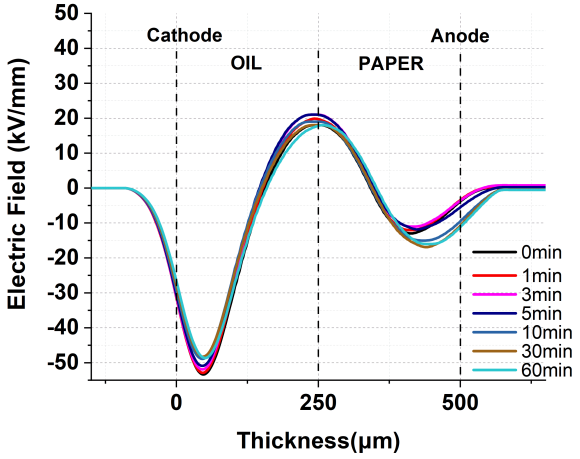

(C)

FIGURE 6.6: Electric Field Distributions of Double Layers of Mineral Oil and the Mineral Oil-impregnated Paper with Different Moisture Contents (A) 0.5 wt%, (B) 2.0 wt%, and (C) 5.0 wt%

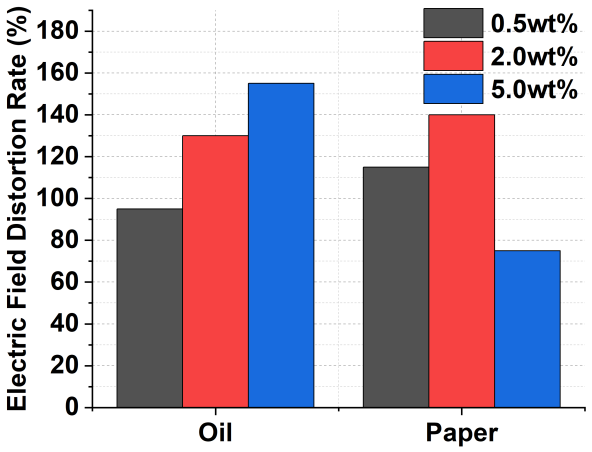

(A)

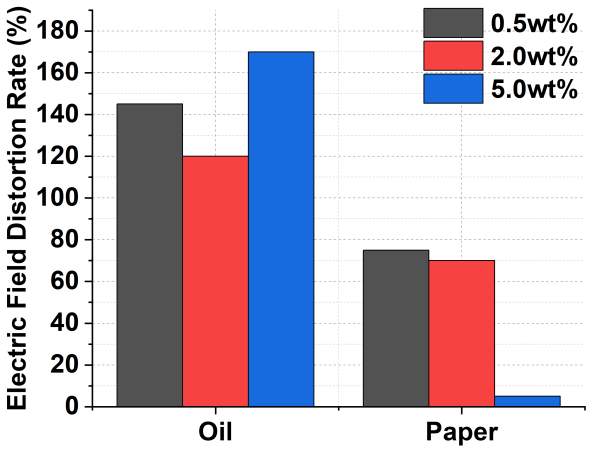

(B)

FIGURE 6.7: Electric Field Distortion Rate with Different Moisture Contents (A) Double Layers of Natural Ester Liquid and the Natural Ester Liquid-impregnated Paper (B) Double Layers of Mineral Oil and the Mineral Oil-impregnated Paper

Figure 6.5 and Figure 6.6 represents electric field distributions in double layer natural ester liquid-impregnated paper and double layer mineral oil-impregnated paper under different moisture conditions. Figure 6.7 illustrates the effect of moisture content on DC electric field distortion in double layer natural ester liquid-impregnated paper and double layer mineral oil-impregnated paper. The natural ester liquid-paper system showed a higher maximum field distortion ratio in the paper when the moisture content was varied from 0.5wt% to 2.0wt%. However, it was measured higher in the oil when the moisture reached 5.0wt%. On the other hand, in the mineral oil-paper system, when the moisture level was 0.5wt% and 2.0wt%, the oil showed a higher maximum field distortion ratio. Similar to the natural ester liquid-paper system, a higher maximum field value was observed for the mineral oil-paper in oil when the moisture level was 5.0wt%.

When the moisture reached 5.0wt%, the maximum field distortion ratio of the double layer natural ester liquid-impregnated paper was 155% in oil and 75% in the paper. On the other hand, the maximum field distortion ratio of the double-layer mineral oil-impregnated paper was 170% in oil and 5% in the paper. The result showed that in an extremely high moisture environment (5.0wt%), the electric field was more uniformly distributed in the natural ester liquid-paper system.

6.6 Space Charge Decay

Figure 7.8 represents the space charge decay of double layer natural ester liquid-impregnated paper and double layer mineral oil-impregnated paper with different moisture levels, respectively.

The natural ester liquid-paper insulation system rapidly discharged most of charges within 10 minutes regardless of the moisture content. This is due to the increased charge mobility caused by the hydrophilic properties of natural ester liquid. On the other hand, in the mineral oil-paper system under dry conditions (0.5wt5%), the charges were still present even after 60 minutes.

Then, as the moisture content increased, the charge dissipation rate gradually increased. In particular, when the double layer mineral oil-impregnated paper was exposed to an extremely high level of moisture (5.0 wt5%), it enhanced the mobility of charges through an increase in conductivity. As a result, at 5.0wt% of moisture, most of the charge was dissipated within 10 minutes, similar to the double layer natural ester liquid-impregnated paper.

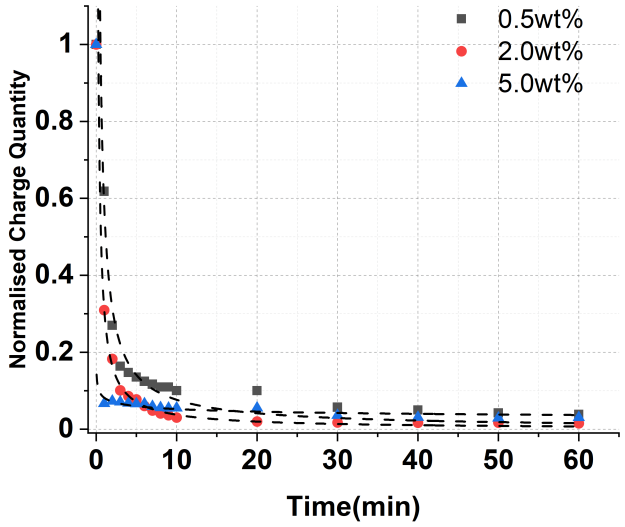

(A)

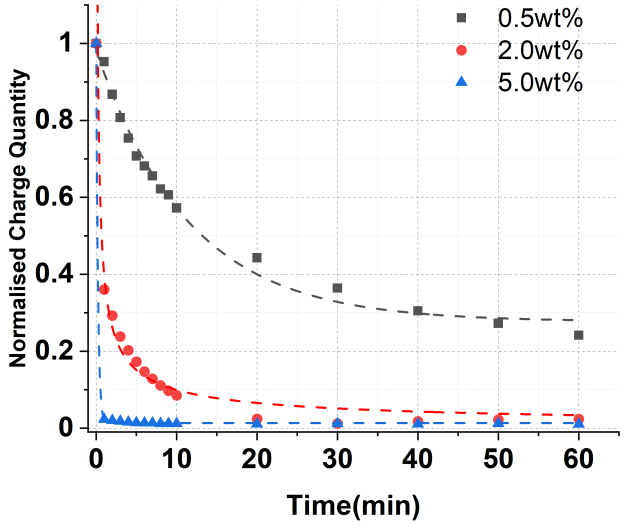

(B)

FIGURE 6.8: Space Charge Decay with Different Moisture Contents (A) Double Layers of natural ester liquid and the natural ester liquid-impregnated Paper (B) Double Layers of Mineral Oil and the Mineral Oil-impregnated Paper (Normalised Charge Quantity)

6.7 DC Breakdown

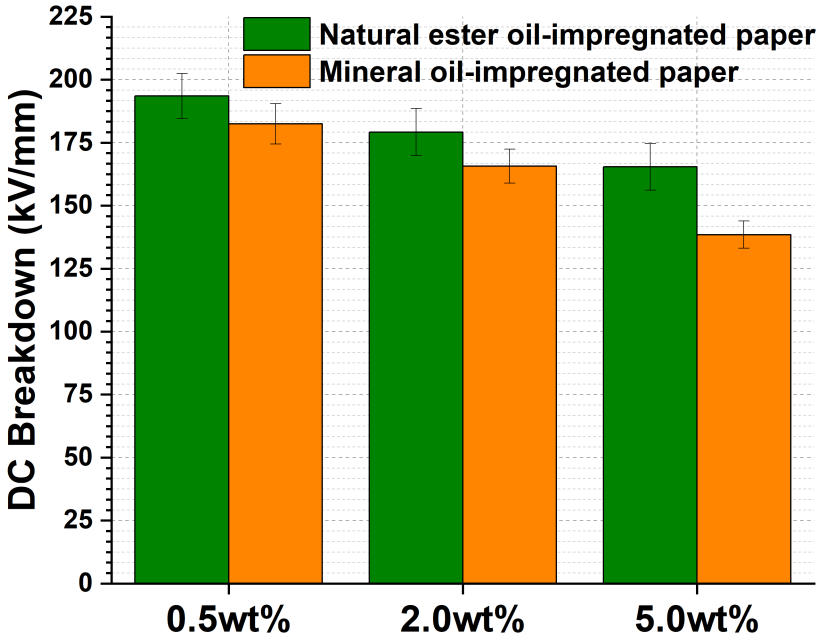

FIGURE 6.9: DC Breakdown of Oil-impregnated Papers with Different Moisture Contents

Figure 6.9 illustrates the DC breakdown of natural ester liquid-impregnated paper and mineral oil-impregnated paper with different moisture contents, respectively. In both samples, the DC breakdown values decreased as the moisture content rose. At 0.5wt%, the natural ester liquid-impregnated paper exhibited a DC breakdown value of 193.52 kV/mm, which decreased to 179.20 kV/mm at 2.0wt% and 165.36 kV/mm at 5.0wt%. On the other hand, the mineral oil-impregnated paper showed DC breakdown values of 182.45 kV/mm at 0.5wt%, 165.71 kV/mm at 2.0wt%, and 138.48 kV/mm at 5.0wt%.

The DC breakdown value of the natural ester liquid-impregnated paper decreased by 14.55% as the moisture content increased from 0.5wt% to 5.0wt%, while that of mineral oil-impregnated paper decreased by 24.09%. While moisture induced more charge accumulation in natural ester liquids compared to mineral oils, the result showed higher DC breakdown values under varying moisture conditions.

6.8 Discussion

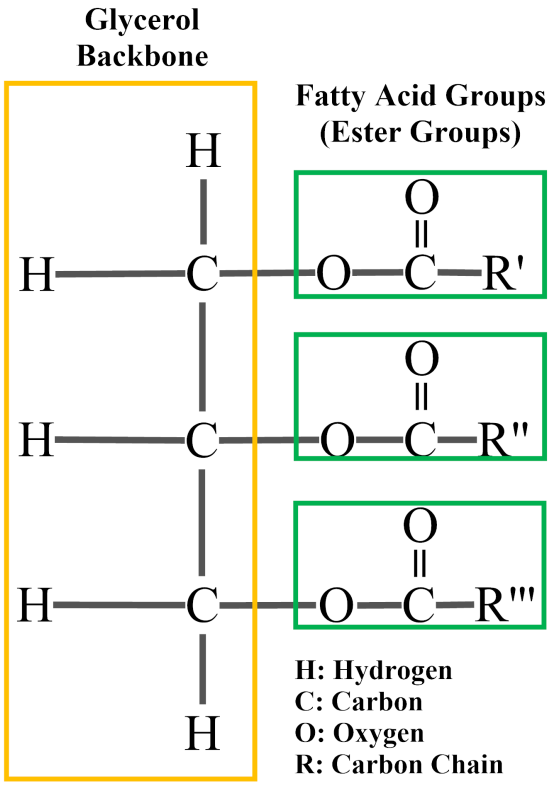

(A)

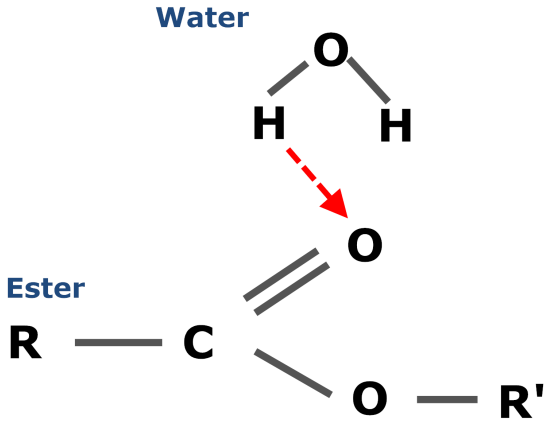

(B)

FIGURE 6.10: (A) Chemical Structure of Natural Ester Liquid and (B) Interaction between Ester Group and Water

The present study investigated the effect of moisture on the space charge properties of double layer natural ester liquid-impregnated paper and double layer mineral oil-impregnated paper. Mineral oil is composed primarily of paraffinic, iso-paraffinic, or naphthenic hydrocarbon structures [110]. Small amounts of polar molecules, such as acids and ketones, are present in mineral oil, but they are mainly removed during the

manufacturing process [110]. Nevertheless, the presence of such polar molecular structures has a direct impact on properties including water solubility, dielectric loss, and interfacial tension [110].

As shown in Figure 6.10, three naturally occurring fatty acid groups are linked to a glycerol backbone in the chemical structure of natural ester liquids [53]. Mineral oil does not contain any ester linkages, whereas natural ester liquid has three ester linkages per molecule [53]. Moisture is considered a very polar molecule. In addition, polar molecules have a strong attraction to each other [53]. Therefore, the hydrogen of water has a strong tendency to combine with the ester linkage through hydrogen bonding [110]. Due to this characteristic of natural ester liquid, more moisture can be dissolved in it without a significant loss of dielectric strength [110]. Consequently, as shown from the results, as the moisture of the Kraft paper increased, the natural ester liquid showed that the moisture was taken away from the paper. On the other hand, mineral oil showed low water solubility even when the moisture of Kraft paper increased due to its hydrophobic characteristic.

In the natural ester liquid-paper system, when the moisture content was low (0.5wt% and 2.0wt%), the charge accumulation was concentrated on the paper over time. This allowed the maximum electric field distortion ratio to have a larger value in the paper. However, when the moisture content reached 5.0wt%, more charges were accumulated in the natural ester liquid. This resulted in a higher maximum field distortion ratio in oil than in paper.

Even with increasing moisture, the mineral oil-paper system showed more charge accumulation in the oil, resulting in a higher maximum electric field ratio in the oil than in the paper. Especially when the moisture reached 5.0wt%, the maximum electric field ratio was 170% in mineral oil and only 5% in the paper. In other words, it showed that the electric field was significantly distorted in mineral oil due to the effect of moisture.

An increase in moisture can contribute to rapid charge dissipation by increasing charge mobility. In other words, because of the water-friendly characteristics of natural ester liquid, the double layer natural ester-impregnated paper dissipated most of the charge within 10 minutes regardless of the increase in moisture. On the other hand, the double layer mineral oil-impregnated paper showed a relatively slow charge dissipation rate when the water content was low (0.5wt% and 2.0wt%). This suggests that mineral oils might be adverse to the polarity reversal effect. When the water content increased from 0.5wt% to 5.0wt%, the mineral oil-impregnated paper significantly reduced the DC dielectric breakdown strength by 24.09%. On the other hand, the DC breakdown strength of the natural ester liquid-impregnated paper decreased by 14.55%. In terms of its molecular structure, cellulose is a more polar substance than natural ester liquids [53]. Therefore, when Kraft paper contains high moisture, natural ester liquid competes with cellulose to dissolve moisture into oil [53]. Therefore, it contributes to maintaining

a higher electric field strength of the natural ester liquid-impregnated paper than the mineral oil-impregnated paper.

6.9 Summary

This chapter investigated how moisture affected the space charge characteristics of double-layer natural ester liquid-impregnated paper by comparing it with double-layer mineral oil-impregnated paper. Interfaces serve as extra electrical barriers between transformer oil and cellulose, allowing space charge to accumulate [106]. The discontinuity between two different materials at the interface could be considered deep traps for charges [106].

A significant heterocharge peak near the cathode in oil was caused by increased moisture in the natural ester liquid-paper system, while paper mainly showed homocharge injections from the anode. This suggests that the natural ester liquid contains the most moisture, leaving the paper dry and free of ionic impurities. As with natural ester liquid, heterocharges were found in mineral oil gaps, indicating that even small amounts of water in mineral oil can generate free ions, potentially affecting heterocharge formation. Additionally, natural ester liquids can dissolve more moisture than mineral oils, giving the paper a higher DC breakdown voltage.

Chapter 7

Polarity Reversal Effect on Space Charge Characteristics of Multilayer of Natural Ester Liquid-impregnated Paper with Different Moisture Contents

7.1 Research Motivation

The electric field distribution across the dielectric sample can be substantially enhanced by the accumulated space charge, which might accelerate the degradation process. In the HVDC transmission system, bi-directional transmission is possible through voltage polarity reversal [87].

Nonetheless, when the transmission direction is reversed, the existing accumulated charges have a significant impact on the redistribution of the electric field in dielectrics [87]. Therefore, it is critical to investigate how polarity reversal affects space charge dynamics in natural ester liquid and mineral oil, respectively.

Moisture has a substantial effect on space charge dynamics. In addition, the distinctions in chemical structure between natural ester liquid and mineral oil result in different interactions with moisture.

Furthermore, in an insulating system consisting of an oil gap and paper, charges can accumulate at the interface between the two materials due to the discontinuity of the material.

This chapter investigates the effect of polarity reversal on the space charge characteristics of a multilayer system comprised of natural ester liquid-impregnated paper at various moisture levels. The results are then compared to those obtained using mineral oil.

7.2 Space Charge Characteristics

Figure 7.1 represents space charge characteristics of a double layer of natural ester liquid and paper under different moisture conditions with a polarity reversal effect. First, the applied voltage lowered the potential barrier between the sample and the two electrodes, allowing charges to be injected. In addition, the discontinuity between the fluid and the solid functions as a trap, causing charges to accumulate at the interface.

As shown in Figure 7.1 (A), when natural ester liquid and paper were in a dry condition, charges mainly accumulated in natural ester liquid initially. However, due to the recombination between negative and positive charges, charges were cancelled out in natural ester liquid over time. On the other hand, more charges accumulated on paper over time. The symmetrical charge distribution was observed following the application of polarity reversal, but existing charges induced a higher charge density peak value in the bottom electrode.

When natural ester liquid and paper were in a moderately wet condition (2.0 wt%), more charges were initially observed in the oil due to the increased mobility of the charges as shown in Figure 7.1 (B). However, as with dry conditions, charges in the oil were cancelled out due to the recombination effect, and the amount of charge in the paper increased over time. After reversing the polarity, the charges, which had moved towards the oil due to the presence of moisture, induced a higher peak value of charge density at the bottom electrode. On the other hand, immediately after the polarity reversal, due to the majority of the charges transferred to the oil, the charge in the paper decreased at 0 seconds and then increased over time. When a voltage was cut off for 60 seconds just before polarity reversal, it was likely that the charge mobility increased due to moisture would have caused a faster discharge. As a result, it was considered that the increase in the amount of charge in the paper right after the polarity reversal was not serious.

When natural ester liquid and paper contained 5.0 wt% moisture as shown in Figure 7.1 (C), it caused high mobility of charge. This allowed more charges to penetrate deeper inside the sample. In particular, most charges were deposited on the oil side, and the charge in the oil increased over time, as opposed to the 0.5 wt% and 2.0 wt% of moisture levels. The water-friendly nature of natural ester liquid takes moisture from paper, which is thought to contribute to the increase in charge on the oil side.

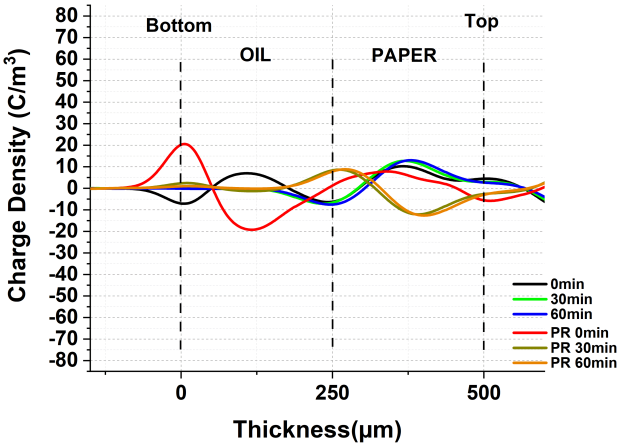

(A)

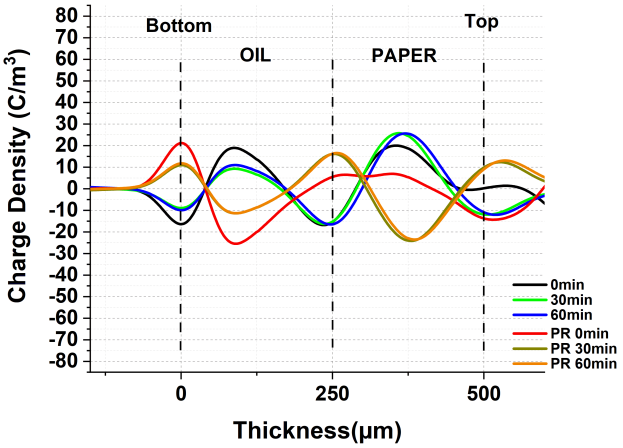

(B)

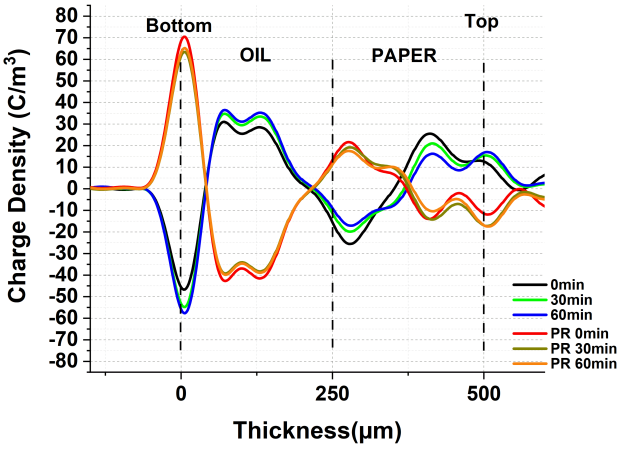

(C)

FIGURE 7.1: Polarity Reversal Effect on Space Charge Characteristics of Double Layers of Natural Ester Liquid and the Natural Ester Liquid-impregnated Paper with Different Moisture Contents (A) 0.5 wt%, (B) 2.0 wt%, and (C) 5.0 wt%, PR: Polarity Reversal

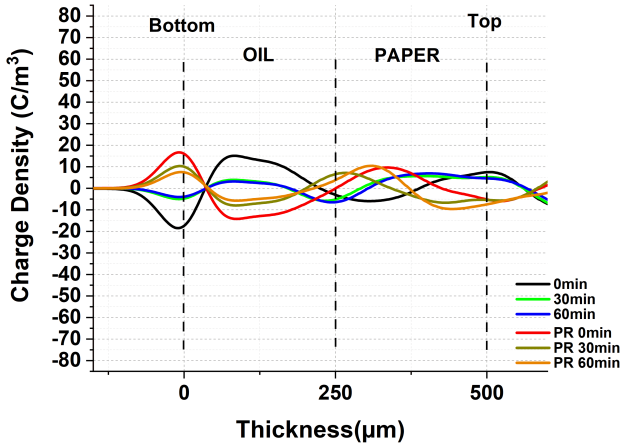

(A)

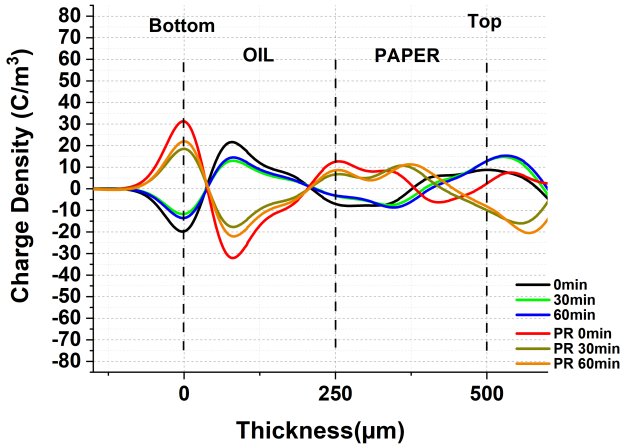

(B)

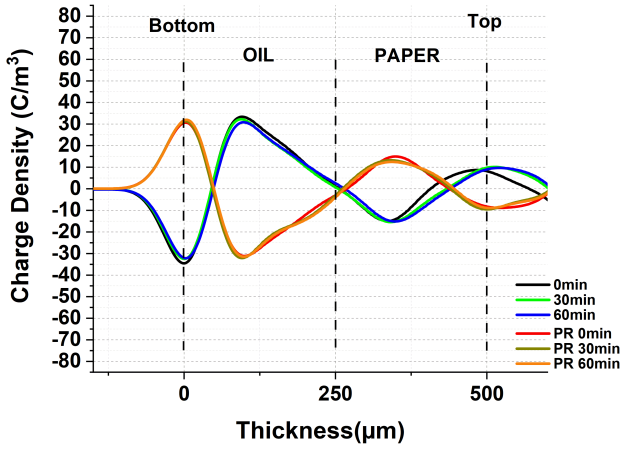

(C)

FIGURE 7.2: Polarity Reversal Effect on Space Charge Characteristics of Double Layers of Mineral Oil and the Mineral Oil-impregnated Paper with Different Moisture Contents (A) 0.5 wt%, (B) 2.0 wt%, and (C) 5.0 wt%, PR: Polarity Reversal

Figure 7.2 represents space charge characteristics of a double layer of mineral oil and paper under different moisture conditions with a polarity reversal effect. Like natural ester liquid-paper, under dry conditions of mineral oil and paper, as illustrated in Figure 7.2 (A), charges are initially accumulated in the oil. However, due to the recombination effect, the charges in the mineral oil are offset, reducing the amount of charge. Charges injected from the top electrode shifted over time toward the mineral oil-paper interface. Right after the polarity was reversed, the amount of charge increased rapidly due to the charges present at 60 minutes.

When mineral oil and paper contained 2.0 wt% moisture as shown in Figure 7.2 (B), the initial charge in mineral oil was higher than that in mineral oil under dry conditions due to increased charge mobility. As mentioned in previous chapters, mineral oil-paper shows a relatively slower charge dissipation rate than natural ester liquid-paper. Due to these characteristics, when the polarity was reversed, the amount of charge was more rapidly induced than the amount of charge at 60 minutes instantaneously.

When the mineral oil and paper were under extremely wet conditions as depicted in Figure 7.2 (C), moisture quickly increased the charge's mobility, allowing it to move more freely inside the sample. Therefore, the maximum amount of charge was accumulated from the beginning, and the movement of the charge did not change significantly over time. The symmetrical charge distribution was also observed after the polarity was reversed. However, the movement of the charge was not much different from the case before the polarity reversal. This probably means that in an environment where moisture is extremely high, the polarity reversal does not have a significant impact.

7.3 Total Charge Amount

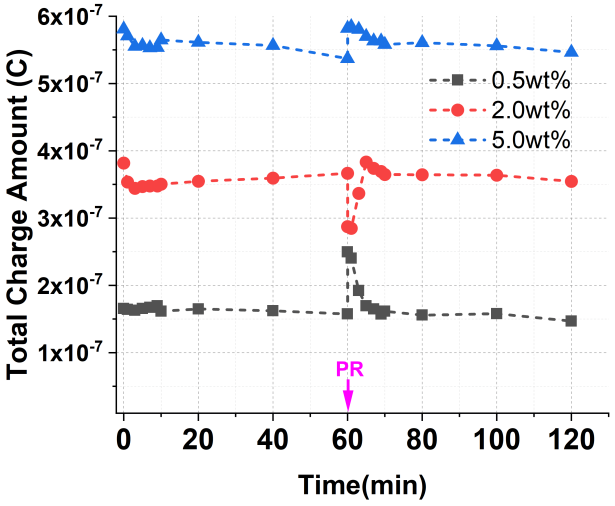

(A)

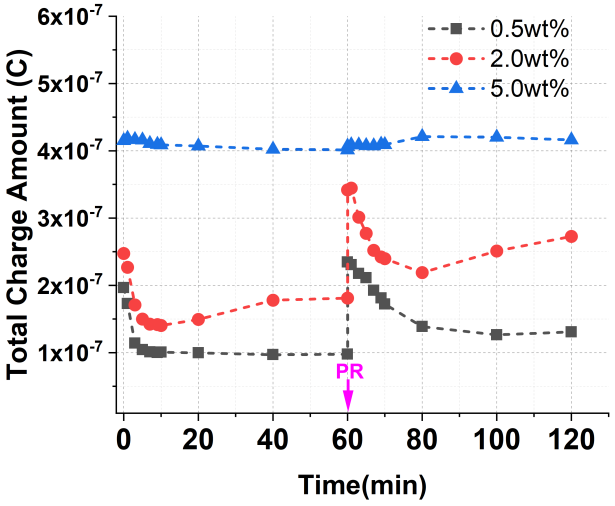

(B)

FIGURE 7.3: Total Amount of Charge with Different Moisture Contents under Polarity Reversal Effect (A) Double Layer of Natural Ester Liquid and Natural Ester Liquid-impregnated Paper (B) Double Layer of Mineral Oil and Mineral Oil-impregnated Paper, PR: Polarity Reversal

Figure 7.3 represents the total amount of charge with different moisture contents for the double layer of natural ester liquid-paper and mineral oil-paper. Both natural ester liquid-paper and mineral oil-paper exhibited an increase in charge amount in response to an increase in moisture.

When the natural ester liquid and paper were in a dry condition (0.5 wt%), the total charge amount was increased by 58.6% instantly due to polarity reversal. On the other

hand, the total charge momentarily decreased by 21.6% after the polarity was reversed when the paper and natural ester liquid contained 2.0 wt% of moisture. This might be because the increased moisture caused a faster charge dissipation rate just before the polarity reversal than when it was in a dry state. Under the condition of 5.0 wt% moisture, the polarity reversal effect increased the charge amount of natural ester liquid and paper by only 8.3%. This could be because the total amount of charge has already significantly increased as a result of the extremely wet conditions, making the polarity reversal effect insignificant.

When moisture levels are low, mineral oil-paper dissipates charges more slowly than natural ester liquid-paper, as discussed in earlier chapters. Therefore, polarity reversal contributed instantaneously raising the amount of charge by 140.2% when the mineral oil and paper were in dry conditions (0.5wt%). In addition, when mineral oil and paper had a moisture level of 2.0 wt%, the total amount of charge was instantaneously increased by 88.6% due to polarity reversal. It seems that the increased moisture, like natural ester liquid, contributed to the increase in the charge dissipation rate. When the moisture content was 5.0 wt%, the polarity reversal only increased the amount of charge by about 1.3%. In other words, it indicates polarity reversal does not significantly contribute to the increase in the total amount of charge in extremely humid environments.

7.4 Electric Field Distortion

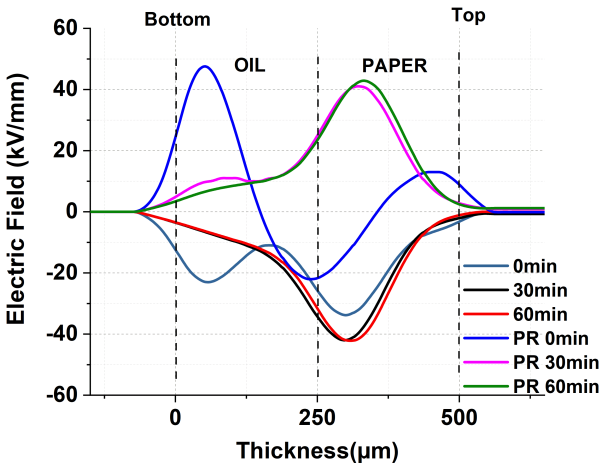

(A)

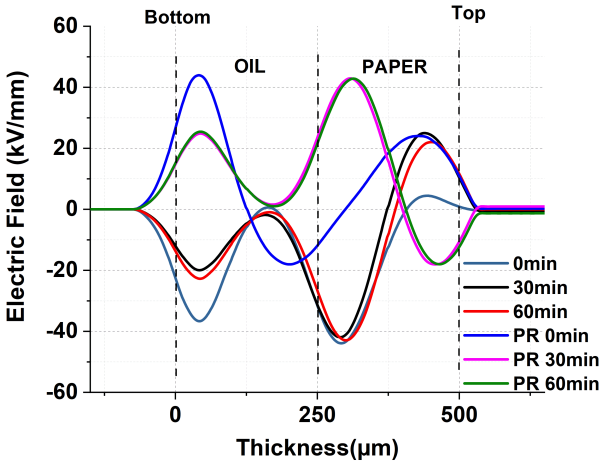

(B)

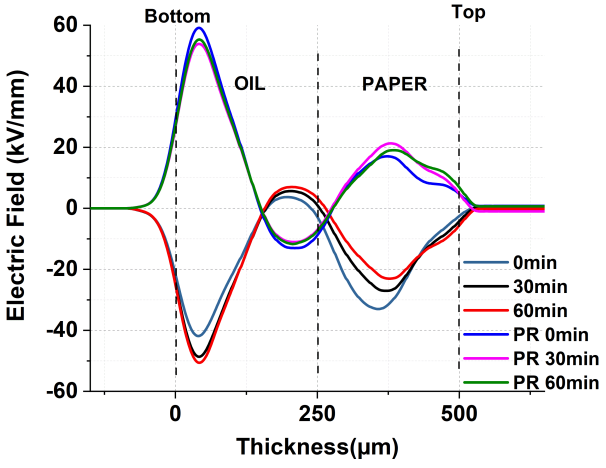

(C)

FIGURE 7.4: Polarity Reversal Effect on Electric Field Distributions of Double Layers of Natural Ester Liquid and the Natural Ester Liquid-impregnated Paper with Different Moisture Contents (A) 0.5 wt%, (B) 2.0 wt%, and (C) 5.0 wt%, PR: Polarity Reversal

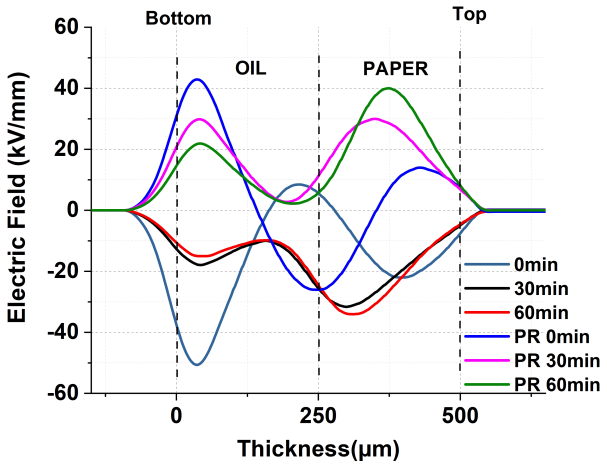

(A)

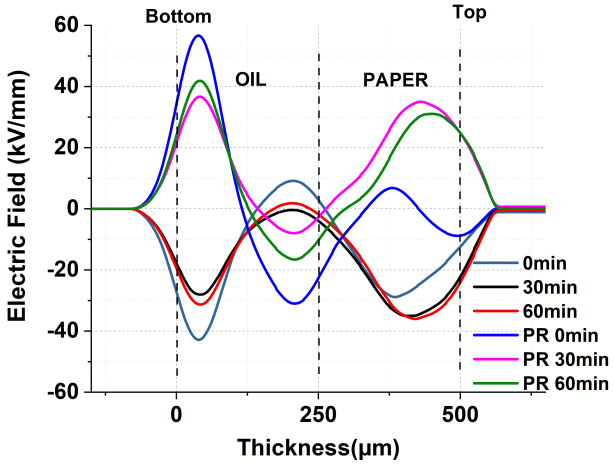

(B)

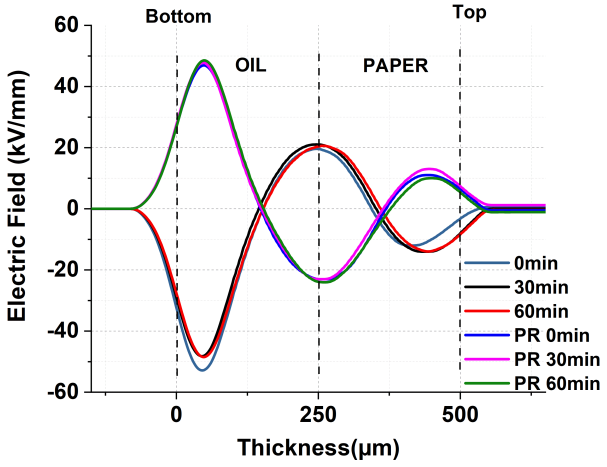

(C)

FIGURE 7.5: Polarity Reversal Effect on Electric Field Distributions of Double Layers of Mineral Oil and the Mineral Oil-impregnated Paper with Different Moisture Contents (A) 0.5 wt%, (B) 2.0 wt%, and (C) 5.0 wt%, PR: Polarity Reversal

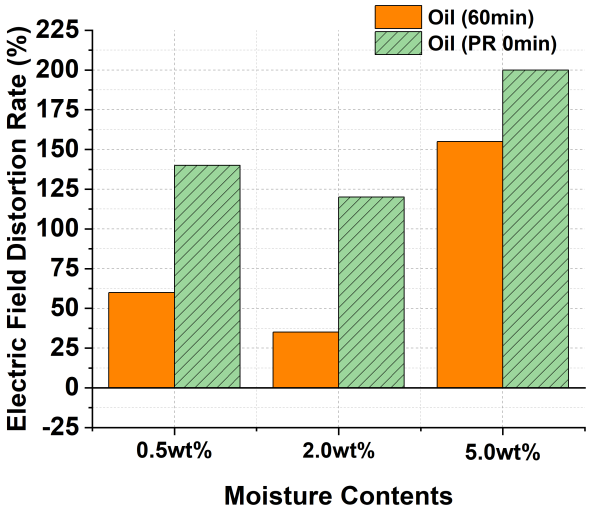

(A)

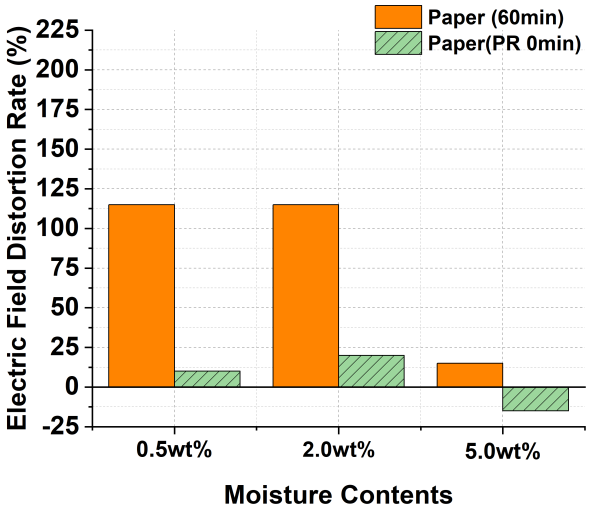

(B)

FIGURE 7.6: Maximum Electric Field Distortion Rate in Double Layer of Natural Ester Liquid and Natural Ester Liquid-impregnated Paper, (A) Maximum Electric Field Distortion Rate at Natural Ester Liquid (B) Maximum Electric Field Distortion Rate at Natural Ester Liquid-impregnated Paper, PR: Polarity Reversal

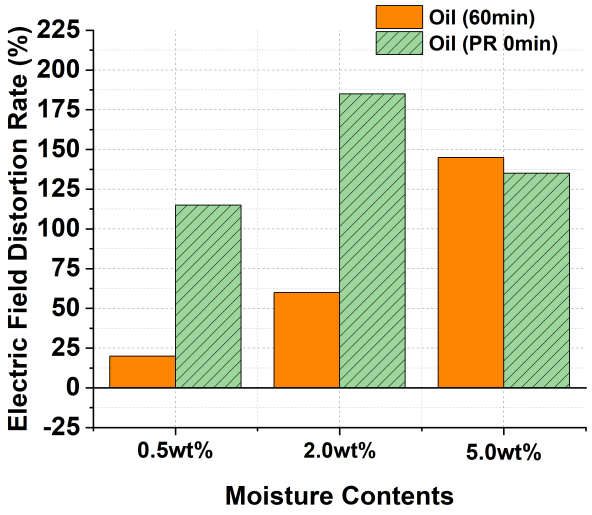

(A)

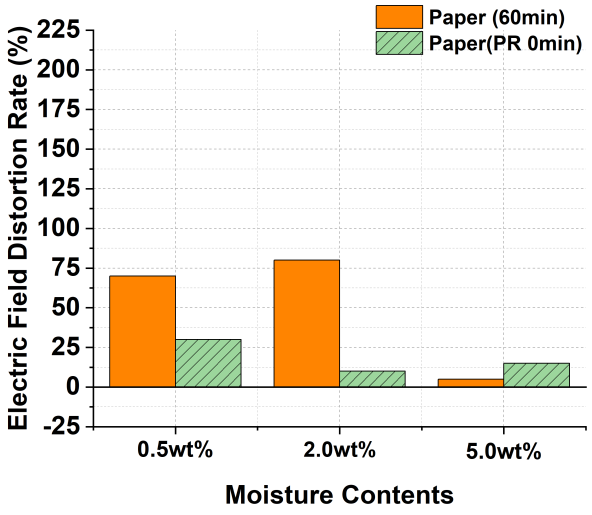

(B)

FIGURE 7.7: Maximum Electric Field Distortion Rate in Double Layer of Mineral Oil and Mineral Oil-impregnated Paper, (A) Maximum Electric Field Distortion Rate at Mineral Oil (B) Maximum Electric Field Distortion Rate at Mineral Oil-impregnated Paper, PR: Polarity Reversal

Figure 7.4 and Figure 7.5 represent the polarity reversal effect on electric field distributions of a double layer of natural ester liquid-paper and mineral oil-paper systems, respectively.

Figure 7.6 illustrates the maximum electric field distortion rate in a double layer of natural ester liquid and natural ester liquid-impregnated paper, respectively, under different moisture conditions. The increase in moisture also increased the maximum electric field distortion rate in natural ester liquid. In addition, polarity reversal contributed to the increase in the maximum field distortion rate. Under dry conditions such as 0.5wt% and 2.0wt%, polarity reversal significantly influences the electric field distortion rate, while under 5.0wt% moisture conditions, the electric field distortion was not as great as in dry conditions. Furthermore, the paper's maximum electric field distortion rate decreased as the moisture increased.

Especially, when the moisture content was 0.5wt%, the maximum electric field distortion rate in natural ester liquid gap increased by 2.33 times from 60min to PR 0min. Regarding 2.0wt% of moisture contents, the maximum electric field distortion rate was raised by 3.42 times right after the polarity reversal. However, the polarity reversal with 5.0wt% moisture caused only 1.23 times an increase in natural ester liquid.

Figure 7.7 depicts the maximum electric field distortion rate in a double layer of mineral oil and mineral oil-impregnated paper under different moisture levels. Regarding the mineral oil gap, except 5.0wt% of moisture level, polarity reversal affected to raise the maximum electric field distortion rate for 0.5 wt%. However, like natural ester liquid, in extremely humid conditions, moisture became a dominant factor regarding charge movement. Therefore, in this case, the polarity reversal became less effective.

In particular, when mineral oil-paper had 0.5wt% and 2.0wt% of moisture contents, it was more susceptible to the effect of the polarity reversal. In other words, when the moisture content was 0.5wt%, the maximum electric field distortion rate in the mineral oil gap from 60 min to PR 0min was raised by 5.75 times due to the polarity reversal. Furthermore, 2.0wt% of moisture content with the polarity reversal caused an increase of the maximum electric field distortion rate by 3.08 times in the mineral oil gap. However, with 2.0wt% of moisture content with the polarity reversal, the maximum electric field distortion rate in the natural ester liquid gap was 120% at PR 0min, whilst the mineral oil gap showed 185% at PR 0min. When the mineral oil-paper was in extremely wet condition (5.0wt%), the maximum electric field distortion rate in the mineral oil gap from 60 min to PR 0min decreased from 145%*to*135%.

7.5 Space Charge Decay

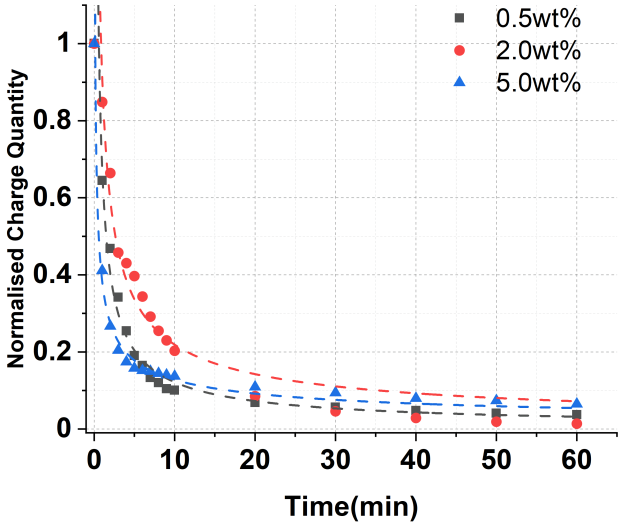

(A)

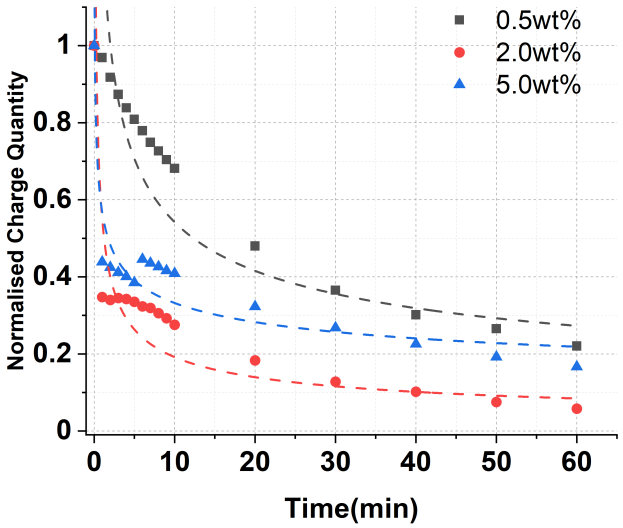

(B)

FIGURE 7.8: Space Charge Decay with Different Moisture Contents after PR (A) Double Layers of natural ester liquid and the Natural Ester Liquid-impregnated Paper (B) Double Layers of Mineral Oil and the Mineral Oil-impregnated Paper (Normalised Charge Quantity)

After 60 minutes of polarity reversal condition, the voltage was cut off in order to measure space charge decay. The results showed that a double layer of natural ester liquid and natural ester liquid-impregnated paper had a faster charge dissipation rate than that of a double layer of mineral oil and mineral oil-impregnated paper.

The higher polarity of the natural ester liquid attracts water easily due to the existence of a double bond in its chemical structure [111]. This can cause the high conductivity of natural ester liquid. Therefore, these characteristics caused most charges to dissipate within 10 minutes in the natural ester liquid-paper system. In other words, the inherent properties of natural ester liquid facilitate rapid charge dissipation regardless of moisture levels after the voltage removal. Probably, the higher conductivity of natural esters, compared to mineral oil, accelerates charge migration away from the sample.

During the refining process, most polar compounds in mineral oil are removed [111]. Therefore, paraffinic and naphthenic-based mineral oils have saturated chemical bonds, which make them difficult to react with water [111]. Therefore, this might cause some difficulties when ionised water escapes from cellulose to the electrode during charge decay. Therefore, this is probably why the mineral oil-paper system showed a much slower charge dissipation rate compared to the natural ester liquid-paper system.

7.6 Discussion

HVDC technology requires a bi-directional transmission system, which can be achieved by reversing the polarity. However, when the polarity is reversed to change the power flow, the oil-paper insulation system in the HVDC converter transformer is inevitably affected by the remaining charges, which influence electric field distribution. Therefore, investigating space charge characteristics under the polarity reversal effect is important.

Moisture is one of the most undesirable substances for HVDC converter transformers because it can significantly weaken the dielectric performance and accelerate the insulation's ageing process. Mineral oil mainly consists of paraffinic and naphthenic-based compounds, which have saturated hydrocarbon bonds. They are usually single bonds, so it is difficult to react with water [111]. On the other hand, natural ester liquid contains a triglyceride structure, which consists of a glycerol backbone with three fatty acids [111]. Those fatty acids possess unsaturated double bonds, which can be easily reacted with water. This characteristic allows natural ester liquid to have a high water solubility.

When the moisture level was 0.5wt%, the mineral oil-paper showed that the polarity reversal caused a rise in the total charge amount by 140.2%, while the total amount of charge increased by 58.6% in the natural ester liquid-paper. In addition, regarding 2.0wt% of moisture level, due to polarity reversal, the total amount of charge in the mineral oil-paper increased by 88.6%, but the total amount of charge in the natural ester liquid-paper decreased by 21.6%. This indicates that mineral oil-paper is more susceptible to the polarity reversal compared to natural ester liquid-paper when the

moisture level is less than 2.0wt%. Therefore, the hydrophilic characteristics of the natural ester liquid can provide the benefit, which can mitigate the effect of polarity reversal. However, when mineral oil-paper and natural ester liquid-paper were in extremely wet conditions (5.0wt%), high moisture levels made the effect of polarity reversal less effective.

7.7 Summary

Polarity reversal is critical when the direction of power flow is reversed. This is because the remaining charges may accelerate the electric field instantaneously by inducing opposite charges. This chapter investigated how space charge characteristics were affected when the polarity was reversed under different moisture conditions.

As previously discussed, natural ester liquid generally showed faster charge dissipation than mineral oil. Then, this can be advantageous when the polarity reversal occurs. Especially when the moisture contents were low (0.5 wt% and 2.0 wt%), natural ester liquid showed the ability to somewhat suppress instantaneous charge induction due to polarity reversal through its fast charge dissipation rate.

On the other hand, mineral oil usually showed a relatively slower charge dissipation rate than natural ester liquid when the moisture content was low. Therefore, when the polarity was reversed, the amount of charge instantly increased due to the remaining charges. This suggests that the insulating oil's charge dissipation rate is one of the essential factors in a polarity reversal situation.

Chapter 8

Conclusions

The sharp rise in energy demand has driven the entire energy industry to develop more efficient energy transmission systems. HVDC power transmission system is the next generation of the power grid due to its advanced technology. In order to achieve the reliable and sustainable performance of HVDC transmission systems, HVDC converter transformers take a key role. Then, the insulation system heavily influences the performance of HVDC converter transformers.

Cellulose and mineral oil are mainly utilised as main insulating materials for HVDC converter transformers. However, mineral oil is fire-hazardous and environmentally harmful. Thus, natural ester liquid is currently considered a possible substitute for mineral oil. Natural ester liquid and mineral oil have different chemical structures. Natural ester liquid contains a triglyceride structure connected to ester linkages. On the other hand, mineral oil is composed of hydrocarbon chains. Hence, the difference in chemical structure between natural ester liquid and mineral oil affects the dielectric performance. Natural ester liquids may contain unsaturated double bonds in their fatty acid chains. These double bonds can enhance the polarity and attract the water easily. Conversely, mineral oil generally has saturated hydrocarbon bonds, making it less polar and less likely to form a hydrogen bond with the water molecule. This difference plays a significant role when the space charge characteristic of natural ester liquid is compared to mineral oil.

Therefore, this thesis has explored the impact of moisture and ageing on space charge characteristics of natural ester liquid-impregnated paper by comparing it with mineral oil-impregnated paper. The impact of moisture on space charge characteristics of the natural ester liquid-impregnated paper and the mineral oil-impregnated paper was investigated. By comparing the characteristics of natural ester liquid and mineral oil, it is possible to estimate whether natural ester liquid may be used as HVDC power transformer oil. Natural ester liquid is a hydrophilic liquid, whereas mineral oil is a hydrophobic liquid. Thus, when the Kraft paper contained a high moisture level, natural

ester liquid absorbed a larger amount of moisture from the Kraft paper than mineral oil. Moisture helped that space charges penetrate deeper into both oil-impregnated papers. As moisture increased, heterocharges accumulated near the cathode, inducing more negative charges. This caused a high electric field distortion in both oil-impregnated papers near the cathode. Compared to the natural ester liquid-impregnated papers, the faster heterocharge formation occurred in the mineral oil-impregnated papers. When the moisture content was low, mineral oil-impregnated paper still performed better than the natural ester liquid-impregnated paper in terms of the electric field distortion rate. However, the electric field distortion rate in both oil-impregnated papers became similar when the Kraft paper contained 5.0wt% moisture content. This indicates that natural ester liquid can provide some benefits under certain moisture levels such as 0.5wt% and 2.0wt%. Also, when the moisture level in Kraft paper is high, natural ester liquid-impregnated paper can expect a similar dielectric performance to mineral oil-impregnated paper, and the high water solubility of natural ester liquid can keep Kraft paper drier [110]. After removing the applied dc voltage, most space charges in the natural ester liquid-impregnated paper decayed rapidly within the first 10 minutes for 0.5wt%, 2.0wt%, and 5.0 wt%. Under the dry state, it took 30 minutes to dissipate most charges in the mineral oil-impregnated paper, which might be disadvantageous for the polarity reversal. Mineral oil is still a decent dielectric liquid in a dry environment. However, in very humid environments, the hydrophobic characteristic of mineral oil can be a severe drawback for the oil-paper insulation system in the HVDC converter transformer compared to natural ester liquid.

Also, the effect of thermal ageing on the space charge characteristics of the natural ester liquid-impregnated paper and the mineral oil-impregnated paper was studied. The natural ester liquid produced more acids than the mineral oil during thermal ageing, which may have contributed to more charge accumulation in the natural ester liquid-impregnated paper. Nevertheless, both oil-impregnated papers did not experience a significant change in their electrical strength during thermal ageing. During thermal ageing, it was also discovered that the natural ester liquid-impregnated paper had a higher DC breakdown voltage than the mineral oil-impregnated paper. DC breakdown strength of natural ester liquid-impregnated paper decreased from 180.04kV/mm to 129.50 kV/mm during 30 days of thermal ageing, while that of mineral oil-impregnated paper reduced from 150.10kV/mm to 124.42kV/mm. Under fresh conditions, the DC breakdown strength of the natural ester liquid-impregnated paper was 20% higher than that of the mineral oil-impregnated paper. In addition, when thermal ageing reached 30 days, the DC breakdown strength of the natural ester liquid-impregnated paper was still 4% higher than that of the mineral oil-impregnated paper.

The impact of moisture on space charge characteristics of multilayer of natural ester liquid-impregnated paper showed that natural ester liquids are polar substances. Therefore, when Kraft paper has a high moisture content, natural ester liquid tends to

take moisture away from the paper. On the other hand, the low water solubility of mineral oil allows moisture to stay on the Kraft paper. Under varying moisture conditions, the double-layer natural ester liquid-impregnated paper always showed more charge than the double-layer oil-impregnated paper. The polar property of natural ester liquids, absorbing moisture, enhances conductivity. This increased conductivity facilitates a more uniform electric field distribution, contributing to the natural ester liquid-impregnated paper's higher DC dielectric breakdown strength compared to mineral oil-impregnated paper. Although mineral oil is an efficient dielectric liquid in dry environments, its hydrophobic nature can be more harmful to oil-paper insulation systems in HVDC transformers in extremely humid environments compared to natural ester liquid.

Finally, the effect of polarity reversal on space charge characteristics of a double-layer natural ester liquid and natural ester liquid-impregnated paper under different moisture contents was investigated. Regarding dry and moderately wet conditions, the high water solubility of natural ester liquid can be advantageous in reducing the effect of polarity reversal. On the other hand, when moisture levels were 0.5wt% and 2.0wt%, the polarity reversal sharply increased the total amount of charges in mineral oil-paper. In other words, the slow charge dissipation rate of mineral oil-paper might be disadvantageous when the polarity is reversed.

This study contributes to the field by investigating the space charge dynamics in multilayer configurations, exploring the oil gap and natural ester liquid-impregnated paper, and providing key comparisons with mineral oil. The main point is that the high permittivity of natural ester liquid, absorbing moisture, leads to an increase in conductivity. This increase in conductivity contributes to a more uniform distribution of the electric field compared to mineral oil.

Natural ester liquid is a promising candidate to replace mineral oil for HVDC converter transformers. Even though natural ester liquid can provide various advantages, additional research is still required to adopt it for HVDC converter transformers.

Chapter 9

Future Work

Ionisation Effect

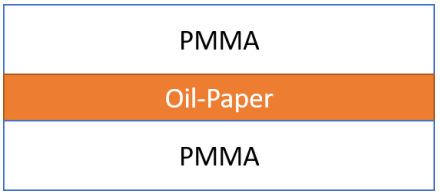

FIGURE 9.1: Configuration for Ionisation Effect

In a natural ester liquid-paper insulation system, the amount of charge can be generated either by charge injection or ionisation. Therefore, by covering the natural ester liquid-paper with PMMA (polymethyl methacrylate) as shown in Figure 9.1, charge injection from electrodes can be prevented. In this case, any charge movement between two PMMAs can be expected from the ionisation effect in the natural ester liquid-paper.

Electrical Ageing

Electrical ageing (DC condition) is critical to understand the dielectric performance of the natural ester liquid-paper because this can simulate the electrical performance of the natural ester liquid in a more realistic way. This might provide valuable insights into the long-term performance of natural ester liquid as a dielectric liquid.

Thermal Ageing with Double Layer

Thermal ageing condition is essential to studying space charge dynamics of natural ester liquid because it causes chemical and physical changes in samples. The double

layer is usually composed of liquid and solid materials. Then, the discontinuity of the two materials creates the interface between liquid and solid. The interface can serve as a trap for charges. Thus, it is crucial to investigate the double layer of the natural ester liquid-paper system under thermal ageing conditions.

References

[1] T. Halder, "Comparative Study of HVDC and HVAC for a Bulk Power Transmission," in *Proceedings of 2013 International Conference on Power, Energy and Control, ICPEC 2013*, IEEE, 2013, pp. 139–144.

[2] V. K. Sood, *Power Electronics Handbook*, 4th ed., Muhammad H. Rashid, Ed. Joe Hayton, 2018, pp. 847–860.

[3] P. Schavemaker and L. van der Sluis, *Electrical Power System Essentials*. Chichester: Wiley, 2008, pp. 5–6, ISBN: 9780470510278.

[4] K. Meah, S. Member, S. Ula, and S. Member, "Comparative Evaluation of HVDC and HVAC Transmission Systems," in *2007 IEEE Power Engineering Society General Meeting*, IEEE, 2007, pp. 1–5.

[5] M. Yea, K. J. Han, J. Park, S. Lee, and J. Choi, "Design Optimization for the Insulation of HVDC Converter Transformers under Composite Electric Stresses," in *IEEE Transactions on Dielectrics and Electrical Insulation*, vol. 25, IEEE, 2018, pp. 253–262.

[6] D. Westermann, D. van Hertem, G. Real, M. Meisingset, T. Rauhala, and M. Kurra, *Voltage Source Converter (VSC) HVDC for Power Transmission - Economic Aspects and Comparison with other AC and DC Technologies*. 2012, pp. 12–35.

[7] J. Fabian, M. Muhr, S. Jaufer, and W. Exner, "Partial Discharge Behavior of Mineral Oil and Oil-Board Insulation Systems at HVDC," in *2012 IEEE International Conference on Condition Monitoring and Diagnosis*, 2012, pp. 285–288.

[8] Y. Shuai, X. Han, L. Zhang, C. Yang, X. Hu, and H. Wu, "Major Insulation Design Consideration of Converter Transformer," in *2016 International Conference on Condition Monitoring and Diagnosis (CMD)*, 2016, pp. 1004–1007.

[9] M. Hao, Y. Zhou, G. Chen, G. Wilson, and P. Jarman, "Space Charge Behaviour in Oil and Impregnated Pressboard Combined Insulation System," in *2014 IEEE 18th International Conference on Dielectric Liquids (ICDL)*, IEEE, 2014, pp. 1–4.

[10] M. Maharana, N. Baruah, S. K. Nayak, and N. Sahoo, "Nanofluid and Transformer Oil Impregnated Aged Kraft Paper: Analysis of its Mechanical Strength," in *2018 IEEE PES Asia-Pacific Power and Energy Engineering Conference (APPEEC)*, vol. 2018-Oct, IEEE, 2018, pp. 302–305.

[11] N. Pattanadech, K. Jariyanurat, S. Maneerot, and P. Nimsanong, "Electrical Characteristic Comparison of Mineral Oil and Natural Ester for Transformer Applications," in *2017 International Electrical Engineering Congress (iEECON)*, 2017, pp. 8–10.

[12] V. H. Dang, A. Beroual, and C. Perrier, "Investigations on Streamers Phenomena in Mineral, Synthetic and Natural Ester Oils under Lightning Impulse Voltage," *IEEE Transactions on Dielectrics and Electrical Insulation*, vol. 19, no. 5, pp. 1521–1527, 2012.

[13] T. Leibfried, W. Zaengle, and V. D. Houhanessian, "Ageing and Moisture Analysis of Power Transformer Insulation Systems Submitted for Publication," in *CIGRE Session Paris*, 2002, pp. 1–6.

[14] M. Daghrah, Z. D. Wang, Q. Liu, D. Walker, C. Krause, and G. Wilson, "Experimental Investigation of Hot Spot Factor for Assessing Hot Spot Temperature in Transformers," in *2016 International Conference on Condition Monitoring and Diagnosis (CMD)*, IEEE, 2016, pp. 948–951.

[15] Y. Li, M. Yasuda, and T. Takada, "Pulsed Electroacoustic Method For Measurement Of Charge Accumulation In Solid Dielectrics," *IEEE Transactions on Dielectrics and Electrical Insulation*, vol. 1, no. 2, pp. 188–195, 1994.

[16] D. Van Hertem and M. Delimar, *Electricity Transmission, Distribution and Storage Systems*, Z. Melhem, Ed. Woodhead Publishing Limited, 2013, pp. 143–173.

[17] J. Setreus and L. Bertling, "Introduction to HVDC Technology for Reliable Electrical Power Systems," in *Proceedings of the 10th International Conference on Probablistic Methods Applied to Power Systems*, 2008, pp. 560–567.

[18] The China Electric Power Research Institute, Ed., *UHV Transmission Technology*. Elsevier, 2018, pp. 387–399. DOI: 10.1016/B978-0-12-805193-1.00009-4.

[19] D. Jovcic, *High Voltage Direct Current Transmission*, 2nd. Wiley, 2019, pp. 140–245.

[20] D. Jovcic, H. Zhang, D. Findlay, A. Z. Annuar, and B. Li, "Subsea DC Collection Grid with High Power Security for Offshore Renewables," *International Transactions on Electrical Energy Systems*, vol. 27, no. 2, pp. 1–14, 2017.

[21] O. E. Oni, I. E. Davidson, and K. N. Mbangula, "A Review of LCC-HVDC and VSC-HVDC Technologies and Applications," in *2016 IEEE 16th International Conference on Environment and Electrical Engineering (EEEIC)*, IEEE, 2016.

[22] M. P. Bahrman, "HVDC Transmission Overview," in *2008 IEEE/PES Transmission and Distribution Conference and ExpositionIEEE/PES Transmission and Distribution Conference and Exposition*, 2008, pp. 1–7.

[23] G. Li, C. Li, and D. van Hertem, *HVDC Grids For Offshore and Supergrid of the Future*, D. Hertem, O. Gomis-Bellmunt, and J. Liang, Eds. IEEE PRESS WILEY, 2016, pp. 45–76.

[24] Z. Liu, "Characteristics of uhv dc transmission system," in *Ultra-High Voltage Ac/dc Grids*, Z. Liu, Ed., Boston: Academic Press, 2015, pp. 95–132.

[25] M. A. Hannan, I. Hussin, P. J. Ker, M. M. Hoque, M. S. Hossain Lipu, A. Hussain, M. S. Rahman, C. W. Faizal, and F. Blaabjerg, "Advanced Control Strategies of VSC Based HVDC Transmission System: Issues and Potential Recommendations," *IEEE Access*, vol. 6, pp. 78 352–78 369, 2018.

[26] J. Burr, S. Finney, and C. Booth, "Comparison of Different Technologies for Improving Commutation Failure Immunity Index for LCC HVDC in Weak AC Systems," in *11th IET International Conference on AC and DC Power Transmission*, vol. 2015, 2015, pp. 1–7.

[27] M. Eremia, C.-C. Liu, and A.-A. Edris, *Advanced Solutions in Power Systems*, 1st ed., M. Eremia, R. Mihalic, and B. Blazic, Eds. 2016, pp. 125–267.

[28] B. D. Gemmell, J. Dorn, D. Retzmann, and D. Soerangr, "Prospects of Multilevel VSC Technologies for Power Transmission," in *2008 IEEE/PES Transmission and Distribution Conference and Exposition*, 2008, pp. 1–16.

[29] M. Carlen and P. Rohan, "ABB Review Special Report - Transformers," Tech. Rep., 2012, p. 17.

[30] A. Carlson, "Specific Requirements on HVDC Converter Transformers," Tech. Rep., 1996, pp. 1–4.

[31] M. Fu, B. Luo, S. Hou, Y. Liao, M. Hao, and G. Chen, "Space Charge Dynamics in Pressboard-oil-pressboard Multilayer System under DC Voltages," in *2015 IEEE 11th International Conference on the Properties and Applications of Dielectric Materials (ICPADM) Space*, IEEE, 2015, pp. 112–115.

[32] R. Nakane, K. Kato, N. Hayakawa, and H. Okubo, "Time and Space Transition of DC Electric Field Distributions in Oil-Pressboard Composite Insulation in AC/DC Converter Transformer," in *2019 IEEE 20th International Conference on Dielectric Liquids (ICDL)*, IEEE, 2019, pp. 1–5.

[33] H. Morooka, A. Yamagishi, K. Kawamura, H. Kojima, and N. Hayakawa, "Thermal-degradation Mechanism of Mineral-oil-immersed Pressboards and Influence of Aging on Pressboard Properties," in *2018 Condition Monitoring and Diagnosis (CMD)*, IEEE, 2018, pp. 1–4.

[34] H. Okubo, "HVDC Electrical Insulation Performance in Oil/Pressboard Composite Insulation System Based on Kerr Electro-Optic Field Measurement and Electric Field Analysis," *IEEE Transactions on Dielectrics and Electrical Insulation*, vol. 25, no. 5, pp. 1785–1797, 2018.

[35] T. K. Saha, P. Purkait, Y. Cui, H. Ma, J. Chan, M. Fairouz, C. Ekanayake, and K. Bandara, *Transformer Ageing: Monitoring and Estimation Techniques*, 1st ed., T. K. Saha and P. Purkait, Eds. Singapore: IEEE PRESS, 2017, pp. 1–403.

[36] T. A. Prevost and T. V. Oommen, "Cellulose Insulation in Oil-Filled Power Transformers: Part I - History and Development," *IEEE Electrical Insulation Magazine*, vol. 22, no. 1, pp. 28–34, 2006.

[37] T. A. Prevost and T. Oommen, "Cellulose insulation in oil-filled power transformers: Part II – maintaining insulation integrity and life," *IEEE Electrical Insulation Magazine*, vol. 22, no. 1, pp. 5–9, 2006.

[38] A. A. Abdelmalik, J. C. Fothergill, and S. J. Dodd, "Aging of Kraft Paper Insulation in Natural Ester Dielectric Fluid," in *Proceedings of IEEE International Conference on Solid Dielectrics, ICSD*, IEEE, 2013, pp. 541–544.

[39] C. Krause, "Power Transformer Insulation - History, Technology and Design," *IEEE Transactions on Dielectrics and Electrical Insulation*, vol. 19, no. 6, pp. 1941–1947, 2012.

[40] P. Bajpai, *Biermann's Handbook of Pulp and Paper*, 3rd ed., M. W. Fisher, Ed. Amsterdam: Joseph P. Hayton, 2018, pp. 1–18.

[41] R. A. Abd El-Aal, K. Helal, A. M. Hassan, and S. S. Dessouky, "Prediction of Transformers Conditions and Lifetime Using Furan Compounds Analysis," *IEEE Access*, vol. 7, pp. 102 264–102 273, 2019.

[42] Z. Shen, F. Wang, Z. Wang, and J. Li, "A Critical Review of Plant-based Insulating Fluids for Transformer: 30-year Development," *Renewable and Sustainable Energy Reviews*, vol. 141, no. October 2020, pp. 1–19, 2021.

[43] T. Rouse, "Mineral Insulating Oil in Transformers," *IEEE Electrical Insulation Magazine*, vol. 14, no. 3, pp. 6–16, 1998.

[44] C. B Pahlavanpour, A. D. Pablo, W. Tumiatti, M. Martins, M. Dahlund, G. Wilson, L. Ritchie, and P. Koestinger, *Insulating Oil Regeneration and Dehalogenation*, 2010.

[45] D. K. Mahanta and S. Laskar, "Electrical Insulating Liquid: A Review," *Journal of Advanced Dielectrics*, vol. 7, no. 4, pp. 1–9, 2017.

[46] X. Wang, C. Tang, B. Huang, and J. Hao, "Review of Research Progress on the Electrical Properties and Modification of Mineral Insulating Oils Used in Power Transformers," *Energies*, pp. 2–31, 2018.

[47] E. Casserly, "Mineral Insulating Liquids – Where They Are From, Where They Are Going," *Transformer Technology*, no. 5, pp. 27–34, 2020.

[48] S. D. Smith and B. L. Beaster, "Design and Test Experience with Natural Ester Fluid for Power Transformers Update," in *2009 IEEE Power and Energy Society General Meeting*, IEEE, 2009, pp. 14–16.

[49] J. Jacob, P. Preetha, and S. Thiruthi Krishnan, "Review on Natural Ester and Nanofluids as an Environmental Friendly Alternative to Transformer Mineral Oil," *IET Nanodielectrics*, vol. 3, no. 2, pp. 33–43, 2020.

[50] "Increased Fire Safety-MIDEL eN 1204," MIDEL, Tech. Rep., 2016, pp. 1–2.

[51] K. Sindhuja, M.Srinivasan, and N.Niveditha, "Natural Esters as an Alternative to Mineral Oil In Transformer Applications," *International Journal of Pure and Applied Mathematics*, vol. 118, no. 20, pp. 723–732, 2018.

[52] "MIDEL eN 1204-Natural Ester Transformer Fluid (Rapeseed) Fire Safe and Biodegradable," MIDEL, Tech. Rep., 2019, pp. 1–4. [Online]. Available: http:

//www.midelsafetyinside.com/wp-content/uploads/2017/05/Midel-eN-1204-SP.pdf.

[53] R. Martine, H. Athanassatou, J. Duart, C, C. Perrier, I. Sitar, J. Walker, C. Claiborne, T. Boche, D. Cherry, A. Darwin, E. Gockenbach, H. Jassen, Y. Shirasaka, and Z. Wang, "Experiences in service with new insulating liquids," Cigre, Tech. Rep. A2.35 (436), 2010, pp. 1–50.

[54] C. Rajotte, M. Foata, P. Jarman, and F. Larese, "Guide for Transformer Maintenance," Cigre Publication, Tech. Rep. 445, 2011, p. 48.

[55] K. J. Rapp, J. Luksich, and A. Sbravati, "Application of Natural Ester Insulating Liquids in Power Transformers," *Engineering, Environmental Science*, no. November, pp. 1–7, 2014. [Online]. Available: http://www.envirotempfluids.com/content/uploads/2013/10/Natural_Ester_Power_Transformers_My_Transfo_2014Final.pdf.

[56] W. Choo, G. Chen, and S. G. Swingler, "Space Charge Accumulation under the Effects of Temperature Gradient on Solid Dielectric DC Cable," in *The 16th International Symposium on High Voltage Engineering*, Johannesburg: SAIEE, 2009, pp. 1–5.

[57] J. Hornak, P. Trnka, P. Totzauer, and M. Gutten, "The Effect of Space Charge Accumulation in High Voltage Insulation Systems," in *2017 18th International Scientific Conference on Electric Power Engineering (EPE)*, IEEE, 2017, pp. 1–5.

[58] I. S. Kwon, S. J. Kim, M. Asif, and B. W. Lee, "Evaluation of Electric Field and Space Charge Dynamics in Dielectric under DC Voltage with Superimposed Switching Impulse," *Energies*, vol. 12, no. 10, pp. 1–15, 2019.

[59] V. N. Kestelman, L. S. Pinchuk, V. A. Goldade, V. N. Kestelman, L. S. Pinchuk, and V. A. Goldade, *Electret Effect and Electric Technologies*. Boston, MA: Springer, 2000, pp. 1–45.

[60] P. Morshuis and M. Jeroense, "Space Charge Measurements on Impregnated Paper: A Review of the PEA Method and a Discussion of Results," *IEEE Electrical Insulation Magazine*, vol. 13, no. 3, pp. 26–35, 1997.

[61] T. T. N. Vu, L. Berquez, and G. Teyssedre, "Space charge measurement by electroacoustic method: Impact of acoustic properties of materials on the response for different geometries," *International Journal on Electrical Engineering and Informatics*, vol. 10, no. 4, pp. 631–647, 2018, ISSN: 20875886. DOI: 10.15676/ijeei.2018.10.4.2.

[62] G. Ala, M. Caruso, V. Cecconi, S. Ganci, A. Imburgia, R. Miceli, P. Romano, and F. Viola, "Review of Acoustic Methods for Space Charge Measurement," in *2015 AEIT International Annual Conference (AEIT)*, IEEE, 2015, pp. 1–6.

[63] T. K. Saha, M. Darveniza, Z. T. Yao, D. Hill, and G. Yeung, "Investigating the Effects of Oxidation and Thermal Degradation on Electrical and Chemical Properties of Power Transformers Insulation," *IEEE Power Engineering Review*, vol. 19, no. 3, p. 1359, 1999.

[64] J. Zhang, J. Li, X. Li, H. Ran, and Z. Wu, "Correlation Analysis of Dispersion Staining Color of Cellulose Fibers in Insulating Oil and Paper Degradation," in *2016 IEEE International Conference on High Voltage Engineering and Application (ICHVE)*, IEEE, 2016, pp. 1–4.

[65] A. Ciuriuc, L. M. Dumitran, and P. V. Notingher, "Dielectric Properties of Paper Insulation Aged in the Presence of Vegetable Transformer Oil," in *Proceedings of IEEE International Conference on Solid Dielectrics, ICSD*, IEEE, 2013, pp. 549–552.

[66] G. K. Frimpong, T. V. Oommen, and R. Asano, "A Survey of Aging Characteristics of Cellulose Insulation in Natural Ester and Mineral Oil," *IEEE Electrical Insulation Magazine*, vol. 27, no. 5, pp. 36–48, 2011.

[67] R. Liu, A. Jaksts, C. Tornkvist, and M. Bergkvist, "Moisture and Space Charge in Oil-Impregnated Pressboard under HVDC," in *The 1998 IEEE 6th International Conference on Conduction and Breakdown in Solid Dielectrics*, IEEE, 1998, pp. 5–6.

[68] L. E. Lundgaard, W. Hansen, D. Linhjell, and T. J. Painter, "Aging of Oil-Impregnated Paper in Power Transformers," *IEEE Transactions on Power Delivery*, vol. 19, no. 1, pp. 230–239, 2004.

[69] N. Azis, Q. Liu, and Z. D. Wang, "Ageing assessment of transformer paper insulation through post mortem analysis," *IEEE Transactions on Dielectrics and Electrical Insulation*, vol. 21, no. 2, pp. 845–853, 2014, ISSN: 10709878. DOI: 10.1109/TDEI.2013.004118.

[70] C. Tang, B. Huang, M. Hao, Z. Xu, J. Hao, and G. Chen, "Progress of space charge research on oil-paper insulation using pulsed electroacoustic techniques," *Energies*, vol. 9, no. 1, pp. 1–35, 2016, ISSN: 19961073.

[71] G. Mazzanti, G. C. Montanari, and J. M. Alison, "A space-charge based method for the estimation of apparent mobility and trap depth as markers for insulation degradation-theoretical basis and experimental validation," *IEEE Transactions on Dielectrics and Electrical Insulation*, vol. 10, no. 2, pp. 187–197, 2003.

[72] Y. X. Zhou, M. Huang, W. J. Chen, and F. B. Jin, "Space charge behavior of oil-paper insulation thermally aged under different temperatures and moistures," *Journal of Electrical Engineering and Technology*, vol. 10, no. 3, pp. 1124–1130, 2015.

[73] R. Zou, J. Hao, and R. Liao, "DC breakdown and space charge characteristics of mineral oil impregnated thermally upgraded paper with different ageing conditons," in *IEEE International Conference on Dielectric Liquids*, IEEE, 2019, pp. 1–4, ISBN: 9781728117188. DOI: 10.1109/ICDL.2019.8796784.

[74] S. Ellingson, *Electromagnetics*. VT Publishing, Aug. 2018, vol. 1, pp. 124–143.

[75] J. S. Kim, B. C. Choi, H. K. Yang, J. H. Jeong, S. T. Chung, and S. B. Cho, "Low-frequency Dielectric Dispersion and Electrical Conductivity of Pure and La-Doped $SrBi_2Nb_2O_9$ Ceramics," *Journal of the Korean Physical Society*, vol. 52, no. 2, pp. 415–416, 2008.

[76] T. Liu, J. Fothergill, S. Dodd, and U. Nilsson, "Dielectric Spectroscopy Measurements on Very Low Loss Cross-linked Polyethylene Power Cables," *Journal of Physics: Conference Series*, vol. 183, pp. 1–6, 2009.

[77] E. Tavar, E. Turk, and S. Kreft, "Simple Modification of Karl-Fischer Titration Method for Determination of Water Content in Colored Samples," *Journal of Analytical Methods in Chemistry*, vol. 1, no. 1, pp. 1–, 2012.

[78] Y. Li and T. Takada, "Progress in Space Charge Measurement of Solid Insulating Materials in Japan," *IEEE Electrical Insulation Magazine*, vol. 10, no. 5, pp. 16–28, 1994.

[79] T. Takada, Y. Tanaka, N. Adachi, and X. Qin, "Comparison Between the PEA Method and the PWP Method for Space Charge Measurement in Solid Dielectrics," *IEEE Transactions on Dielectrics and Electrical Insulation*, vol. 5, no. 6, pp. 944–951, 1998.

[80] T. Takada, J. Holboell, A. Toureille, J. Densley, N. Hampton, J. Castellon, R. Hegerberg, M. Henriksen, G. Montanari, M. Nagao, and P. Morshuis, *Space Charge Measurement in Dielectrics and Insulating Materials*, February. Cigre, 2006, pp. 1–51.

[81] Y. Li, M. Yasuda, and T. Takada, "Pulsed Electroacoustic Method For Measurement Of Charge Accumulation In Solid Dielectrics," *IEEE Transactions on Dielectrics and Electrical Insulation*, vol. 1, no. 2, pp. 188–195, 1994.

[82] S. Lubricants, "Shell Diala S3 ZX-IG Technical Data Sheet," Tech. Rep., 2012, pp. 1–2.

[83] MI MATERIALS, "MIDEL eN 1204," Tech. Rep., pp. 1–4.

[84] C. Perrier and T. Stirl, "Moisture-equilibrium Charts: Monitoring Natural-ester Green Transformers," *Transformers Magazine*, vol. 4, no. 2, pp. 98–102, 2018.

[85] K. J. Rapp, C. P. McShane, and J. Luksich, "Interaction mechanisms of natural ester dielectric fluid and Kraft paper," in *2005 IEEE International Conference on Dielectric Liquids (ICDL)*, IEEE, 2005, pp. 393–396, ISBN: 0780389549. DOI: 10.1109/icdl.2005.1490108.

[86] H. Yoon and G. Chen, "Space charge characteristics of natural ester oil-impregnated paper with different moisture contents," *IEEE Transactions on Dielectrics and Electrical Insulation*, vol. 29, no. 6, pp. 2139–2140, 2022, ISSN: 15584135. DOI: 10.1109/TDEI.2022.3202740.

[87] G. Nagaraju and R. Sarathi, "The Effect of Voltage Polarity Reversal on Space Charge Behavior of Epoxy MgO Nanocomposites," in *Electrical Insulation Conference, EIC*, IEEE, 2021, pp. 317–320, ISBN: 9781665415644. DOI: 10.1109/EIC49891.2021.9612383.

[88] S. Maneerot, N. Pattanadech, Y. Kittikhuntharadol, P. Nimsanong, and C. Bunlaksananusorn, "Polarization and Conduction Characteristics of Mineral Oil and Natural Ester Mixed with Nanoparticles," *Advances in Materials Science and Engineering*, vol. 2022, G. Carotenuto, Ed., pp. 1–10, Mar. 2022, ISSN: 1687-8442.

DOI: 10.1155/2022/9225170. [Online]. Available: https://www.hindawi.com/journals/amse/2022/9225170/.

[89] O. Roizman, "Water in Transformers," *Transformer Magazine*, vol. 6, no. 1, pp. 68–74, 2019.

[90] R. Villarroel, B. García de Burgos, and D. F. García, "Moisture dynamics in natural-ester filled transformers," *International Journal of Electrical Power and Energy Systems*, vol. 124, no. December 2019, pp. 2–3, 2021. [Online]. Available: https://doi.org/10.1016/j.ijepes.2020.106172.

[91] B. Huang, Z. Xu, M. Hao, and G. Chen, "Multilayers Oil and Oil-impregnated Pressboard Electric Field Simulation based on Space Charge," *IEEE Transactions on Dielectrics and Electrical Insulation*, vol. 26, no. 2, pp. 532–533, 2019. DOI: 10.1109/TDEI.2019.007429.

[92] L. Che, J. Wu, G. Zhou, Y. Yin, and Q. Wang, "Effect of moisture content on space charge behavior in oil-paper insulation under DC electric field," *IEEE Transactions on Dielectrics and Electrical Insulation*, vol. 27, no. 5, pp. 1570–1572, 2020, ISSN: 15584135. DOI: 10.1109/TDEI.2020.008799.

[93] R. Liao, J. Hao, G. Chen, Z. Ma, and L. Yang, "A comparative study of physicochemical, dielectric and thermal properties of pressboard insulation impregnated with natural ester and mineral oil," *IEEE Transactions on Dielectrics and Electrical Insulation*, vol. 18, no. 5, pp. 1626–1637, 2011, ISSN: 10709878. DOI: 10.1109/TDEI.2011.6032833.

[94] Z. Xing, C. Zhang, H. Cui, Y. Hai, Q. Wu, and D. Min, "Space charge accumulation and decay in dielectric materials with dual discrete traps," *Applied Sciences (Switzerland)*, vol. 9, no. 20, p. 2, 2019, ISSN: 20763417. DOI: 10.3390/app9204253.

[95] B. Huang, M. Hao, J. Hao, J. Fu, Q. Wang, and G. Chen, "Space charge characteristics in oil and oil- impregnated pressboard and electric field distortion after polarity reversal," *IEEE Transactions on Dielectrics and Electrical Insulation*, vol. 23, no. 2, p. 883, 2016. DOI: 10.1109/TDEI.2015.005413.

[96] R. J. Heywood, A. M. Emsley, and M. Ali, "Degradation of cellulosic insulation in power transformers . Part 1 : Factors affecting the measurement of the average viscometric degree of polymerisation of new and aged electrical papers," *IEE Proceedings - Science Measurement and Technology*, vol. 147, no. 2, pp. 86–90, 2000.

[97] C. Perrier, M. Ryadi, Y. Bertrand, and C. Tran Duy, "Comparison between mineral and ester oils," CIGRE, Tech. Rep., 2010, pp. 1–6.

[98] N. Azis and Z. D. Wang, "Acid generation study of natural ester," in *International Symposium on High Voltage Engineering*, 2011, pp. 1–6.

[99] K. D. Kouassi, I. Fofana, L. Cissé, Y. Hadjadj, K. M. Lucia Yapi, and K. Ambroise Diby, "Impact of low molecular weight acids on oil impregnated paper insulation degradation," *Energies*, vol. 11, no. 6, pp. 1–13, 2018, ISSN: 19961073. DOI: 10.3390/en11061465.

[100] U. M. Rao, I. Fofana, and J. S. N'Cho, "On some imperative IEEE standards for usage of natural ester liquids in transformers," *IEEE Access*, vol. 8, pp. 145 446–145 448, 2020, ISSN: 21693536. DOI: 10.1109/ACCESS.2020.3014600.

[101] J. Hao, W. Ye, C. Gao, M. Zhu, L. Yang, and R. Liao, "Experimental and molecular level analysis of natural ester delaying degradation of cellulose insulation polymer," *High Voltage*, vol. 7, no. 5, pp. 1001–1015, 2022, ISSN: 23977264. DOI: 10.1049/hve2.12151.

[102] K. L. Kato and R. E. Cameron, "A review of the relationship between thermally-accelerated ageing of paper and hornification," *Cellulose*, vol. 6, no. 1, pp. 23–40, 1999, ISSN: 09690239. DOI: 10.1023/A:1009292120151.

[103] Z. Mu, S. Y. Matharage, Z. D. Wang, and Q. Liu, "Effect of Low Molecular Weight Acids and Moisture on Space Charge of Oil Impregnated Paper Insulation," in *2018 IEEE International Conference on High Voltage Engineering and Application (ICHVE)*, 2019, pp. 1–2, ISBN: 9781538650868. DOI: 10.1109/ICHVE.2018.8641887.

[104] K. Wang, F. Wang, Z. Lou, Q. Han, Q. Zhao, K. Hu, Z. Huang, and J. Li, "Relationship between the electrical characteristics of molecules and fast streamers in ester insulation oil," *International Journal of Molecular Sciences*, vol. 21, no. 3, pp. 1–7, 2020, ISSN: 14220067. DOI: 10.3390/ijms21030974.

[105] B. X. Du, J. G. Zhang, and D. S. Liu, "Interface charge behavior of multi-layer oil-paper insulation under DC and polarity reversal voltages," *IEEE Transactions on Dielectrics and Electrical Insulation*, vol. 22, no. 5, pp. 2628–2636, 2015, ISSN: 10709878. DOI: 10.1109/TDEI.2015.005052.

[106] X. Zhao, N. Feng, L. Pu, J. Liu, W. Duan, Z. Ju, H. Sun, B. Huang, M. Hao, and G. Chen, "Temperature gradient effect on the space charge behaviour in multi-layers of oil and pressboard," *IEEE Transactions on Dielectrics and Electrical Insulation*, vol. 26, no. 5, pp. 1645–1653, Oct. 2019, ISSN: 1070-9878. DOI: 10.1109/TDEI.2019.008216. [Online]. Available: https://ieeexplore.ieee.org/document/8858136/.

[107] F. Vahidi, S. Haegele, S. Tenbohlen, K. Rapp, and A. Sbravati, "Study on moisture influence on electrical conductivity of natural ester fluid and mineral oil," in *2017 IEEE Electrical Insulation Conference*, IEEE, 2017, pp. 290–293, ISBN: 9781509039654. DOI: 10.1109/EIC.2017.8004614.

[108] S. O. Oparanti, U. M. Rao, and I. Fofana, "Natural Esters for Green Transformers: Challenges and Keys for Improved Serviceability," *Energies*, vol. 16, no. 1, 2023, ISSN: 19961073. DOI: 10.3390/en16010061.

[109] I. L. Hosier, A. S. Vaughan, and R. D. Chippendale, "Permittivity mismatch and its influence on ramp breakdown performance," in *IEEE International Conference on Solid Dielectrics, ICSD*, IEEE, 2013, pp. 644–647, ISBN: 9781479908073. DOI: 10.1109/ICSD.2013.6619665.

[110] M. Lashbrook, H. Al-Amin, and R. Martin, "Natural ester and synthetic ester fluids, applications and maintenance," in *2017 10th Jordan International Electrical and Electronics Engineering Conference, JIEEEC 2017*, 2017, p. 2, ISBN: 9781538618363. DOI: 10.1109/JIEEEC.2017.8051397.

[111] J. Malde, M. Daghrah, and A. Gyore, "Natural and Synthetic Ester Liquids-How They Differ, What They Deliver," *Transformer Technology*, pp. 56–67, 2020.